JOURNAL OF THE

Electrochemical Society

ol. 105, No. 12 December 1958

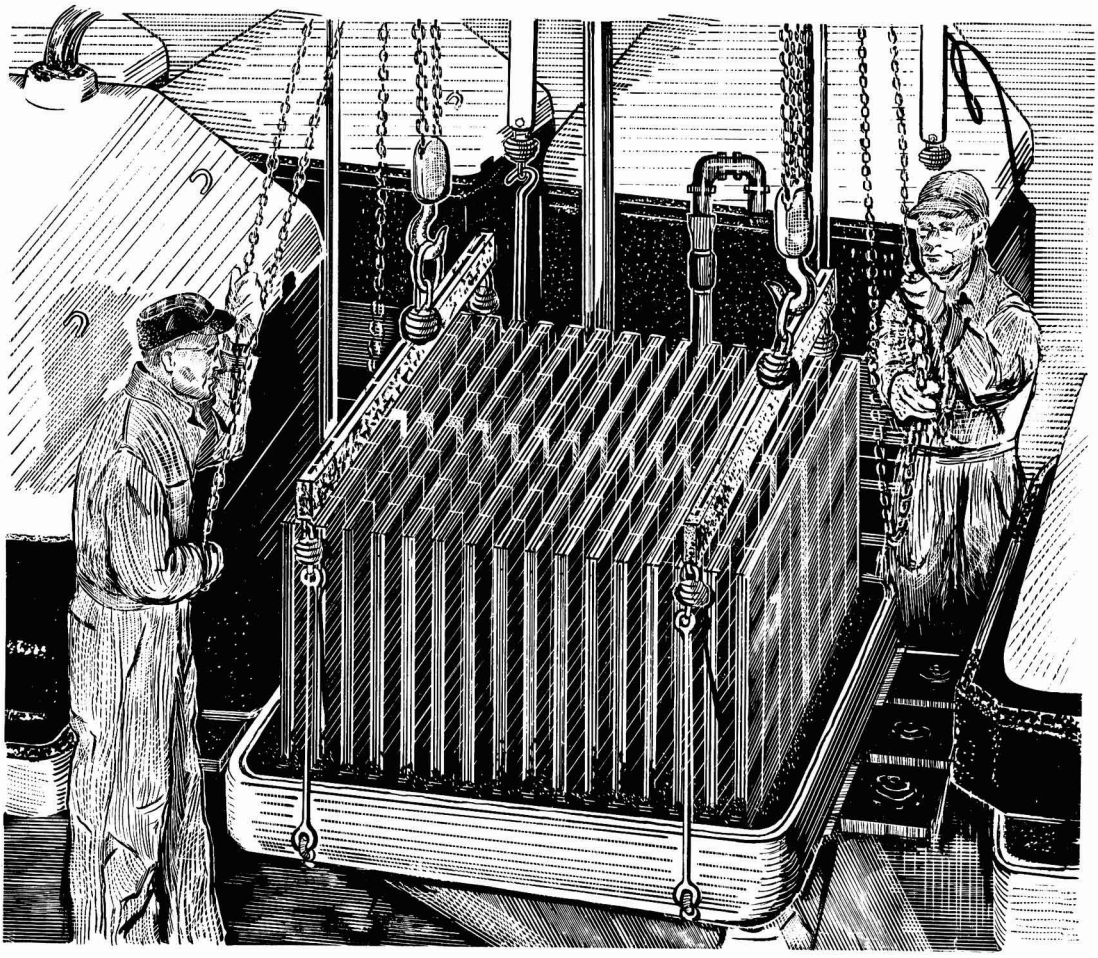

Efficiency in the making

Depth of experience in the building, installation and operation of Hooker cells is a highly important factor in their production efficiency.

High efficiency is also a characteristic of **GLC Anodes,** which are "custom made" to individual cell requirements.

FREE—*This illustration of cell renewal has been handsomely reproduced with no advertising text. We will be pleased to send you one of these reproductions with our compliments. Simply write to Dept. J-12.*

ELECTRODE
GLC®
DIVISION

GREAT LAKES CARBON CORPORATION

18 EAST 48TH STREET, NEW YORK 17, N.Y. OFFICES IN PRINCIPAL CITIES

Journal of the Electrochemical Society

DECEMBER 1958 **VOL. 105 • NO. 12**

CONTENTS

Published monthly by The Electrochemical Society, Inc., from Manchester, N. H., **Executive Offices, Editorial Office** and **Circulation Dept.,** and **Advertising Office** at 1860 Broadway, New York 23, N. Y., combining the JOURNAL and TRANSACTIONS OF THE ELECTROCHEMICAL SOCIETY. Statements and opinions given in articles and papers in the JOURNAL OF THE ELECTROCHEMICAL SOCIETY are those of the contributors, and The Electrochemical Society assumes no responsibility for them. Nondeductible subscription to members $5.00; subscription to nonmembers $18.00. Single copies $1.25 to members, $1.75 to nonmembers.

Entered as second-class matter at the Post Office at Manchester, N. H., under the act of August 24, 1912.

Now . . . Ratings > 120 kw for rectifiers made with

DU PONT SILICON

compact units can eliminate need for dc lines

A wide range of rectifiers made with Du Pont Hyperpure Silicon—*with ratings from a few microwatts to > 120 kw per cell*—are now available. Manufacturers cite efficiencies up to 99% in units operated at 60 cps, operation at temperatures from –65° to 175°C., rectification ratios as high as 10 million with negligible reverse conductance, and the elimination of special dc lines when these compact rectifiers are used in bridges.

Du Pont, pioneer and first commercial producer of silicon, supplies manufacturers of rectifiers, diodes and transistors with several grades of Hyperpure Silicon. (Du Pont does not produce devices.)

Write today for our free booklet containing full data on Du Pont Silicon: E. I. du Pont de Nemours & Co. (Inc.), 2420 Nemours Bldg., Pigments Department, Wilmington 98, Delaware.

DUPONT REG. U.S. PAT. OFF **HYPERPURE SILICON**

Better Things for Better Living
. . . through Chemistry

Editorial

Anniversary Greetings to AES

CONCEIVED in the year 1908, the "National Electro-Platers Association of the United States and Canada" was born early in 1909. In 1913, NEPA, with a membership of some 350, was reorganized as the American Electroplaters' Society. After a half century of growth and progress, AES is now observing its Fiftieth Anniversary during the period of July 1, 1958 through June 30, 1959. The year's activities will be climaxed by the society's Golden Jubilee Convention and Industrial Finishing Exposition, including the Fifth International Conference on Electrodeposition and Metal Finishing, to be held in Detroit next June. The official journal of AES, *Plating*, is preparing a special feature Golden Jubilee Issue for June.

This JOURNAL takes the opportunity to extend anniversary greetings to AES, and to congratulate the society on the high position it has attained among American Industrial Scientific Societies. Recognized leader in a field of utmost importance to modern society, its interests range from the encouragement of theoretical research through the activities of many of the largest industrial corporations to the practical problems of the smallest plating and finishing laboratory. In addition to the encouragement of basic research, AES is able to offer financial support to worthy projects in a way which our own Society cannot do, and we congratulate the organization on its wise decisions in this direction.

Our Society and the American Electroplaters' Society have enjoyed cordial and mutually profitable relations for many years, and there seems to be no reason why this should not continue indefinitely. We have a considerable area of overlapping interests on the one hand, and on the other hand a wide separation of interests. Electrodeposition is the largest Division of our Society, with more than 700 members, of whom several hundred are also members of AES. There are members common with our Corrosion and other Divisions as well. Our Society could not, and would not wish to, extend its activities over the full range of AES interests, and the opposite is certainly equally true. We are happy that the work of each Society supplements that of the other.

Our Society is fortunate in having similarly overlapping interests with many other scientific organizations. We like to feel that we can provide a common meeting ground, with our National (and International) Meetings and JOURNAL, for scientists of widely divergent primary interests. Our growth during the past several years, and the increasing support we have received, are measures of our success. These things have not come at the expense of the other societies at all, but are the result of mutual desires for the interchange of knowledge and stimulation.

—CVK

SARGENT-SLOMIN ANALYZERS
are standard equipment
in prominent laboratories

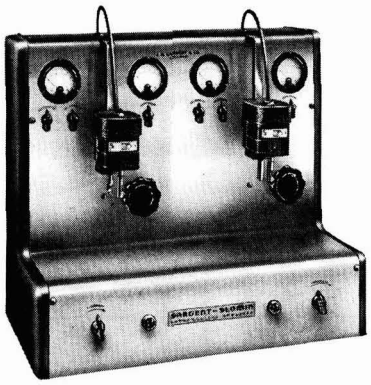

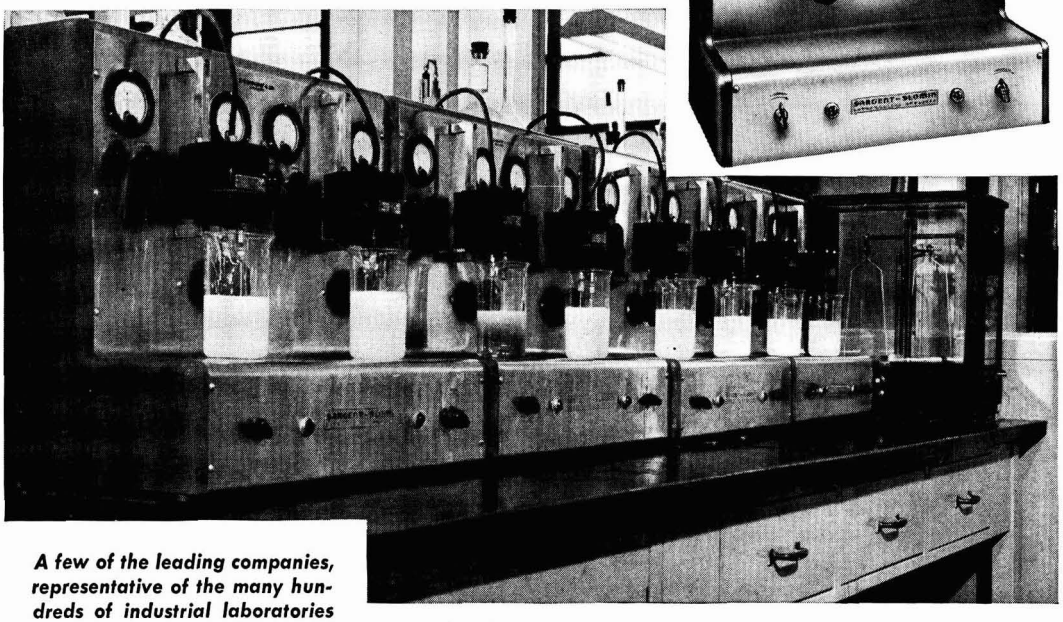

A few of the leading companies, representative of the many hundreds of industrial laboratories using the Sargent - Slomin and Heavy Duty Analyzers for control analyses . . .

AMPCO METAL, Inc.
ANDERSON LABORATORIES
CALERA MINING COMPANY
EUREKA WILLIAMS COMPANY
THE FEDERAL METAL CO.
FORD MOTOR COMPANY
THE GLIDDEN COMPANY—Chemical, Metal and Pigment Division
HOT POINT CO.
HOWARD FOUNDRY COMPANY
INTERNATIONAL HARVESTER COMPANY
KENNAMETAL Inc.
McQUAY - NORRIS MANUFACTURING CO.
NATIONAL LEAD COMPANY, Fredericktown, Missouri
PIASECKI HELICOPTER CORPORATION
REVERE COPPER & BRASS INCORPORATED
THE RIVER SMELTING & REFINING COMPANY
SILAS MASON COMPANY
THE STUDEBAKER CORPORATION
THOMPSON PRODUCTS, INC.

Photo Courtesy INTERNATIONAL HARVESTER COMPANY, Melrose Park, Illinois

Sargent-Slomin Electrolytic Analyzers are recommended for such electro analytical determinations as: Copper in—ores, brass, iron, aluminum and its alloys, magnesium and its alloys, bronze, white metals, silver solders, nickel and zinc die castings. Lead in—brass, aluminum and its alloys, bronze, zinc and zinc die castings. Assay of electrolytical copper, nickel and other metals.

Sargent analyzers are completely line operated, employing self-contained rectifying and filter circuits. Deposition voltage is adjusted by means of autotransformers, with meters indicating volts and amperes and controls on the panel. An easily replaceable fuse guards against circuit overload. Maximum D.C. current capacity is 5 to 15 amperes; maximum D.C. voltage available, 10 volts.

Sargent-Slomin Analyzers stir through a rotating chuck operated from a capacitor type induction motor, having a fixed speed of 550 r.p.m. with 60 cycle A.C. current or 460 r.p.m. with 50 cycle A.C. current. Motors are sealed against corrosive fumes and are mounted on cast metal brackets, sliding on ½" square stainless steel rods, permitting vertical adjustment of electrode position over a distance of 4". Pre-lubricated ball-bearings support the rotating shaft. All analyzers accommodate electrodes having shaft diameters no greater than 0.059 inch. Stainless steel spring tension chucks permit quick, easy insertion of electrodes and maintain proper electrical contact. Special Sargent high efficiency electrodes are available for these analyzers. Illustrated above is one model of the five types of Sargent-Slomin and Heavy Duty Analyzers.

S-29465 ELECTROLYTIC ANALYZER—Motor stirred, Two Position, 5 Ampere. With two adjustable heaters, pilot lights and control knobs. For operation from 115 volt, 50 or 60 cycle A.C. circuits.....**$530.00**

SARGENT

SCIENTIFIC LABORATORY INSTRUMENTS • APPARATUS • SUPPLIES • CHEMICALS

E. H. SARGENT & COMPANY, 4647 W. FOSTER, CHICAGO 30, ILLINOIS
DETROIT 4, MICH. • DALLAS 35, TEXAS • BIRMINGHAM 4, ALA. • SPRINGFIELD, N. J.

FUTURE MEETINGS OF
The Electrochemical Society

Philadelphia, Pa., May 3, 4, 5, 6, and 7, 1959

Headquarters at the Sheraton Hotel

Sessions probably will be scheduled on

Electric Insulation, Electronics (including Luminescence

and Semiconductors), Electrothermics and Metallurgy

(including a Projected Symposium on "Mechanical Properties of Intermetallic Compounds"),

Industrial Electrolytics, and Theoretical Electrochemistry

★ ★ ★

Columbus, Ohio, October 18, 19, 20, 21, and 22, 1959

Headquarters at the Deshler-Hilton Hotel

★ ★ ★

Chicago, Ill., May 1, 2, 3, 4, and 5, 1960

Headquarters at the Lasalle Hotel

★ ★ ★

Houston, Texas, October 9, 10, 11, 12, and 13, 1960

Headquarters at the Shamrock Hotel

★ ★ ★

Papers are now being solicited for the meeting to be held in Philadelphia, Pa., May 3-7, 1959. Triplicate copies of each abstract (*not exceeding 75 words in length*) are due at Society Headquarters, 1860 Broadway, New York 23, N. Y., *not later than January 2, 1959* in order to be included in the program. *Please indicate on abstract for which Division's symposium the paper is to be scheduled, and underline the name of the author who will present the paper.* Complete manuscripts should be sent in triplicate to the Managing Editor of the JOURNAL at 1860 Broadway, New York 23, N. Y.

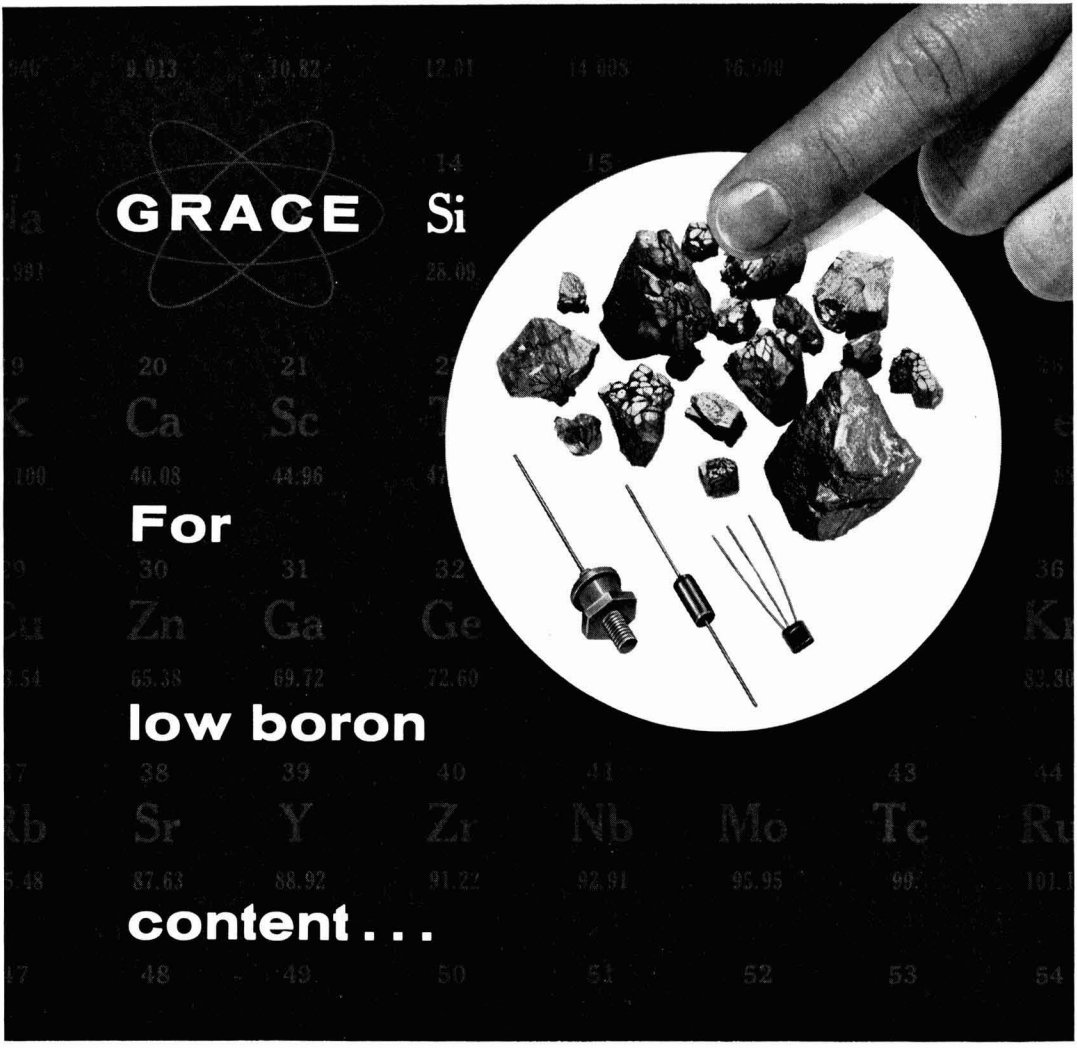

GRACE SILICON

(ultra-high-purity)

"For want of a nail the battle was lost" becomes painfully true when translated to lack of purity in the semi-conductor material you choose for your transistors, diodes or other silicon devices.

The Pechiney process, used in the manufacture of Grace Silicon, is noted for a product with low boron content as well as overall high purity.

May we suggest that whenever top quality silicon is desired—silicon combining both high purity and uniform quality—you get in touch with GRACE ELECTRONIC CHEMICALS, INC., at PLaza 2-7699, 101 N. Charles Street in Baltimore.

GRACE ELECTRONIC CHEMICALS, INC.
101 N. Charles St., Baltimore, Maryland
Subsidiary of W. R. GRACE & CO.

Diffusion Control in Silicon by Carrier Gas Composition

C. J. Frosch and L. Derick

Bell Telephone Laboratories, Inc., Murray Hill, New Jersey

ABSTRACT

A single heating process is described for producing controlled p-n and n-p-n diffused structures in silicon by changing the carrier gas composition during diffusion. The process is shown to depend on large changes in the rate of evaporation from a Ga_2O_3 source at a given temperature in carrier gases of different composition. The weight loss from a Ga_2O_3 source at a given temperature is quite large in reducing gases, extremely small in neutral gases, and essentially zero in oxidizing gases. The weight loss from a Ga_2O_3 source in reducing gases also decreases with increasing concentrations of water vapor in the carrier gas. The weight loss from a Sb_2O_4 source at a given temperature is relatively large in all of these carrier gases.

The diffusion apparatus consists essentially of a fused silica tube extending through separately controlled temperature zones for the location of the diffusant sources and the silicon samples. Carrier gases at controlled rates of flow carry the diffusant vapors past the silicon samples at atmospheric pressure.

Data are presented for single diffusions from Ga_2O_3 and Sb_2O_4 sources in several carrier gas compositions. P-type layers are formed in 5 ohm-cm n-type silicon in the Ga_2O_3 diffusions in reducing gases but not in oxidizing gases. A controlled number of gallium atoms can be introduced into silicon by heating first in a reducing gas and then in an oxidizing gas. N-type layers are formed in 5 ohm-cm p-type silicon in the Sb_2O_4 diffusions in all of the carrier gases studied. Data also are presented on double diffusions from As_2O_3-Ga_2O_3 and Sb_2O_4-Ga_2O_3 sources to illustrate the control of layer thickness by heating first in wet N_2 and then in wet H_2. These double diffused structures are shown to be suitable for the fabrication of high alpha transistors.

The introduction and control of impurities in semiconductors by vapor-solid diffusion techniques has been described by Fuller and Ditzenberger (1, 2) and Frosch and Derick (3). These techniques can be employed for producing controlled single and multiple diffusion layers by the proper choice of processing parameters such as temperature, time, gas flow, and gas composition. However, the control of multiple diffusion layers and often single diffusion layers generally requires more than one heating of the Si in separate diffusion apparatus. For example, a diffusion apparatus contaminated with Ga could not be employed by the older techniques for introducing Sb or As into a semiconductor to make a controlled n-p-n transistor structure.

This paper describes a new single heating process for producing controlled single and multiple diffusion layers in semiconductors by changing the carrier gas composition during the diffusion. The diffusion control is shown to depend on large changes in the volatility of certain impurities in carrier gases of different composition. However, the formation of SiO_2 layers on Si during heating in oxidizing carrier gases also is an important factor in the control of diffusion layers. This results from the partial masking (3) by a SiO_2 layer against the diffusion of certain impurities into Si at elevated temperatures. An SiO_2 layer on Si does not mask against Ga but does mask against Sb and As. For example, the surface concentration obtained for a Ga diffusion is essentially the same for an unoxidized or preoxidized Si sample. On the other hand, the surface concentration obtained for a Sb or As diffusion decreases with increasing thickness of a SiO_2 layer on the Si surface. Further discussion of these masking effects is given below.

Apparatus and Procedure

The diffusion apparatus is shown schematically in Fig. 1. It is the same as that described previously (3) except for the addition of a third controlled temperature zone. The apparatus consists essentially of a fused silica tube extending through three separately controlled temperature zones. The first

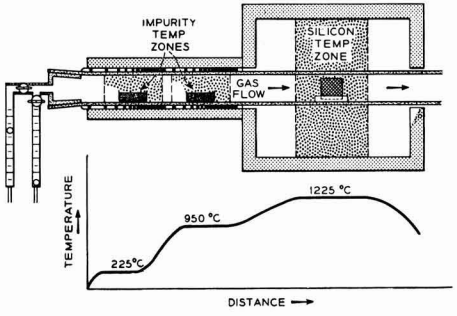

Fig. 1. Apparatus for vapor-solid diffusion at atmospheric pressure.

two temperature zones together with the carrier gases serve to regulate the volatility of the impurities placed therein. The third temperature zone is the location of the Si samples. The temperatures are regulated to ±2°C by means of Pt-Pt 10% Rh thermocouples and automatic controllers.

Flowmeters attached to one end of the furnace tube regulate the flow of the carrier gases. In this investigation flow rates of 1500 cc/min of the carrier gas were employed in furnace tubes of 2.5 cm ID. A temperature-controlled fritted-glass water bubbler is inserted between the flowmeters and the furnace tube when water vapor is being added to the carrier gas.

In the weight loss studies, a single controlled temperature zone is employed. Each carrier gas composition is allowed to flow through the apparatus for several minutes to establish a steady-state condition. Then a weighed amount of impurity (approximately 2 g) in a tared fused silica crucible is inserted into the cool end of the furnace tube. After 10 min the sample is moved quickly into the controlled temperature zone for a measured time. Then the sample is withdrawn rapidly to the cool end of the furnace tube. It is allowed to cool for 10 min before weighing. The same procedure is repeated for several successive weight losses. A new supply of impurity is employed for each carrier gas composition. The exact conditions are given on Fig. 1-3 and in the later discussion.

In the diffusion studies the impurities in fused silica or platinum crucibles are placed in the controlled temperature zones. The carrier gas composition is allowed to flow through the apparatus for several minutes to establish a steady-state condition. Then the Si samples held vertically in slotted fused-silica holders are introduced rapidly into the controlled temperature zone. Depending on the particular experiment, the carrier gas composition may be changed without removing the Si samples from the furnace. Silicon samples are removed rapidly after the heating interval. The exact process parameters are reported in Tables I-IV.

Methods for determining the electrical characteristics, surface concentrations, and diffusion depths are essentially the same as those described elsewhere (1, 2).

Samples

The Si samples were cut from approximately 5 ohm-cm n-type (arsenic doped) or p-type (boron doped) single-crystal ingots grown in the [111] direction by pulling from the melt. The ingots were sawed perpendicular to the growth direction into slices approximately 1 mm thick. These were machine lapped on both surfaces with No. 1800 emery powder to a thickness of about 7×10^{-2} cm. After cutting into squares of 0.75 x 0.75 cm, the samples were etched for 4-5 min in a mixture of 5 parts of concentrated HNO_3 to 1 part of concentrated HF. Reproducible surfaces of excellent appearance were obtained by maintaining the etchant temperature at about 20°C and employing mechanical agitation during etching. The etched samples were heated for 1 hr at 1300°C in 100% O_2 when preoxidized samples were employed in the diffusions.

Impurity Volatility

The volatility of elemental diffusants or their compounds at a given temperature in carrier gases of different composition is the basic control variable in this study. Hence, volatility data are of importance in establishing diffusion process parameters. Such data are presented in this section for a single donor and a single acceptor impurity. These are sufficient to illustrate the effect of carrier gas composition on volatility. The volatility is expressed in terms of a weight loss from a heated impurity source. However, the volatile molecular species or the impurity vapor in the carrier gas stream is not necessarily of the same composition as the impurity source.

Some typical weight loss data for a Ga_2O_3 powder and elemental Ga are plotted in Fig. 2 and 3, respectively, as a function of heating time at 950°C in several carrier gas compositions. Note particularly the large weight losses in wet H_2 and the essentially zero loss in wet N_2 for the Ga_2O_3 source. The weight loss decreases rapidly with increasing H_2O concentration in the H_2. The Ga_2O_3 is reduced to Ga in dry H_2 at these fast flow rates. Weight losses from a Ga_2O_3 source also are appreciable in a CO carrier gas. Volatility decreases with increasing concentrations of H_2O or CO_2 in the CO. For com-

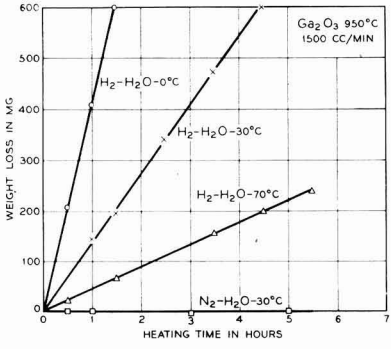

Fig. 2. Effect of carrier gas composition on weight loss from a heated Ga_2O_3 source.

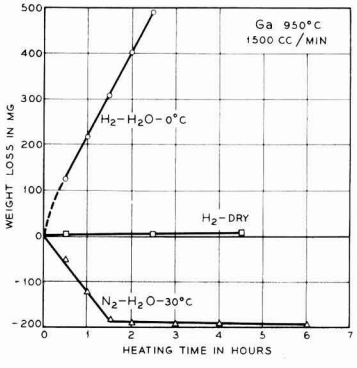

Fig. 3. Effect of carrier gas composition on weight loss from a heated Ga source.

parable conditions, weight losses in CO are from about 5 to 10 times lower than those in H_2. Weight losses from a Ga_2O_3 source are extremely small or zero over the temperature range studied up to 1200°C in gases such as N_2, He, A, and O_2 with or without added H_2O or O_2.

In the case of the Ga source the weight losses as shown in Fig. 3 are large in wet H_2 but very small in dry H_2. A gain in weight occurs in the wet N_2 with a conversion of the source material to Ga_2O_3.

The large changes in volatility from Ga_2O_3 sources at a given temperature in carrier gases of different composition must depend on an increase in the concentration of a volatile molecular species in the vapor phase. Such a reaction need take place only at the evaporating surface and probably occurs rapidly. Information on these thermodynamic equilibria of impurity vapors at different temperatures in different carrier gas compositions would be helpful in establishing diffusion controls. It would lead also to a better understanding of the diffusion process.

The higher weight losses from a Ga_2O_3 source in reducing gases as compared to inert or oxidizing gases suggests the reduction of the impurity to a more volatile species. Unpublished vapor pressure data (4) show that the reactions can be expressed by the following equations:

$$Ga_2O_3 + 2H_2 = Ga_2O + 2H_2O \quad [1]$$

$$Ga_2O_3 + 2CO = Ga_2O + 2CO_2 \quad [2]$$

in which Ga_2O is the volatile molecular species being formed. These equations explain the decrease in weight loss from a Ga_2O_3 source with increasing concentrations of H_2O or CO_2 added to the H_2 or CO carrier gases, respectively. The weight loss for a Ga source in wet H_2 as shown in Fig. 3 probably occurs also as Ga_2O.

The weight losses from Sb_2O_4 and Sb sources at a given temperature are appreciable in dry or wet N_2, H_2, A, or He. For example, as shown in the second column of Table I, the weight losses from an Sb_2O_4 source are large at 950°C in N_2. They also show no definite trend or appreciable change with water content over the concentration range studied. Weight loss determinations could not be made in H_2 since Sb_2O_4 reduces to Sb even in the presence of fairly large concentrations of H_2O. However, the weight losses for Sb_2O_4 or Sb sources are known to be appreciable in all of the dry or wet carrier gases studied with the exception of O_2. The weight loss for an Sb_2O_4 source at 950°C in O_2 is very small as compared to that in other carrier gases such as H_2 or N_2. However, the loss at 1100°C in O_2 is somewhat higher than the loss in wet or dry N_2 at 950°C. This effect of O_2 might be explained by a shift upward in the transition temperature above that predicted by the equations

$$2Sb_2O_5 \underset{\leftrightarrows}{380°C} 2Sb_2O_4 + O_2 \quad [3]$$

$$2Sb_2O_4 \underset{\leftrightarrows}{930°C} 2Sb_2O_3 + O_2 \quad [4]$$

in which the Sb_2O_3 would be assumed to be the more volatile molecular species. It is reported elsewhere (5) that Sb_2O_4 is probably Sb_4O_8 which is a mixture of Sb_2O_3 and Sb_2O_5 below 900°C. This may account for some of the volatility effects observed with this oxide.

Table I. Effect of carrier gas composition on the diffusion of Sb in Si. Diffusion, 1 hr; Si, 1200°C; Sb_2O_4, 950°C

Water temp, °C	Sb_2O_4, wt loss, mg	Ohms per square	Layer thick., cm x 10^5	Surface concen., at./cc x 10^{17}
		Hydrogen		
0	—	263	15	30
70	—	495	13	12
		Nitrogen		
Dry	255	64	15	330
0	224	151	15	78
30	260	212	15	42
50	—	286	15	27
70	244	647	13	8

Single Diffusion Layers

Single diffusion data are included to illustrate the relation between the previous volatility data and the diffusion depth, sheet resistance, and surface concentration. These data also provide the necessary processing parameters for the double diffusions.

In Table I single diffusion data are presented for an Sb_2O_4 source at 950°C in H_2 and N_2 carrier gases of different H_2O content. The diffusions were made for 1 hr with 5 ohm-cm p-type Si samples at 1200°C. Note particularly the progressive increase in sheet resistance and decrease in surface concentration with increasing water content in both the H_2 and N_2 carrier gases. The measurements are not sufficiently accurate to show the probable progressive decrease in diffusion depth with increasing water content in the carrier gases. However, the weight losses in column 2 of Table I show no progressive or large change with increasing water content in the N_2 carrier gas. This apparent discrepancy between the weight loss and diffusion data is explained by the masking (3) effect of the SiO_2 layer which is being formed continuously during the introduction of the impurity. For example, no conversion layer will form under the same conditions even in dry N_2 if the Si samples first are preoxidized for 1 hr at 1300°C in O_2. This 1300°C SiO_2 surface layer reduces the surface concentration of Sb to below about 10^{15} atoms/cc. The results in Table I are explained as being due to an increase in the rate of SiO_2 formation and hence more effective masking with increasing water content in the carrier gas. In other words, the competition between the introduction of Sb into the Si and the formation of an SiO_2 layer favors the latter as the concentration of water vapor in the carrier gas is increased.

Single diffusion data for a Ga_2O_3 source at 950°C are presented in Table II for several carrier gas compositions. The diffusions were made for 1 hr at 1200°C using preoxidized 5 ohm-cm n-type Si. An SiO_2 layer does not mask (3) against the diffusion of Ga. This absence of masking by an SiO_2 layer against the diffusion of Ga is a necessary control

Table II. Effect of carrier gas composition on the diffusion of Ga in Si. Diffusion, 1 hr; Si, 1200°C; Ga_2O_3, 950°C

Water temp, °C	Ga_2O_3, wt loss, mg	Ohms per square	Layer thick., cm x 10^5	Surface concen., at./cc x 10^{16}
		Hydrogen		
0	407	149	66	340
30	136	361	61	150
50	—	1455	43	14
70	45	>6000	25	<6
		Carbon Monoxide		
Dry	135	165	74	280
0	45	1117	56	15
30	24	>6000	20	<6
		Nitrogen-Helium-Oxygen		
0	0	N	0	—

requirement in the double diffusions described later, since oxidation occurs during the introduction of the donor impurity. Preoxidized samples are preferred in Ga diffusions since surface pitting is avoided. Surface pitting of unoxidized Si by Ga is especially bad at high-diffusion temperatures.

Note particularly in Table II the absence of a conversion layer in either wet N_2, He, or O_2. The same result is obtained with dry O_2 or inert gases containing even a small trace of O_2. However, completely dry and oxygen-free inert gases such as N_2 and He give a conversion layer of low surface concentration. Note also in Table II the progressive increase in sheet resistance and decrease in layer thickness and surface concentration with increasing water content in the H_2 and CO carrier gases. The direct relation between weight loss and diffusion data also is evident from the table. The results in Table II clearly demonstrate the basic principle for controlling the introduction of Ga atoms into Si. Thus Ga atoms can be introduced by first heating in wet H_2 and then diffusing in wet N_2 to produce the desired diffusion depth without introducing more Ga atoms. The following diffusion data illustrates this principle more clearly.

The data in Table III illustrate the control of single diffusion layers by changing the carrier gas composition during the heating operation. The diffusions were made with preoxidized 5 ohm-cm n-type Si for 1 hr at 1350°C with the Ga_2O_3 source at 950°C. The carrier gas composition during the heating operation was either wet H_2 or wet N_2 for the time intervals shown in column 1 of Table III. Both the H_2 and N_2 were bubbled through water at 30°C in these experiments.

With the exception of the first and last experiments in Table III, note the progressive decrease in sheet resistance and increase in surface concentration with increasing time in wet H_2. The layer thickness also tends to increase slightly with increasing heating time in wet H_2. An n-p-n type structure results from the experimental conditions shown in the first row of the table. The appearance of n-type surface layers in single carrier gas Ga diffusions also occurs with unoxidized Si samples when a high water content reducing gas or pure N_2, He, or A are used. In other words, an n-type surface layer is formed when the Ga surface concentration falls below a limiting value which depends upon the processing conditions. The n-type surface layer is believed to result from the presence of a small concentration of a donor impurity in the Ga_2O_3. This seems reasonable since the diffusion conditions, which are required for the appearance of these n-type layers, differ with the source of supply of the Ga_2O_3. The presence of a donor impurity has not been confirmed by spectrographic analysis since it is difficult to determine small concentrations of elements such as P, As, or Sb.

The last experiment in Table III is included to illustrate the flexibility of this procedure for device development. In this case a final short heating in wet H_2 produces a high surface concentration (about 10^{17} atoms/cc) on a previously established diffusion gradient. The high surface concentration facilitates ohmic electrical contact.

The data in Table III clearly demonstrate the effectiveness of wet H_2 and wet N_2 for controlling the introduction of Ga atoms into Si at high temperatures. The method is essentially a predeposition technique. However, unlike the one described previously (3), it requires only a single heating of the Si at one temperature for both the predeposition and diffusion.

A second method for controlling the introduction of Ga atoms into Si from a Ga_2O_3 source is illustrated by the H_2 and CO experiments in Table II. In these the diffusion characteristics are determined by the water content of the reducing carrier gas rather than the time interval of heating in wet H_2 followed by wet N_2. The diffusion layers may be varied further by changing the water content of the reducing carrier gas during the heating operation. In addition, the diffusion layers may be produced by a combination of the conditions shown in Tables II and III. Thus Ga diffusion layers can be controlled over wide limits by changing the carrier gas composition during a single heating operation.

A few experimental diffusions were made with In and In_2O_3 sources using wet H_2 or wet N_2 as the carrier gas. Conversion layers were obtained in wet H_2 but not in wet N_2. Except for fundamental differences such as vapor pressure, diffusion constant, and surface solubility in silicon, In and In_2O_3 sources can be employed to produce controlled diffusion layers by varying the carrier gas composition in the manner described for the Ga and Ga_2O_3 sources.

Table III. Diffusion control of Ga in Si by heating first in wet H_2 followed by wet N_2. Si, 1350°C; Ga_2O_3, 950°C; H_2O, 30°C

Time in min, H_2-N_2-H_2	Ohms per square	Layer thick., cm x 10^4	Surface concen., at./cc x 10^{16}
5—55—0	N	20*	—
10—50—0	566	22	7
20—40—0	221	23	19
30—30—0	192	24	23
60— 0—0	112	23	95
5—50—5	270	20	—

* P layer.

Table IV. Control of double diffusion layers by heating first in wet N_2 followed by wet H_2. Ga_2O_3, 900°C; H_2O, 30°C

Silicon temp, °C	Time in min N_2	H_2	Total	Layer thick., cm x 10^5 N	P	N + P
		Sb_2O_4, 900°C				
1300	30	90	120	51	130	181
1300	60	90	150	56	134	190
1300	150	90	240	71	114	185
1300	210	90	300	84	101	185
1300	330	90	420	97	81	178
		As_2O_3, 220°C				
1200	180	60	240	33	15	48
1200	120	120	240	36	46	82
1350	5	10	15	36	61	97
1350	9	6	15	38	33	71

Double Diffusion Layers

The design of electronic devices such as transistors requires double diffused layers of controlled thicknesses and doping concentrations in semiconductors. Such layers can be produced in a single heating operation by varying the carrier gas composition in controlled time intervals as illustrated by the data in Table IV.

The diffusions were made with unoxidized 5 ohm-cm n-type Si with the Ga_2O_3 source at 900°C and the carrier gases bubbled through water at 30°C. The other diffusion conditions are listed in the table. A new supply of each impurity was employed in each run. The Si samples were introduced into the furnace with the wet N_2 carrier gas flowing. The carrier gas was changed to wet H_2 after a time which was predetermined from single diffusion experiments. The heating was continued in wet H_2 until the desired double diffused layer thicknesses were obtained.

In the Sb_2O_4-Ga_2O_3 diffusion data in Table IV, the heating time in wet N_2 is increased progressively while the heating time in wet H_2 is held constant. Note the progressive increase in the n-type layer thickness with increasing heating time in the wet N_2. On the other hand the Ga diffusion layer (N+P) remains essentially constant or independent of the heating time in wet N_2. This is in agreement with the previous single diffusion data in which Sb but not Ga is introduced into Si in wet N_2. Thus the Sb diffusion depth is determined by the total heating time while the Ga diffusion depth is determined by the heating time in wet H_2. The double diffused layers result since Sb has a higher doping level and smaller diffusion constant than Ga.

In the As_2O_3-Ga_2O_3 diffusion data in Table IV, the total heating time was held constant for each temperature while the heating time in both wet N_2 and wet H_2 was varied. Note the large changes in the p-layer thicknesses and the small changes in the n-layer thicknesses for each diffusion temperature. The control again is based on Ga since As forms conversion layers in p-type Si in both wet N_2 and wet H_2.

The data in Table IV demonstrate the control of double diffused layers in a single heating operation by changing the carrier gas composition. However, a wide range of controlled double diffusion layers can be produced by further carrier gas composition changes. For example the n-layer doping level may be increased by reducing the water content in the N_2. The p-layer doping level may be decreased by increasing the water content of the H_2 or by completing the heating in wet N_2 after an interval in wet H_2. A large number of diffusion conditions obviously are possible to meet specific structural requirements.

In order to test the suitability of the single heating process for producing transistor structures, d-c alpha measurements were made on a number of double diffused silicon samples. The contacts were applied by essentially the same evaporation and alloying techniques described by Tanenbaum and Thomas (6). The d-c measurements were made on several approximately 5×10^{-2} cm diameter etched dots on one surface of each sample. About 90% of the d-c alpha values were 0.90-0.98 with about 50% above 0.95 at a collector voltage of 10 v and an emitter current of 5 ma. The d-c alpha values remained quite flat over an emitter current range of 0.1-15 ma.

It is possible also by this single heating process to produce controlled structures by the SiO_2 masking technique (3). For example, the Sb_2O_4 diffusions in Table IV would result in only a single p-layer if the Si was preoxidized for 1 hr at 1300°C in O_2. Thus controlled structures with double and single diffused layer patterns can be produced with preoxidized Si by first removing the SiO_2 from the regions which are to become double diffused layers.

Summary

A single heating process has been described for the production of controlled single and double diffusion layers in Si. The process is designed to meet a large range of design parameters for electronic devices.

Acknowledgment

The authors are indebted to M. Tanenbaum and C. D. Thurmond for their helpful suggestions during the preparation of this paper.

Manuscript received June 24, 1958. This paper was prepared for delivery before the New York Meeting, April 27-May 1, 1958.

Any discussion of this paper will appear in a Discussion Section to be published in the June 1959 JOURNAL.

REFERENCES

1. C. S. Fuller and J. A. Ditzenberger, *J. Appl. Phys.*, **25**, 1439 (1954).
2. C. S. Fuller and J. A. Ditzenberger, *ibid.*, **27**, 544 (1956).
3. C. J. Frosch and L. Derick, *This Journal*, **104**, 547 (1957).
4. C. J. Frosch and C. D. Thurmond, Unpublished data.
5. N. V. Sidgwick, "Chemical Elements and Their Compounds," Vol. 1, p. 789 (1950).
6. M. Tanenbaum and D. E. Thomas, *Bell System Tech. J.*, **34**, 105 (1955).

Diffusion into Silicon from Glassy Layers

J. E. Cline[1] and R. G. Seed[2]

Semiconductor Division, Sylvania Electric Products Inc., Woburn, Massachusetts

ABSTRACT

The diffusion of boron into silicon from glassy layers containing the system K_2O-SiO_2-B_2O_3 was investigated. These glassy layers can be formed by dehydrating aqueous solutions, and they are fluid at the diffusion temperature of 1200°C. Methods were explored for obtaining controllable initial concentrations and penetrations of diffusant. Uniformly flat junctions were obtained, apparently due to the solvent action of the glassy layers in preventing masking by silicon dioxide.

An important technique in the fabrication of semiconductor devices is the high-temperature diffusion of donor and acceptor impurities into single-crystal material. Diffusion is governed by the expression:

$$C_{(x,\,t)}=C_{(x=0,\,t)}\,erfc\left[\frac{x}{\sqrt{4Dt}}\right]=C_o\left[1-\frac{2}{\sqrt{\pi}}\int_0^{\frac{x}{\sqrt{4Dt}}}e^{-a^2}da\right]$$

The function, *erfc y*, is plotted semilogarithmically as the solid line in Fig. 1 (1, 2).

Reproducible and uniform impurity penetration, resulting in flat junctions, can be produced only from a uniform planar source concentration.

Frosch and Derick (3) found that under special conditions of carrier-gas composition surface layers of SiO_2 could reduce C_o by factors up to 200. Under the conditions ordinarily used in diffusion processes, it is difficult to avoid localized masking effects due to accidentally produced oxide layers.

This investigation of the effects of various glassy layers on the diffusion of boron into Si was undertaken to explore means of controlling C_o in both level and uniformity.

Precoating Procedure

The glassy layers were prepared by dehydration of aqueous solutions of silicates or borates of potassium. From the phase equilibrium diagram (4) of the binary system K_2O-SiO_2 it is apparent that a liquid phase can be maintained at temperatures above 1165°C if the SiO_2 concentration is below 78.8 wt %.

The following solutions were used: solution 1, potassium silicate solution, sp gr 1.25 (Sylvania Electric Products Inc.); solution 2, 10 g potassium tetraborate, $K_2B_4O_7 5H_2O$ (Fisher Scientific Co.), 3.5 g potassium hydroxide (Baker Analyzed), 15 g deionized water; solution 3, equal parts by weight of solutions 1 and 2.

It is calculated that these solutions form glassy layers, after dehydration, with the following mole ratios: solution 1, $K_2O:SiO_2$ = 1:3.44; solution 2, $K_2O:B_2O_3$ = 1:1; solution 3, $K_2O:SiO_2:B_2O_3$ = 1.37:1.25:1.

The n-type Si slices used in these experiments were oxidized by heating in air at 1200°C for 2 hr. After cooling they were each coated with one of the solutions. The coatings were then dried under a heat lamp.

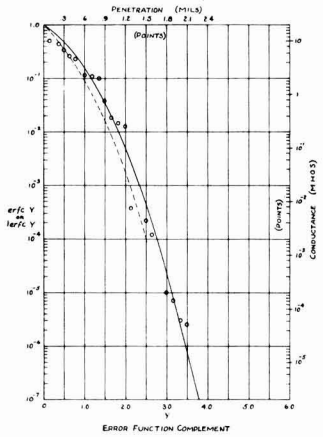

Fig. 1. The solid curve is a plot of erfc y vs. y and the dashed curve that of i erfc y vs. y. The points are experimental conductance values plotted against penetration for the 90-hr diffusion of silicon coated with solution 2.

Diffusion Experiments

The diffusion runs were carried out in a Kanthal-wound furnace with a high-temperature combustion tube (McDanel) open to the air. Two alundum boats were placed in the hot zone; one contained B_2O_3 and the other the Si slices. Diffusion temperatures were in the range 1165°-1190°C. The time of a run was generally 20 hr, although one run was made for 90 hr. It is not believed that appreciable diffusion of Al occurred due to the Al_2O_3 in the boats used in these experiments.

The penetration of diffusant was determined after each diffusion run by carefully lapping down the Si slices and by taking electrical measurements with a linear 4-point probe (5) at thickness steps of 0.1 mil. The point at which the glassy layer was considered to be removed by the lapping was determined by the sudden increase in conductivity. The resulting measure of the ratio of volts to amperes from the probe readings is a complicated function of the resistivity

[1] Present address: Raytheon Manufacturing Co., Semiconductor Division, Newton, Mass.
[2] Present address: 258 East St., Lexington, Mass.

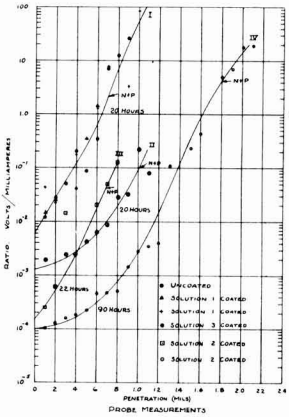

Fig. 2. Results of probe studies on 6 diffusion runs

of the material depending on how the resistivity varies with thickness in the layers below the probe. However, the ratio of amperes to volts is a direct measure of the conductance of the sample, in this case the sheet conductance. It can be shown easily that the conductance is directly proportional to the total number of carriers in the sample (sheet) which, in turn, is equal to the number of impurity atoms beneath the probe. The total number of diffused impurity atoms, N_T, which have penetrated beyond a depth y, is just

$$N_T = C_o \int_y^\infty erfc \frac{x}{\sqrt{4Dt}}\, dx = \left[\frac{1}{\sqrt{4Dt}}\, i\, erfc\, y\right] C_o$$

where i, the commonly used symbolic representation for integration of the error function complement, is itself not a closed expression. The values, normalized to one at $x = 0$, are plotted as the dashed curve in Fig. 1. It is seen that the difference between the error function and this integral is only slight.

The position of the p-n junction was determined by hot-probe measurements on the lapped slices and also by metallographic examination of sections of the slices.

Discussion of Results

The results of the probe studies on 6 diffusion runs are shown in Fig. 2 in which the volt-milliampere ratios are plotted against penetrations in mils. The penetrations at which the p-n junctions occurred, as determined by hot-probe measurements, are indicated by the symbol "n + p." Curve I fits the data for diffusion in uncoated Si and in two slices coated with solution 1. Curve II is for the slice coated with solution 3, and curve III for the slice coated with solution 2.

The main effect noted for the potassium silicate coating (solution 1) was to promote the formation of a flat junction as was observed by metallographic examination. Solution 3 led to an increase in C_o which was indicated by the decrease in volt-milliampere ratio at zero penetration. Solution 2 caused an even greater increase in C_o.

A 90-hr run with solution 3, curve IV, showed both a relatively high C_o and deep penetration of the diffusant. Using the same data, relative conductance was plotted against penetration in Fig. 1, the points being the experimental conductance values. The scales of ordinate and abscissa were normalized and adjusted to give the best fit to the theoretical curves. The value of $1.8 \cdot 10^{-12}$ cm^2/sec for the diffusion constant, D, was deduced from the data and agrees within experimental error of the temperature 1175°C with that reported by Fuller and Ditzenberger (6). The source-plane concentration, C_o was calculated by the method of differential conductances and found to be $4.8 \cdot 10^{20}$. It would be expected that a discontinuity in the slope of the curve of conductance vs. penetration would appear at the position of the p-n junction due to the contribution of the n-type impurity to the conductance. The fact that our data do not show such discontinuities may be attributed to lack of refinement of the probe technique. The agreement of the data in the region beyond the p-n junction with the theoretical curve is fortuitous.

The flat junctions observed under the glassy coatings are apparently due to the removal of masking by localized silicon dioxide layers by the solvent action of the glasses. Increasing the boron content of the glasses increases the value of C_o.

Acknowledgment

The authors are grateful to George Shaw for his contributions to the experimental work in this investigation.

Manuscript received May 20, 1958. This paper was prepared for delivery before the New York Meeting, April 27-May 1, 1958.

Any discussion of this paper will appear in a Discussion Section to be published in the June 1959 JOURNAL.

REFERENCES

1. "Tables of Probability Functions," Vol. 1. Federal Works Agency, Work Projects Administration. New York, 1941.
2. W. Jost, "Diffusion," p. 61, Academic Press, Inc., New York (1952).
3. C. J. Frosch and L. Derick, *This Journal*, **104**, 547 (1957).
4. F. C. Kracek, N. L. Bowen, and G. W. Morey, *J. Phys. Chem.*, **33**, 1857 (1929).
5. A. Uhlir, Jr., *Bell Syst. Tech. J.*, **34**, 105 (1955).
6. C. S. Fuller and J. A. Ditzenberger, *J. Appl. Phys.*, **27**, 544 (1956).

Diffusion Concentration Profiles by Analog Computation

Worden Waring[1]

Semiconductor Division, Raytheon Manufacturing Company, Newton, Massachusetts

ABSTRACT

Simulation of diffusion processes on an analog computer permits solutions to the diffusion equations under boundary conditions which make analytical solutions impractical. Effects on transistor structure are shown for "slumping" and "outdiffusion" of the first diffusant in a double diffusion. Diffusion from a liquid alloy dot through a regrown region is well represented by an analytical solution except for very thin regrown regions or very long diffusion times. Diffusion through two layers of material with different diffusion coefficients gives profiles which may deviate widely from the error function complement.

In order to study the various diffusion processes with semiconductor materials, an analog computer has been wired and programmed so as to simulate the actual diffusions in a one-dimensional geometry. This permits the solution of the diffusion equations under boundary conditions making an analytical solution impractical. It also permits making changes in conditions and following their effects readily. Unfortunately the analog computer can integrate with respect to only one variable, so an approximation must be used in solving the diffusion (or heat flow) equations. Also, its numerical results are limited to about 3 orders of magnitude.

The machine used is a Reeves Electronic Analog Computer (REAC), Model C400. Its behavior is directed by the wiring on a patchboard, which is varied somewhat for the different problems. Its output is obtained as a series of readings on a digital voltmeter and as curves drawn on graph paper. In the present work, integration is along the time axis and continuous curves with time may be obtained for concentration at a particular location. The variation of concentration in space is represented by concentration values at 12 equally spaced stations; curves drawn through these points are shown in the present figures.

A number of runs were made simulating simple diffusion in from a constant surface concentration. Results were tested against the error function complement, which is the correct theoretical solution (1, 2) and were found to be uniformly within about 1 percentage unit of the correct values for C/C_o, where C is the concentration as a function of distance (h) and time (t) and C_o is the constant surface concentration.

Double Diffusion

One of the first problems was a simulation of double diffusion: silicon is heated to an appropriate temperature, gallium is diffused in from the vapor, then the sample is placed for a shorter time in phosphorus vapor at the same temperature, which diffuses in and overdopes the gallium near the surface. To simulate this, a normal indiffusion was run on the machine; then the surface concentration was set at zero and the diffusion continued. During this second diffusion the first material, which is then initially distributed according to the error function complement, tends to "slump"; its concentration tends to level out. In addition, it escapes from the surface, or "outdiffuses." Outdiffusion from an initially uniform concentration has been discussed elsewhere (3-5). The present simulation gives the results of outdiffusion from a concentration distribution initially described by the error function complement.

Runs of varying lengths of time on the REAC, as shown in Fig. 1, show successive stages in the concentration profile as these processes go on. The parameter on the curves is the ratio of the time of second diffusion to the time of first diffusion. The figure shows how the concentration near the surface drops abruptly, but further in the bulk the concentration rises gradually.

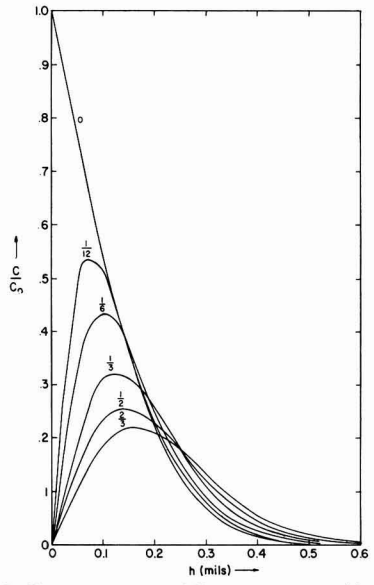

Fig. 1. Slumping and outdiffusion processes. Number on curves is ratio of second diffusion time to first.

[1] Present address: Fairchild Semiconductor Corp., Palo Alto, Calif.

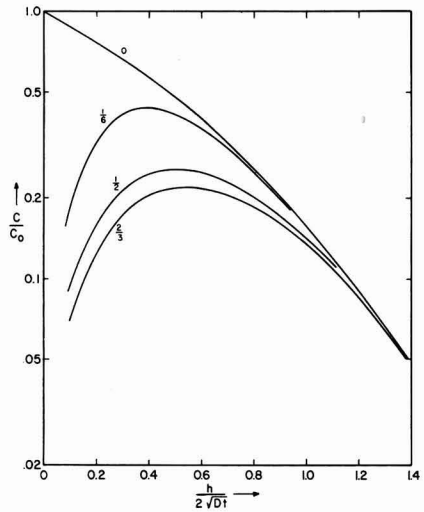

Fig. 2. Slumping and outdiffusion; reduced parameters. Number on curves is ratio of second diffusion time to first.

In order to make these results more generally useful, the concentration ratios are next plotted against a dimensionless abscissa, $h/2\sqrt{Dt}$. This would put all simple indiffusion processes on the same curve, the error function complement, which is the initial, or "0" curve in Fig. 1 and 2. In addition, in Fig. 2 a logarithmic scale is used for concentration. All the curves go down to zero (minus infinity) at zero abscissa value.

Two principal conclusions are that concentrations of the first diffusant near the surface may be considerably less than is predicted by assuming it is static during the second diffusion, and that a good approximation to concentrations of the first diffusant in the interior is to assume simple indiffusion occurs, but for the total time of both diffusions (see later).

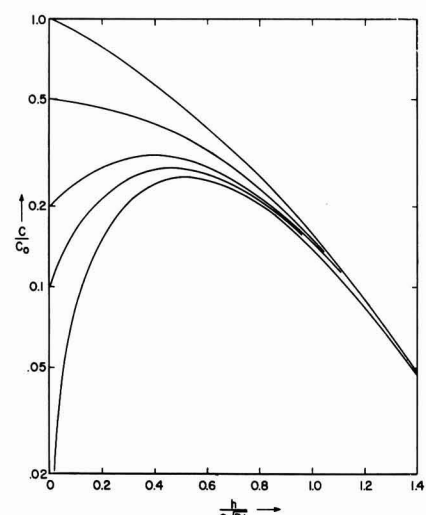

Fig. 3. Effect of surface concentration on slumping and outdiffusion.

However, the curves of Fig. 2 should be modified. It is unlikely that the surface concentration will be zero. In order to test the effects of various surface concentrations on the outdiffusion (and slumping) process, runs were made wherein the surface concentration was held constant at different values. Results are shown in Fig. 3. The second diffusion was just half the time of the first diffusion in all these runs. The bottom curve goes to zero at zero abscissa.

Rather limited data indicate that the surface concentration (in an atmosphere essentially devoid of the outdiffusing material) is several orders of magnitude less than the initial saturation value. Figure 3 shows that in such cases it should be perfectly satisfactory to assume zero surface concentration for practical outdiffusion problems.

Application to a Transistor

The results of simulated runs such as these were applied to a hypothetical device fabrication. Gallium was diffused into n-type silicon, followed by phosphorus (with a different diffusion coefficient) in a gallium-free atmosphere. Conversion of concentrations to resistivities gave the curves of Fig. 4. The dashed curves show the resistivity and type profiles if the gallium had been static during the phosphorus diffusion, that is, using the error function complement distribution for the time of gallium diffusion alone. The junctions would be just where the vertical dashes reach the upper boundary of the figure. The solid curves show the results when outdiffusion and slumping are included; for the gallium outdiffusion, its surface concentration was set at zero, as discussed above. The junctions are located now where the lines project above the upper boundary of the figure. The inner, collector junction is seen to have moved in about 0.12 mil; the outer, emitter junction has moved out very little, 0.014 mil; the base width has thus increased by about 0.13 mil. In addition, the resistivity in the base region has decreased decidedly, and its minimum has fallen from 0.11 ohm-cm to 0.045 ohm-cm.

If the gallium distribution were calculated on the basis of simple indiffusion with constant surface con-

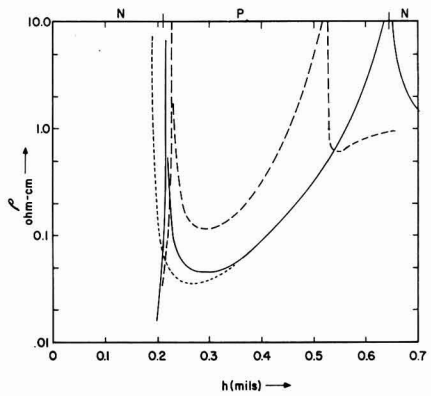

Fig. 4. Effect on device resistivity of slumping and outdiffusion. - - - - - no slumping and outdiffusion; ——— with slumping and outdiffusion; . . . . . base diffusion calculated for total time.

centration (error function complement) but for the total time of both diffusions, its distribution would be as shown by the dotted curve. This is an excellent fit for the inner junction, but introduces some error in the position of the outer, emitter junction. As mentioned before, this is a much better approximation than assuming the first diffusant is static during the second diffusion.

The effects of such changes in concentration profiles on the properties of transistors can be demonstrated readily.

Bulk Diffusion Process

A second type of problem was to obtain the concentration profile for a material which initially had a fixed concentration of impurity in a regrown region and zero concentration in the adjacent bulk material, when the impurity diffused from the regrown region into the bulk. Transistor structures of approximately this nature have been described by various authors (6-10). The diffusion processes are similar to those in the grown-diffused technique (11, 12). The analytical, exact solution is simple for the case where both regions are of infinite extent (1). But now a liquid alloy dot is placed on the regrown region and is assumed to maintain a constant surface concentration at a fixed distance (thickness of regrown region) from the inner boundary of the regrown region. Results for this situation are compared in Fig. 5 with the analytical solution for the doubly infinite case. Solid curves are smoothed from the REAC results, and dashed curves represent the doubly infinite solution. Curves 1 are for a short time of diffusion and curves 2 for a longer time. Arrows show the boundary of the regrown region.

It is clear that the doubly infinite solution is satisfactory for a short diffusion (or, what amounts to the same thing, a thick regrown region). For a long diffusion, however, the doubly infinite solution is in error. It must always pass through the value 0.50 at the boundary of the regrown region, so it becomes poorer as time goes on. This is another example where a major value of the machine solution is in establishing limits within which simpler analytical solutions are satisfactorily accurate.

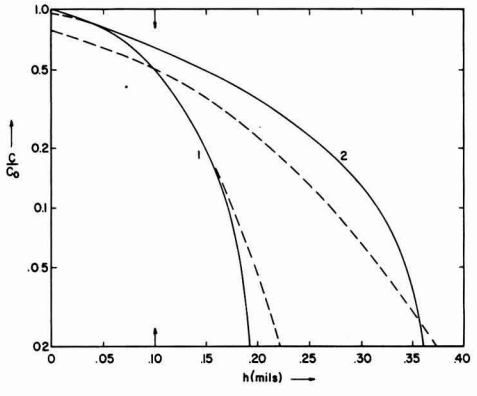

Fig. 5. Diffusion through a regrown region. Arrow shows boundary. ————calculated by REAC; - - - - - doubly infinite solution; 1 after short time; 2 after longer time.

The abrupt dropping off of the REAC results at large distances and especially at long times is an error. It occurs because the circuitry used forces the concentration curve to go through zero just beyond the last concentration value actually read. This error is easy to recognize, however, and can be corrected by greater sophistication in directing the machine behavior. The runs shown in Fig. 5 were from unusually long machine running times, which ordinarily are rejected.

A third type of problem concerns a two-layer system, wherein there is one value of the diffusion coefficient in one layer and a different value in the other. This is not quite an oxide layer representation, because the distribution coefficient at the interface is assumed to be unity, and because the differences in coefficient values are not extreme, but it might represent a disturbed layer on a semiconductor surface.

Figure 6 shows the results when the doping material diffuses faster in the outer layer and slower in the semiconductor bulk; the ratio is 5:1. The solid curves are for two particular times, with t_2 later than t_1. The dashed curve shows what the concentration profile would have been if diffusion had occurred in the inner layer for the same length of time but with a constant "surface" concentration in the interface equal to its value at time t_1. The ratio of concentrations (deviation from the actual) increases with distance. The concentration at any fixed point within the material moves upward and to the left with time, on this graph.

Figure 7 shows the results when the doping material diffuses only 0.1 as fast in the outer layer as in the bulk. Again the hypothetical profile is shown for the shorter time, to indicate how the increase with time of the boundary concentration causes a profile different from the error function complement. Again,

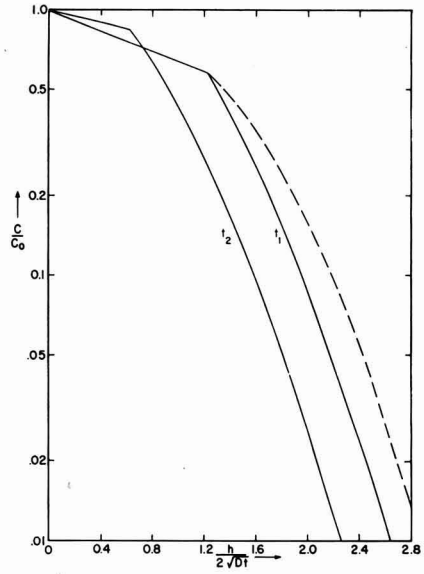

Fig. 6. Diffusion into bulk through layer with higher diffusion coefficient.

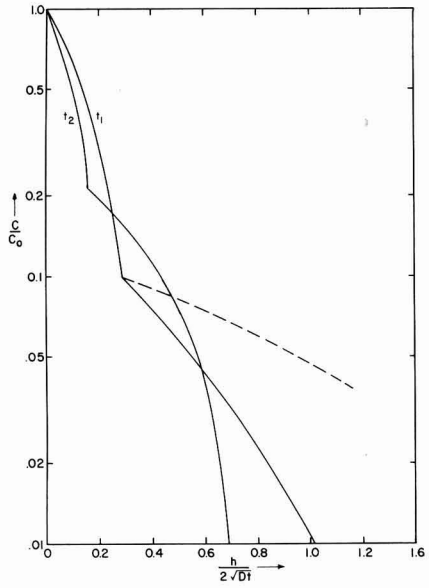

Fig. 7. Diffusion into bulk through layer with lower diffusion coefficient.

concentrations at particular locations move upward and to the left with time, on this graph. In Fig. 6 and 7 the break in each curve occurs where the diffusion coefficient changes value.

In addition to the problems discussed here, simulation of diffusion may be applied to cases where the diffusion coefficient varies with distance, as when one type of doping material is diffused through material with significant concentrations of the opposite type of dope. The diffusion coefficient may vary with time rather than with position. This will occur during the heating and cooling process involved in diffusion, and especially when slow cooling is utilized in order to maintain lifetime or resistivity of the material. Or the surface concentration may be a function of time, as when a two-temperature furnace is used and the doping material is slowly heated, or if the dope must diffuse along a rather long path in order to reach the semiconductor material.

In all such problems, a major advantage of the simulation technique is its flexibility: it is easy to represent a wide variety of diffusion conditions. It gives answers readily, when an exact analytical solution may be complex to solve or difficult to evaluate numerically. In addition to giving adequate solutions, it is also valuable in indicating limits within which simple analytical solutions are sufficiently accurate.

Acknowledgment

The author is indebted to Norman Nicol, supervising the REAC at Raytheon's Research Division, for assistance in setting up the general problem and for stimulating discussions with regard to this and other analog computations.

The work on this paper was supported in part by Signal Corps Contract No. DA36-039-sc-72710.

Manuscript received April 29, 1958. This paper was prepared for delivery before the New York Meeting, April 27-May 1, 1958.

Any discussion of this paper will appear in a Discussion Section to be published in the June 1959 JOURNAL.

REFERENCES

1. W. Jost, "Diffusion in Solids, Liquids, Gases," Academic Press, Inc., New York (1952).
2. H. S. Carslaw and J. C. Jaeger, "Conduction of Heat in Solids," Oxford University Press (1950).
3. K. Lehovec, K. Schoeni, and R. Zuleeg, *J. Appl. Phys.*, **28**, 420 (1957).
4. R. C. Miller and F. M. Smits, *Phys. Rev.*, **107**, 65 (1957).
5. J. Halpern and R. H. Rediker, *Proc. I.R.E.*, **46**, 1068 (1958).
6. C. E. Benjamin and R. L. Longini, I.R.E.-A.I.E.E. Semiconductor Device Research Conference, Philadelphia, June 20-22, 1955.
7. H. Statz, W. Leverton, and J. Spanos, I.R.E.-A.I.E.E. Semiconductor Device Research Conference, Philadelphia, June 20-22, 1955.
8. J. R. A. Beale, *Proc. Phys. Soc. (London)*, **B70**, 1087 (1957).
9. G. Freedman, *et al.*, I.R.E. National Convention, New York, March 24-27, 1958.
10. R. S. Schwartz and S. B. N. Slade, I.R.E. Electron Devices Meeting, Washington, D. C., Oct. 31-Nov. 1, 1957.
11. K. Lehovec and A. Levitas, *J. Appl. Phys.*, **28**, 106 (1957).
12. B.Cornelison and W. Adcock, Paper presented at WESCON; p. 22 Part 3 of Convention Record, August 1957.

A Sensitive Method for Measuring Optical Scattering in Silicon

G. H. Schwuttke, O. A. Weinreich, and P. H. Keck

Central Research Laboratories, Sylvania Electric Products, Inc., Bayside, New York

ABSTRACT

An instrument has been developed for the observation of optical scattering in silicon and in intermetallic compounds. It is considered as a supplementary tool suitable for studying crystal imperfections in conjunction with other optical methods. Scattering patterns of heat-treated, crucible-grown silicon crystals have been discussed as examples. The observations are in complete agreement with previously published results obtained by several other investigators on the clustering of oxygen in silicon caused by heat treatment.

Optical observations on silicon in the wavelength range greater than 1.1 μ, that is, in the region of its infrared transmission, have led to significant progress in the study of crystal perfection. In particular, the investigations of Dash (1) on birefringence in Si as observed in transmission between crossed polarizers have revealed many details such as strain patterns, growth rings, and multiple twinning. In his studies an infrared converter tube is used for visual observations. While this method is quite sensitive, it does not reveal certain types of imperfections, such as very finely dispersed precipitates caused by the presence of oxygen in Si crystals grown in quartz crucibles.

As Kaiser has shown, heat treatment of such crystals at 1000°C causes formation of SiO_2 clusters within the Si matrix, and these clusters in turn give rise to optical scattering (2). While Debye and Lederhandler (3) have reported measurements of the angular distribution of scattering, a sensitive arrangement for observing the intensity distribution of scattered light within the sample is of considerable interest in conjunction with other optical measurements such as 9-μ absorption (4) and the birefringence.

Experimental Arrangement

A sensitive instrument for observing the scattering must use a strong light source to provide a very intense illumination of the sample and at the same time the field of view must be kept as dark as possible when the scattering sample is not in place. This condition is always easy to fulfill if the sample is illuminated through a relatively small aperture and the observation path makes a large angle with the direction of illumination, as it is done in observing the Tyndall scattering, where this angle is usually 90°. In contrast to such an arrangement, we have chosen a large illumination aperture around a conical dark field zone and the integrated scattered light is observed from inside an umbra or shadow cone (5). Figure 1 shows the optical arrangement schematically. The integrating sphere Sph is illuminated by the light source S. This sphere has a small opening, O_2, in front and a larger one, O_1, on the opposite side, which is backed by a black cone, B. The holes O_1 and O_2 define an umbra or shadow cone into which no light originating from the sphere can penetrate. If a sample is put before O_2 it will be illuminated with an aperture of 180°. If scattering occurs, the scattered light will penetrate into the shadow cone, which means that the sample will brighten up according to the degree of scattering when viewed from within the shadow cone.

Figure 2 shows schematically the complete arrangement of the instrument for the study of scattering in Si. This instrument actually consists of a water-cooled integrating sphere Sph of 10 cm diameter which is illuminated by a 200-w projection lamp. The inner wall of the sphere is gold plated, since gold has a high reflectivity in the infrared region. The two aligned holes O_1 and O_2 have a diameter of 60 mm and 8 mm, respectively. The black body B is a cone of 70 cm length; it is covered on

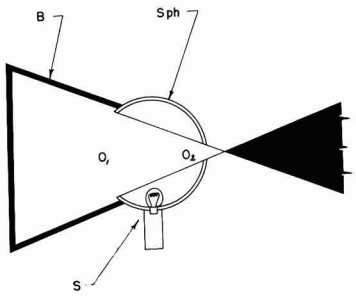

Fig. 1. Optical principle of scattering arrangement

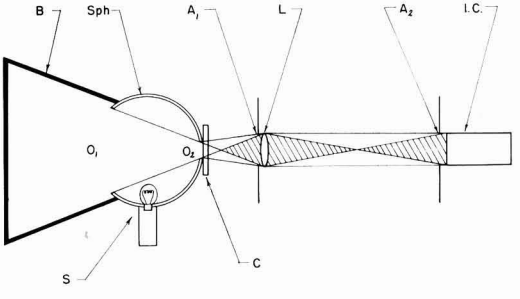

Fig. 2. Scattering meter schematically

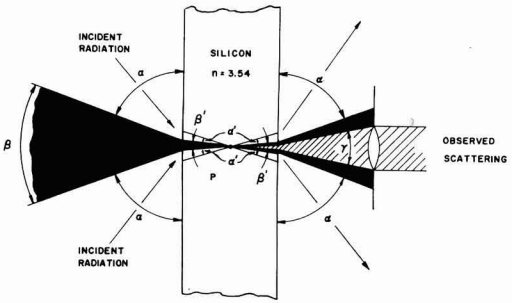

Fig. 3. Optical path in silicon samples

the inside with black velvet. The two holes in the sphere define an umbra, as explained in Fig. 1, which provides a suitable dark field for a sensitive detection of any scattering in the Si sample, which is placed in front of hole O_2. The sample is scanned by moving it across the hole on a microscope stage. The specimens with thickness ranging from a fraction of a millimeter to several millimeters have to have two well-polished planar faces; scratches or dust particles will show up in the scattering picture. The objective L forms a magnified image of the sample on the face of the infrared image converter tube I. C. For a sensitive observation of the scattered light from the sample, it is important that both the objective L and the image converter tube I. C. be located completely within the shadow cone. Light diffraction causes the edge of the front opening of the sphere to appear as a bright ring in the plane of the sample image. This bright ring has to be cut off by a suitable diaphragm A_2 in front of the image converter tube in order to keep the field of view as dark as possible. As a consequence of the dark emission of the image converter cathode, the field of view at room temperature was not very dark.

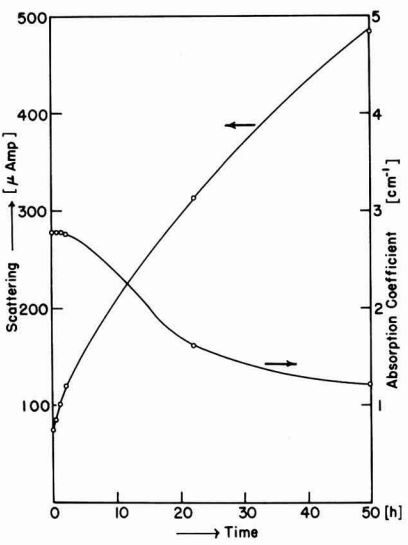

Fig. 4. Scattered intensity and 9-μ absorption vs. heat-treatment time at 1000°C for silicon (n-type, 95 ohm-cm, crucible pulled in [111] direction).

Cooling of the tube resulted in a background close to the visual threshold. For this purpose dry air cooled by liquid nitrogen was blown from a ring-shaped mouthpiece against the front window of the converter tube. For many observations it was not necessary to use cooling.

Since the refractive index of Si is relatively high, the aperture of the cone of illumination and of the cone of the observed scattering are strongly reduced within the sample in comparison to their corresponding values in air; this relation is schematically represented in Fig. 3. We are using a refractive index value of 3.54 for Si at 1.2 μ as published by Salzberg and Villa (6). For this refractive index the aperture of 180° provided by the integrating sphere shrinks to a value of 33°, or, in other words, the illuminating sphere as seen from a scattering particle P inside the Si would appear under an aperture of 33°. Similarly, the black body which appears from the front hole in the sphere under 30° is seen from P under the reduced aperture of 8° 22″. In order to preserve the dark-field arrangement the effective angle under which the scattered light is observed must be smaller than the dark cone. We have used effective observation apertures between 3° and 8°, which corresponds to 10° to 28° apertures in air. It is quite apparent that in our arrangement, due to the high refractive index of Si, essentially forward scattering within ±15° is observed.

Results

Let us discuss some results obtained on Si single crystals. First, it should be emphasized that the described instrument serves best as a supplementary tool in conjunction with the observation of birefringence in transmission and of surface structure in reflected light. Any surface structure of Si samples shows up strongly as scattering and, in order to avoid erroneous results, the samples must be highly polished and their surface quality checked in reflected light. Twinning, lineage, and strain pattern were found to cause very little scattering and therefore are shown up more sensitively in transmission between crossed polarizers than in the scattering instrument. On the other hand, clustering of oxygen in Si caused by heat treatment of crucible-grown crystals at 1000°C produces strong effects that can readily be observed in the scattering instrument.

In Fig. 4 the intensity of scattered light in relative units is plotted against the time of heat treatment at 1000°C for adjacent slices cut from a Si crystal n-type with 95 ohm-cm resistivity. The intensity was measured with a photomultiplier tube facing the image converter tube. The background intensity as mainly caused by the image converter tube was in this case about 40 μa. Samples before heat treatment gave readings between 50 and 70 μa Also plotted is the 9-μ absorption of the samples vs. heat treatment time. The absorption coefficient before heat treatment was 2.76 cm^{-1}. This corresponds to an initial oxygen concentration of 4.5 x 10^{17} O/cc [*see* Fig. 1 in (4)]. While the decay in the 9-μ absorption takes place gradually as observed previously (2, 7), the scattered intensity increases

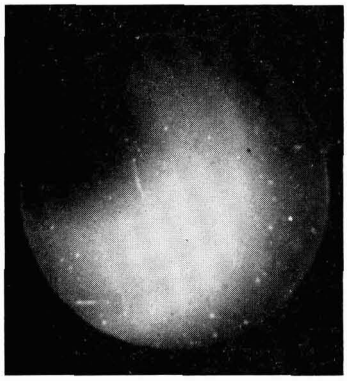

Fig. 5. Scattering pattern of silicon crystal with uniform oxygen content but with large differences in dislocation densities. The crystal was grown in the [111] direction and cut perpendicular to the growth axis. (After 130 hr of heat treatment at 1000°C, magnification 6½ times after reduction for publication.)

steeply, and after 1-2 hr of heat treatment a distinct increase in scattering is evident, while the change in the 9-μ absorption is still very small. The intensity of scattering after a certain heat-treatment period depends on the original concentration of oxygen and, of course, on the concentration of centers that serve to form the nucleus of oxygen cluster. Lederhandler and Patel (7) have shown that the decrease of the 9-μ absorption with heat-treatment time is strongly dependent on the density of dislocations, which apparently serve as nucleation centers for the precipitation of oxygen and for which further evidence was published recently (8, 9). From these results it is concluded that the intensity distribution of scattering after a short heat treatment at 1000°C is a sensitive indication of the original distribution of oxygen concentration and of the distribution of the concentration of the nucleation centers. Since the 9-μ absorption of the crystal before heat treatment provides a good measure for the oxygen concentration, the scattering pattern can be analyzed for the distribution of the nucleation center concentration. Figure 5 gives an example of a scattering pattern in a Si crystal. Before heat treatment this crystal displayed a fairly constant 9-μ absorption, which indicated that the original oxygen concentration over the region shown was uniform within 10%. In the bright area in the picture, high dislocation densities were found by etching. There precipitation of oxygen produced strong scattering, which is in general agreement with the findings of Lederhandler and Patel (7) that dislocations offer favorable sites for the clustering of oxygen.

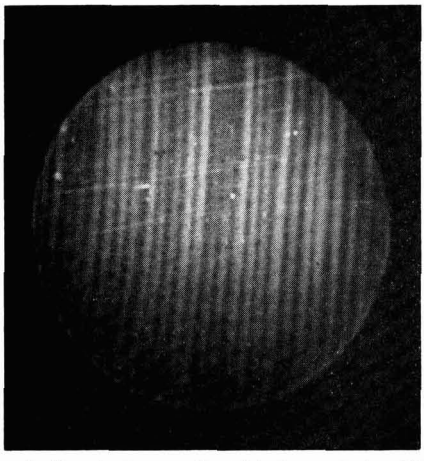

Fig. 6. Growth rings made visible by scattering. The rotated silicon crystal, p-type 130 ohm-cm, was cut parallel to growth direction [111]. (Heat treated at 1000°C for 100 hr, distance between growth rings 0.27 mm, magnification 8 times after reduction for publication.)

Growth rings can be made visible by scattering, as Kaiser (2) has already shown. Figure 6 is a scattering picture of a rotated Si crystal cut parallel to the growth direction and heat treated at 1000°C for 100 hr. The crystal was grown in the [111] direction and the sample was p-type 130 ohm-cm before heat treatment. A very distinct pattern of stripes has developed which checks with the growth rings. The picture is similar to birefringence stripes which Dash (1) has shown on rotated Si crystals to be due to small periodic temperature fluctuations during the crystal growth. Since even very small temperature fluctuations cause appreciable changes in the oxygen concentration, it is quite understandable that a distinct stripe pattern results in the scattering instrument. Heat treatment of 2-4 hr at 1000°C is sufficient to make the stripes clearly visible. Longer heat treatment was applied to the sample shown in Fig. 6 in order to produce a high contrast for reproduction purposes. No birefringence stripes were detected on this particular crystal in transmission between crossed polarizers before heat treatment; after heat treatment there was only a very faint indication of stripes. This proves that in this case the observation with scattered light is more sensitive than the observation of birefringence. In Fig. 7 the same crystal as shown in the previous figure is pictured in the lower half. In the upper half an adjacent slice of the crystal is shown that was gold plated (10) to bring out resistivity changes and junctions but was not heat treated. A close inspection indicates a good match of the two stripe patterns as is to be expected from the knowledge of the donor formation in Si (2, 9) caused by oxygen impurity at temperatures below 500°C. During the normal cooling of the sample, apparently a sufficient donor formation took place to bring out the stripe pattern after plating. This was confirmed by a second plating experiment after half-hour treatment of the sample at 450°C. The stripe pattern was essentially the same before and after this treatment.

The application of the described scattering instrument is not limited to Si, but can as well be used for other crystals which have a suitable transparency range. For instance, we have made some preliminary observations on GaAs and InP crystals that showed appreciable scattering with the appearance of a grainy structure, the understanding of which will require more detailed studies. Intermetallic compounds with a band gap larger than that

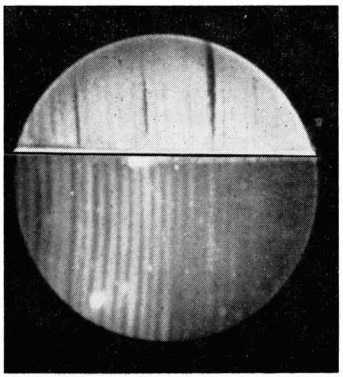

Fig. 7. Match of growth rings (same sample as Fig. 6) with junction delineation by gold plating. (Distance between growth rings 0.27 mm, magnification 6½ times after reduction for publication.)

of Si give a strongly increased sensitivity because the image-converter tube used for the observation of scattering has its maximum sensitivity at 0.8 μ, while in the case of Si the tube is used only near the long wave-length limit of its sensitivity. It appears to be of interest to continue the investigation of scattering in intermetallic compounds, but it should be remembered that it is not easy with some of the materials to prepare plane, highly polished surfaces as required for the measurements.

Acknowledgment

It is a pleasure to acknowledge the able assistance of P. Riggio and F. Wrzesc in building the instrument and of L. Letendre and Mrs. O. Kielbasa in preparing the samples.

The research reported in this paper was sponsored by the Electronics Research Directorate of the Air Force Cambridge Research Center, Air Force and Development Command, under Contract AF19-(604)-3482

Manuscript received May 26, 1958. This paper was prepared for delivery before the New York Meeting, April 27-May 1, 1958.

Any discussion of this paper will appear in a Discussion Section to be published in the June 1959 JOURNAL.

REFERENCES

1. W. C. Dash, *Phys. Rev.*, **98**, 1536 (A) (1955).
2. W. Kaiser, *ibid.*, **105**, 1751 (1957).
3. P. P. Debye and S. Lederhandler, *Bul. Amer. Phys. Soc. Ser. II*, **2**, 66 (1957).
4. W. Kaiser and P. H. Keck, *J. Appl. Phys.*, **28**, 882 (1957).
5. P. H. Keck, *Optik*, **1**, 169 (1946).
6. C. D. Salzberg and J. J. Villa, *J. Opt. Soc. Amer.*, **47**, 244 (1957).
7. S. Lederhandler and J. R. Patel, *Phys. Rev.*, **108**, 239 (1957).
8. R. A. Logan and A. J. Peters, *J. Appl. Phys.*, **28**, 1419 (1957).
9. C. S. Fuller and R. Logan, *ibid.*, **28**, 1427 (1957).
10. S. J. Silverman and D. R. Benn, *This Journal*, **105**, 170 (1958).

Effects of Certain Chemical Treatments and Ambient Atmospheres on Surface Properties of Silicon

T. M. Buck and F. S. McKim

Bell Telephone Laboratories, Incorporated, Murray Hill, New Jersey

ABSTRACT

Measurements of surface conductance, recombination velocity (S), and field effect were made on n- and p-type silicon specimens with certain surface treatments and ambient atmospheres. The conditions covered a wide range in surface potential (0.7 ev) and recombination velocity (40–10^4 cm/sec). Low recombination velocity occurred when the surface was strongly p-type, after treatments in boiling deionized water or sodium dichromate solution, or when the surface was strongly n-type, after treatment in concentrated hydrofluoric acid. Atmospheres which bend the energy bands back toward the middle from these extreme conditions caused S to increase. Curves of S vs. band position at the surface for the various treatments appear to be branches of the type of curve predicted by theory for recombination centers at a discrete energy level. The position of the Fermi level at the surface for a given treatment apparently depended to a small extent on whether the bulk material was n- or p-type. This apparent difference, which is contrary to experience on germanium, may have been caused in part by poor contact between an inversion layer and the bulk material.

Among various types of surface studies on semiconductors in recent years the dependence of surface recombination velocity (S) on surface potential has been used to gain considerable information on the energies, densities, and capture cross sections of surface states, particularly on Ge (1-6). On Si such studies have been hampered by the difficulty in obtaining low S; in fact, only a few treatments have been reported for producing low S on Si (7, 8).

In the present work, three of these low S treatments were studied along with a common etch which does not produce low S. Field-effect and sur-

face conductivity measurements showed that the low S treatments produce rather large shifts in surface potential. [Moore and Nelson (7) had already reported that the dichromate treatment makes the surface p-type.] Smaller shifts were produced by atmosphere cycling of a modified Brattain-Bardeen type in which dry oxygen, wet nitrogen, and, in one case, dry nitrogen were used. The combination of chemical treatments and atmosphere cycling permitted exploration of a large range in surface potential and recombination velocity.

Details of Chemical Treatments

The treatments studied will be identified as (*a*) dichromate (7), (*b*) boiling deionized water (8), and (*c*) HF soak (8). These three can produce low S on both n- and p-type material. A fourth treatment, (*d*) HNO_3:HF, was included for comparison with the others.

Dichromate treatment.—The specimen was soaked in 1% sodium dichromate solution for a few minutes after a preliminary etch in 10/1 HNO_3-HF and a light rinse in deionized water. The dichromate solution usually has been allowed to dry on the surface. The effect is enhanced sometimes by warming the solution to 80°-90°C. Light rinsing in deionized water after this does not seem to destroy the effect. Dry oxygen is a good atmosphere for preserving the effects on surface conductivity and S after this treatment.

Boiling deionized water treatment.—The specimen was immersed in boiling, deionized water for 30 min or longer, after preliminary etching and rinsing. After boiling, the specimen was dried by evaporation or by drawing off excess water with filter paper. It was then quickly placed in a dry oxygen atmosphere.

Conductivity of the water has usually been 0.1 μmho cm^{-1} from the deionizing column and 0.5-0.6 μmho-cm^{-1} after boiling, with most of the increase probably coming from sources other than the specimen. The details of this treatment are rather critical in obtaining low S, e.g., the water must be quite pure, it must be hot, and mere heating in air or oxygen or immersion in a number of other liquids, mostly organic, at about 100°C do not produce low S.

HF *treatment.*—The specimen was soaked in concentrated (48%) HF for 5 min, after a preliminary etch in 10/1 HNO_3:HF. It was then rinsed for about 5 sec in running, deionized water. The most pronounced effect on surface conductivity and S was preserved by quickly placing the specimen in dry nitrogen (within 10-15 sec); helium, argon, etc., would probably do as well, but oxygen should be excluded, as it tends to destroy the effect.

10/1 HNO_3:HF *etch followed by rinse in cold deionized water.*—This is a commonly used etch which removes Si at a moderately slow rate (≈0.6 mil/min) leaving a bright smooth surface. In addition to being one of the treatments under study, this etch was used in preparing the surface for the other treatments, although the effects of the other treatments do not seem to depend critically on the nature of the preliminary etch.

Surface Conductivity

The surface conductivity of a semiconductor is a unique function of the surface potential or surface barrier height for a given bulk resistivity. Since this function has been calculated (9-11), surface conductivity may be used to determine surface potential. The data of Kingston and Neustadter (9), which are convenient for the extrapolation necessary with Si, were used to construct curves of $\Delta\sigma_s$ vs. U_s where σ_s is the surface conductivity and $U_s = (E_F - E_i)/kT$ at the surface. U_B is the corresponding quantity in the interior, E_F is the Fermi level, and E_i the value of E_F in intrinsic material, or approximately the middle of the energy gap. No correction was made for reduced mobility near the surface, of the type calculated by Schrieffer (11); the correction is small for Ge and would be even smaller for Si because of the longer Debye length.

The specimens were thin slabs, about 0.040 cm thick, with high bulk resistivity and high volume lifetime (about 1000 μsec). Resistance was measured on a General Radio Bridge, Type 650-Pl. Temperature was controlled satisfactorily by means of a constant temperature bath at 28°C. Contacts were bonded to the ends of the specimens, gold wire for n-type material and aluminum for p-type, after first plating a small area with gold or aluminum. These contacts were found to have no significant resistance compared to the total resistance of the specimens.

The change in surface conductance, per square, was computed from

$$\Delta\sigma_s = (R_F^{-1} - R_{Max}^{-1})\frac{L}{P} + \Delta\sigma_{T.M.} \qquad [1]$$

where R_F is measured resistance; R_{Max} the maximum which could be observed in certain situations; L the distance between contacts; P the cross-sectional perimeter of the slab; and $\Delta\sigma_{T.M.}$ the minimum value (negative) on the theoretical curve of $\Delta\sigma_s$ vs. U_s.

It was necessary to determine experimentally (during cycling) the minimum in conductance in order to place other points on the curve. Points were placed on the n- or p-side of the minimum on the basis of the assumption that dry oxygen causes a p-type shift while water vapor causes an n-type shift, so that when R_F decreases in dry oxygen or increases in wet nitrogen the surface must be on the p-side of the minimum in surface conductivity. The opposite behavior would indicate the n-side. This assumption was based on the results of separate field-effect measurements on these types of surfaces and it is in accord with the general experience of others with etched Si and Ge surfaces.

Surface Conductivity Results

N-type silicon.—In Fig. 1 the ranges of surface conductivity covered during four or five cycles of alternate exposure to dry oxygen and wet nitrogen (43% R.H.) are indicated for the four different treatments. Exposures to the atmospheres were for 10 min to several hours depending on the time required for conductance to stop changing. Changes were usually more rapid in wet nitrogen than in dry

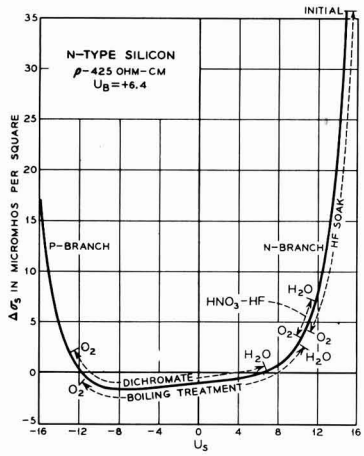

Fig. 1. N-type Si. Ranges of surface conductivity and U_s for four different treatments in atmosphere cycling. Dry oxygen and wet nitrogen extremes are indicated by O_2 and H_2O.

oxygen. The extremes of conductivity reached in these atmospheres are indicated by O_2 or H_2O in the figures.

The behavior after the 10/1 HNO_3:HF etch was erratic at first but after several cycles R_F consistently increased in dry O_2 and decreased in wet N_2 producing the rather small range indicated on the curve, slightly on the n-side of the straight band position which is at $U_s = U_B$, $\Delta\sigma_s = 0$.

With the other treatments the bands could be bent well away from this position in both directions. The HF treatment had a strong n-type effect. Initially (in dry nitrogen) surface conductivity was over 35 μmhos per square; the specimen resistance dropped from about 70,000 to 35,000 ohms. The condition held for about 2 hr in dry nitrogen after which atmosphere cycling was started. During cycling $\Delta\sigma_s$ decreased in dry oxygen and increased in wet nitrogen, but these oscillations were superimposed on a steady downward trend in surface conductivity so that eventually after much cycling $\Delta\sigma_s$ was at the lower extreme of the range in dry O_2 and would not move up very far in wet nitrogen. This irreversible downward trend is probably associated with the growth of an oxide film which has been studied by Archer (12) using ellipsometry, after an HF soak. Similar behavior has been studied on Ge by Kikuchi (13), although S did not behave in the manner which will be described for Si.

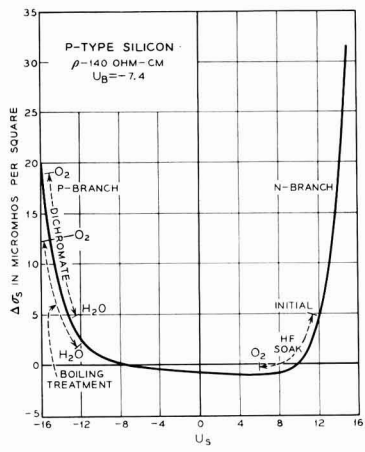

Fig. 2. P-type Si. Ranges of surface conductivity and U_s for three different treatments in atmosphere cycling. Dry oxygen and wet nitrogen extremes are indicated by O_2 and H_2O.

The other two treatments allowed the surface to swing over to the p-side, the dichromate treatment producing a somewhat stronger shift than the boiling treatment. In atmosphere cycling surface conductivity traversed the ranges indicated quite reversibly, going through the minimum.

P-type silicon.—On a p-type specimen (Fig. 2) the treatments produced shifts in the same direction but of somewhat different magnitude. The boiling and dichromate treatments produced larger values of $\Delta\sigma_s$ and $|U_s|$ than they did on the n-type specimen while the n-type treatment (HF) produced smaller values.

On Ge, Brattain and Garrett (4) found U_s the same on n- or p-type material for a given treatment; the surface states determined the position of the Fermi level at the surface regardless of the bulk resistivity or majority carrier type. In the present case, with Si, the differences are not very large but they did seem real and reproducible. Poor contact between an inversion layer and the bulk material could cause an effect in this direction; the inversion layer would not make its full contribution to the change in conductance and this would cause an underestimate of $|U_s|$, e.g., at the O_2 extremes for the dichromate and boiling treatments in Fig. 1. However, it does not seem that this could account entirely for the differences between the wet extremes for these same treatments on the two types of material.

Whatever the explanation of the differences in magnitude, the shifts are in the same direction on both n- and p-type material. The chemical treatments had the predominant influence in determining surface potential while the atmospheres had a secondary modulating influence. Both the chemical treatment and the ambient atmosphere are obviously important in establishing the surface potential.

The mechanisms by which these treatments cause these effects are not clear. The well-known p-type effect of oxygen (and also ozone and chlorine) has been ascribed to its high electron affinity by which it acts as an acceptor (14). Dichromate, being a strong oxidizing agent, also might be expected to provide acceptor levels. Moore and Nelson (7) proposed an electrochemical mechanism. The familiar n-type effect of water vapor is less susceptible to qualitative explanation and the same may be said for the HF soak. One wonders why the surface is so strongly n-type when it is stripped of oxide and has some HF absorbed on it, and why oxide film growth causes it to go back in the p-direction. The p-type effect of the boiling treatment may be due

to cleaning of the surface which allows oxygen to be more effective in producing its normal p-type shift.

Surface Recombination

All the values of S to be reported were computed from filament lifetimes determined by the photoconductivity-decay method (15). A simplified equation (16) was used to compute S from filament lifetime for these specimens with thickness considerably smaller than width. The specimens were cut from crystals which had high volume lifetime and were relatively free of non-recombining traps. In some cases, however, especially when low S was obtained together with a strong inversion layer, "tails" were observed in the photoconductivity decay curves, somewhat similar to those described by Haynes and Hornbeck for volume traps (15). This effect, when observed, was eliminated by very weak d-c light. Since it was usually, if not exclusively, associated with a strong inversion layer condition it may have been caused by surface photovoltage. All values of S were determined from good exponential decay curves, usually with no ambient light but sometimes with weak d-c light when necessary to get a good exponential. The low S values produced by the three special treatments, on both n- and p-type material, were confirmed, at least qualitatively and in some cases quantitatively, by the PME method (17).

It has been mentioned that the success of the low S treatments depends on keeping the specimen in the proper atmosphere. A prominent feature of the behavior is that the direction in which S changes in an atmosphere depends on the previous treatment.

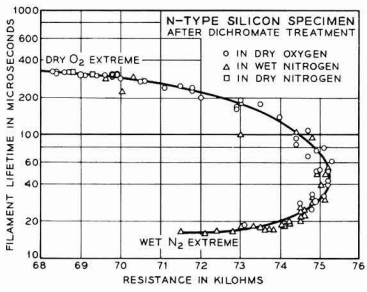

Fig. 3. Filament lifetime vs. resistance during atmosphere cycling after dichromate treatment. N-type Si, $\rho \approx 425$ ohm-cm., $\tau_B \approx 1000$ μsec. Dimensions of slab: 0.040 x 0.270 x 1.75 cm.

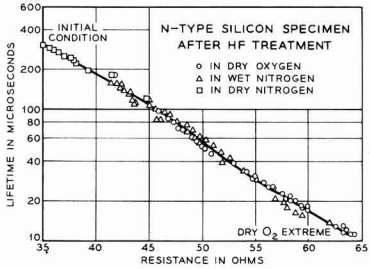

Fig. 4 Filament lifetime vs. resistance during atmosphere cycling after HF soak. N-type silicon, $\rho \approx 425$ ohm cm., $\tau_B \approx 1000$ μ sec. Dimensions of slab: 0.040 x 0.270 x 1.75 cm.

After the boiling and dichromate treatments, dry O_2 favors low S while water vapor causes S to increase drastically. The opposite is true after the HF and HNO_3:HF treatments.

In order to obtain S as a function of U_s, filament lifetime measurements were made during cycling along with the surface conductivity measurements discussed above. The raw data for two such experiments are shown in Fig. 3 and 4 for the dichromate and HF treatments. After the dichromate treatment and with dry O_2 ambient the lifetime was high and resistance rather low. Exposure to wet nitrogen caused the values to traverse the curve in the clockwise direction down to the wet N_2 extreme. Dry oxygen brought them back again counterclockwise. Cycling after the HF treatment caused an oscillating shift toward higher resistance and lower lifetime. In both these cases there was very little scattering; S was a well-behaved function of surface conductivity or surface potential. This was true also for the HNO_3-HF etch after an initial period of instability and erratic behavior. The behavior in these three cases strongly suggested that the atmospheres did not change the recombination states but merely shifted surface potential. After the boiling treatment there was some scattering and hysteresis throughout the cycling but not enough to prevent the drawing of a fairly reasonable smooth curve of lifetime vs. resistance.

Figure 5 shows the cycling data converted to S and U_s values. Low recombination velocity occurs when the surface is strongly n-type or strongly p-type and atmospheres which tend to bend the energy bands back toward the middle from these extreme conditions cause S to increase. The behavior explains why low S is not obtained with most common etches which probably leave the surface in the middle region as does the HNO_3:HF etch. However, it does not follow that any treatment which produces as large a shift in U_s will also produce low S since another treatment might cause recombination states to change in energy or density, or both. An example of this has been observed with an etch in hot sodium hydroxide[1] which caused an n-type shift even stronger than the HF treatment but did not produce very low S. A few measurements indicated that in this case the S vs. U_s curve was displaced to the right of the HF curve in Fig. 5.

Since the data of Fig. 5 represent four different chemical treatments it may be too optimistic to try to analyze the data for energies and capture cross sections of recombination centers, but an attempt has been made. For the case where S varies only because of variation in surface potential without any change in the recombination centers, and where the recombination states are at one discrete energy level, current theories (3, 4) predict curves of the type given by the dashed curves of Fig. 5. Another possibility would be a curve with a broad flat top leading to two possible values of the energy level. More than one of these curves might be observed over a large range of surface potential, representing more than one set of recombination states.

[1] Suggested by I. L. Kalnins.

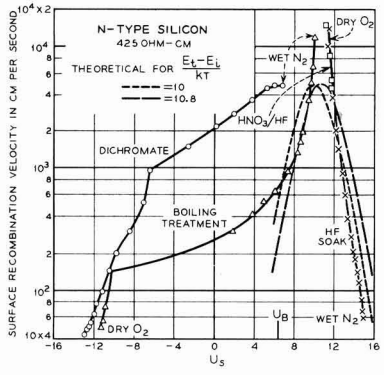

Fig. 5. Surface recombination velocity vs. U_s for four different treatments, with atmosphere cycling. N-type Si. O dichromate treatment; △ boiling treatment; X HF soak; □ HNO_3/HF etch.

Many, et al. (3, 5) have found curves of this type in experiments on Ge in which surface potential was varied by a transverse electric field.

In the present case for Si, the data obviously do not fall on one universal curve. The chemical treatments undoubtedly do change the recombination states to some extent; for example, the density of states was apparently higher for the dichromate treatment than for the boiling treatment. However it is interesting to speculate that the HF and boiling treatment data may form two branches of the same curve and to compare them with the theoretical curves (dashed) which have been sketched in. The curve on the left is for a recombination center 0.26 ev above the middle of the energy gap with a capture cross-section ratio $\sigma_p/\sigma_n \approx 5 \times 10^8$. This is, of course, an unusually high ratio and must be regarded with suspicion in view of the piecing together of data for different treatments which was necessary to cover the range. However, the HF curve, in particular, definitely has the proper slope for one branch of the type of curve predicted by theory for a discrete trap energy and, if the whole range of U_s could have been covered without changing treatments, the data might be analyzed in more detail by current theories.

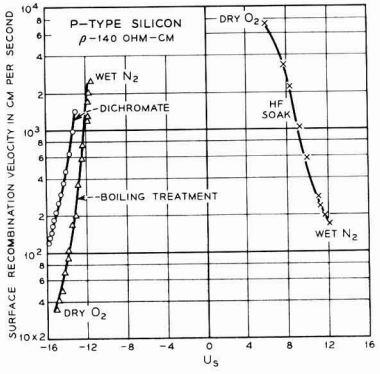

Fig. 6. Surface recombination velocity vs. U_s for three different treatments, with atmosphere cycling. P-type Si.

The data for the p-type specimen, Fig. 6, again show recombination velocity low at the p- or n-type extremes and high in the middle region. And again the curves resemble outside branches of the theoretical type of curve, with S falling off by $\frac{1}{e}$ in one unit (kT) of U_s.

Field Effect

The field effect measurements are not discussed in detail. In relation to the foregoing material their chief value was that they gave qualitative indications of the n- or p-type character of the surface, as influenced by chemical treatment and atmosphere, which permitted a choice of the proper branch of the conductance curve in the d-c measurements.

The method used was that of Aigrain (18) which has been developed and used extensively by Montgomery (19) in studies of time constants of surface states on Ge. A theoretical treatment of high-frequency field-effect phenomena has been given by Garrett (20).

Field-effect mobility ($\mu_{F.E.}$) was determined as a function of frequency of the applied field, over a range of 50 cycles/sec to 60 kc/sec. The interpretation was clear in the case of a strong n-type surface on n-material or a strong p-type surface on p-material. In these cases field-effect mobility was negative or positive, respectively, and was constant over the frequency range. This is the type of behavior Montgomery found with Ge.

But anomalies occurred when strong inversion layers were evidently present. Montgomery found that with inversion layers on Ge, $\mu_{F.E.}$ had positive values at low frequency for p-type inversion layers (or negative for n-type inversion layers) and then changed in one sweep to a value having the sign of the majority carrier and considerably larger than bulk mobility; the change of sign, which occurred with an inflection at $1/(2\pi\tau_f)$ was attributed to failure of regeneration processes to keep up with the alternating field. (τ_f is the filament lifetime.) In inversion layer situations on Si the behavior was similar in that $\mu_{F.E.}$ changed sign in the same directions, but the inflection frequency was not generally equal to $1/(2\pi\tau_f)$ and there were rather sharp minima or maxima in the curves at higher frequency. The inflection frequency usually corresponded to a lifetime higher than actually measured. Again, as with the d-c conductivity measurements, there is the possibility that difficulties may arise from poor contact between the inversion layer and the bulk material. The situation is expected to be worse with Si than Ge because of the smaller reverse current across a junction in Si.

Nevertheless, in spite of the difficulty in detailed interpretation, the general features of the field-effect curves for the various treatments were quite reproducible and gave qualitative evidence of the n- or p-type effects of the various treatments and atmospheres.

Effects on Devices

Information of this sort should be helpful in selection of surface treatments and atmospheres to

improve Si device parameters which depend on surface potential and S. For example, the "p-type" treatments might be expected to improve breakdown voltage in p^+-n diodes (higher bulk resistivity on the n-side), while all three low S treatments should improve α in transistors which have sufficiently high volume lifetime. The HF treatment offers the combination of low S with an n-type surface which in certain situations may be more desirable than the p-type surface of the other two. However, the HF-treated surfaces tend to be less stable than the other two. In some preliminary experiments with p^+-n grown-junction diodes the breakdown voltage increased progressively from about 140 to 310 v in going through the series from the strongest n-type (HF) treatment to the strongest p-type (dichromate) treatment. This is in accord at least qualitatively with the surface breakdown theory of Garrett and Brattain (21). However, while the dichromate treatment produced the highest breakdown voltage it also caused a large saturation current presumably because of the larger effective junction area.

Conclusions

1. The chemical treatments had stronger effects than the atmospheres in determining surface potential. However, both the chemical treatments and ambient atmospheres were important in establishing the surface potential.

2. Low recombination velocity occurred when the surface was strongly p-type, after the dichromate and boiling deionized water treatments, or when it was strongly n-type, after the HF treatment. Atmospheres which pulled the energy bands back toward the middle from these extreme conditions caused S to increase (water vapor in the case of the boiling and dichromate treatments, and dry oxygen after the HF treatment.) The extreme bending in either direction required to obtain low S explains why low S is not produced by most common etching treatments.

3. Curves of S vs. U_s for the various treatments resemble branches of theoretical curves for recombination centers at a discrete energy level. A tentative analysis made by piecing together curves for treatments on the n-type sample indicates $E_T - E_i =$ 0.26 ev and a cross-section ratio $\sigma_p/\sigma_n \approx 5 \times 10^8$ for one set of recombination centers. This extremely large ratio must be viewed with suspicion because of the piecing together required to obtain it. If it had been possible to approach the maximum in S from both sides without changing the chemical treatment, a more detailed and reliable analysis could be made.

4. The apparent difference between U_s values for a given treatment on n- and p-type material may have been due, at least in part, to poor contact between an inversion layer and the bulk material. This would also change the shape of the S vs. U_s curves obtained under inversion layer conditions but would not affect the curves for enhancement layer conditions.

Acknowledgments

A number of people have made helpful suggestions and comments during the course of this work. The authors are especially indebted to H. C. Montgomery for his advice and help in the field-effect measurements and to C. G. B. Garrett and W. H. Brattain for helpful discussions. They also wish to thank E. D. Kolb for supplying the high resistivity, high lifetime Si necessary in this work.

Manuscript received May 26, 1958. This paper was prepared for delivery before the New York Meeting, April 27-May 1, 1958.

Any discussion of this paper will appear in a Discussion Section to be published in the June 1959 JOURNAL.

REFERENCES

1. W. H. Brattain and J. Bardeen, *Bell System Tech. J.*, **32**, 1 (1953).
2. D. T. Stevenson and R. J. Keyes, *Physica*, **20**, 1041 (1954).
3. Many, Harnik, and Margoninski, "Semiconductor Surface Physics," p. 85, U. of Pennsylvania Press (1956).
4. W. H. Brattain and C. G. B. Garrett, *Bell System Tech. J.* **35**, 1019 (1956). C. G. B. Garrett and W. H. Brattain, *ibid.*, **35**, 1041 (1956).
5. A. Many and D. Gerlich, *Phys. Rev.*, **107**, 404 (1957).
6. S. Wang and G. Wallis, *ibid.*, **107**, 947 (1957).
7. A. R. Moore and H. Nelson, *RCA Rev.*, **17**, 5 (1956).
8. T. M. Buck and F. S. McKim, Paper presented Electrochem. Soc. Meeting, Cleveland, Oct. 1956.
9. R. H. Kingston and S. F. Neustadter, *J. Appl. Phys.*, **26**, 718 (1955).
10. C. G. B. Garrett and W. H. Brattain, *Phys. Rev.*, **99**, 376 (1955).
11. J. R. Schrieffer, *ibid.*, **97**, 641 (1955).
12. R. J. Archer, *This Journal*, **105**, 619 (1957).
13. M. Kikuchi, *J. Phys. Soc. Japan*, **12**, 756 (1957).
14. N. F. Mott, "Semiconducting Materials," p. 1 Butterworth Scientific Publications Ltd., London (1951); R. H. Kingston, *J. Appl. Phys.*, **27**, 101 (1956).
15. J. R. Haynes and J. A. Hornbeck, *Phys. Rev.*, **90**, 152 (1953); J. A. Hornbeck and J. R. Haynes, *ibid.*, **97**, 311 (1955).
16. J. P. McKelvey and R. L. Longini, *J. Appl. Phys.*, **25**, 634 (1954).
17. T. M. Buck and F. S. McKim, *Phys. Rev.*, **106**, 904 (1957).
18. Aigrain, Lagrenaudi, Liandrat, *J. phys. radium*, **13**, 587 (1952).
19. H. C. Montgomery, *Phys. Rev.*, **106**, 441 (1957).
20. C. G. B. Garrett, *ibid.*, **107**, 478 (1957).
21. C. G. B. Garrett and W. H. Brattain, *J. Appl. Phys.*, **27**, 299 (1956).

Saturation Currents in Germanium and Silicon Electrodes

John B. Flynn

Sylvania Electric Products Inc., Woburn, Massachusetts

ABSTRACT

Saturation currents observed in germanium electrodes in KOH and in silicon electrodes in dilute HF solutions have been studied with a view to determining the source of generation within the electrode of the carriers involved in the reaction at the electrode solution interface. In n-type germanium anodes the generation is principally in the bulk with negligible contribution from the surface. Cathodes of p-type germanium in KOH show that surface generation is predominant. Generation in the space-charge region of silicon electrodes is probably the limiting process in dilute HF.

The phenomena of saturation current in germanium and silicon electrodes has been studied by several workers (1-5). For n-type Ge anodes in KOH solution their general conclusion is that the limiting currents observed are due to the rate of generation of holes in the bulk which diffuse to the surface and initiate the dissolution of Ge atoms. However, the role of surface generation remains somewhat obscure.

It was the purpose of this investigation to try to confirm the above findings by a more direct method and at the same time evaluate the magnitude of the contribution of surface generation. Similar studies were also carried out on p-type cathodes and Si electrodes.

Experimental

Figure 1 is a diagram of the cell used for the experimental work. It consisted of a three-necked 100-ml round bottomed flask; each neck was provided with a polyethylene stopper. The leads to the different electrodes passed through the stoppers. The counter electrode was a piece of platinized platinum sheet. The reference electrode for Ge was a saturated calomel electrode, connection being made by means of a bridge of saturated KCl solution.

For the work on Si electrodes a Pt wire was used as the reference electrode and the inside wall of the flask was lined with beeswax against the corrosive HF solutions. The outside of the cell was painted black because the Si electrodes were quite sensitive to light.

The HF solutions were ~5% [i.e., 1 vol of 48% HF (C.P.) diluted to 10 vol with demineralized water].[1]

The Ge or Si specimens used for electrodes were cut from single-crystal material in the form of slabs about 0.8 cm thick. The surface exposed to the solution, which was approximately on the (111) plane, varied in the area from 2 to 4 cm^2.

The method of mounting the Ge or Si in the cell is shown in Fig. 2. The samples were Cu plated on the back side (electrolytic for Ge, electroless for Si) which was then smeared with solder. The electrode, except for the face, was then covered with black wax to insulate it from the solution and minimize any photoeffect.

[1] Dr. P. Wang of our laboratory has found that solutions of this dilution permit smooth electrolytic etching of p-type Si.

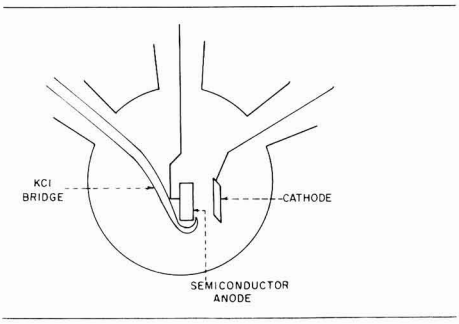

Fig. 1. Electrolytic cell diagram

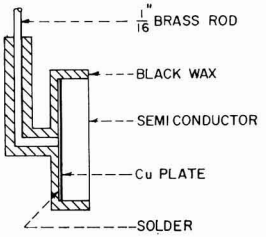

Fig. 2. Semiconductor electrode

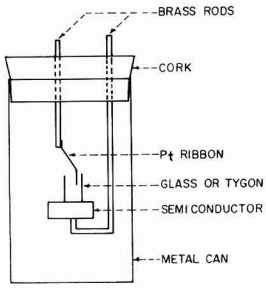

Fig. 3. Diagram of second type of cell used

A second experimental arrangement was used mainly for the purpose of checking the results obtained to see if any current leak significantly affected the results. This is shown in Fig. 3. Here the electrodes were bent in such a way that the unwaxed semiconductor surface was turned up. A glass or Tygon cylinder was mounted on this face. The solution was placed in the cylinder. This arrangement enormously reduces the chance of leakage. A platinum ribbon, serving as a counter electrode, was placed in the solution. This cell was mounted in a metal can which was covered with a cork stopper.

This metal can and the cell shown in Fig. 1 were mounted in a thermostatted water bath kept at 25.0° ±0.1°C for all of the work except where the temperature was deliberately varied.

The resistivities of the Ge and Si were measured by the four point probe method, and the lifetime on Ge was measured by the traveling light-spot technique. Lifetimes of the Si samples were not measured.

The current-voltage curves were obtained as follows. From a d-c power supply a certain voltage was applied across the cell. The voltage of the semiconductor electrode was measured against the reference electrode or counter electrode and the current through the cell was also measured at every applied voltage setting.

Results

Using the arrangement in Fig. 3 showed that the black wax gave adequate electrical insulation between the solution and metal parts of the electrode.

Most of the work reported here deals with n-type Ge anodes. If we assume that the current in n-type Ge anodes is limited by the bulk generation of carriers, it can be shown easily that the limiting current density (i) should obey the relationship

$$i = q^2 D_p u_n N_i^2 \frac{\rho}{L}$$

Here q is the electronic charge, D_p is the diffusion coefficient of holes, u_n is the electron mobility, N_i^2 is the product of electrons and holes at equilibrium, ρ is the resistivity of the material, and L is the diffusion length of holes.

In deriving this expression it is assumed that the hole concentration at the germanium-solution interface is effectively zero and that the resistivity of n-type Ge is determined by electron concentration only.

Therefore, if this relationship holds, a plot of the limiting current density for several n-type Ge specimens against the quantity (ρ/L) should yield a straight line of slope ($q^2 D_p u_n N_i^2$) and zero intercept.

In Fig. 4 some current voltage curves are shown which were obtained with n-type Ge anodes in a 1.35N KOH solution at 25°C. The method of taking a value for the saturation current where the saturation is not perfect is shown. The portion of the curves marked A and B are extrapolated until they intersect. The current at this point is taken as the saturation current.

A plot of the saturation current densities against the ratio of resistivity to diffusion length (ρ/L) for several n-type Ge samples is shown in Fig. 5. Two runs were made on almost all of the samples. While the data appear to fall about a straight line passing through the origin, the value of its slope is 4.4 times the theoretically calculated value for a current multiplication of unity.

In Fig. 6 is the same data plotted a little differently, namely, the current density divided by the resistivity against the reciprocal of the diffusion length. This manner of plotting the data shows a little more clearly the dependence of the limiting current density on the bulk properties alone.

If surface generation was contributing appreciably to the current, then the plot in Fig. 6 would show a definite intercept, which it does not. Hence, in 1.35N KOH and probably other electrolytic etching solutions, the saturation currents observed with

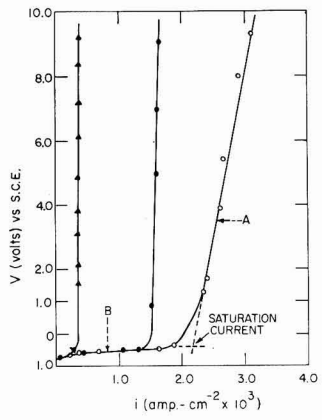

Fig. 4. Examples of voltage vs. current density curves for three n-type Ge anodes in 1.35N KOH at 25°C and method of determining "saturation current." Values of resistivity and diffusion length for these electrodes were: O, 17 ohm-cm, .07 cm; •, 14 ohm-cm, 0.07 cm; ▲, 5.8 ohm-cm, 0.13 cm.

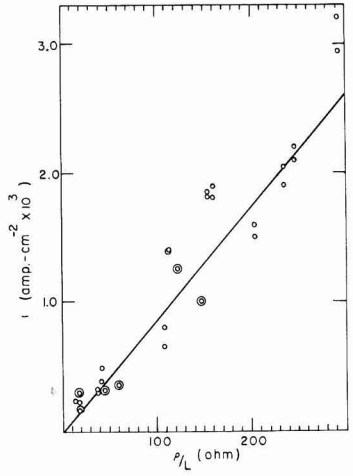

Fig. 5. Plot of i vs. ρ/L for several n-type Ge anodes in 1.35N KOH at 25°C.

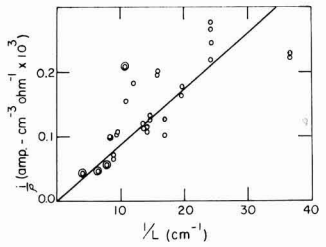

Fig. 6. Current density divided by resistivity vs. the reciprocal of the diffusion length for several n-type Ge anodes in 1.35N KOH at 25°C.

n-type Ge anodes are due to bulk generation alone with a negligible contribution from the surface.

Furthermore, the current multiplication appears to be close to 4 rather than a value of about 2 reported by others (1, 2). We are unable at this time to account for this difference in the values of current multiplication found. A possible mechanism for a current multiplication of 4 is given below:

$$Ge(s) + e^+ \rightarrow Ge(II) + e^- \text{ rate determining}$$

$$Ge(II) \longrightarrow Ge(IV) + 2e^- \text{ rapid}$$

The Roman numerals indicate the valence state of Ge, and the role of OH^- ions is not defined. This mechanism simply requires that the species formed due to the diffusion of a hole to a Ge atom at the surface is spontaneously oxidized electrolytically, and Ge ions, as OH^- complexes (3), go into solution.

A final point on the n-type Ge anodes is the question of the temperature dependence of the saturation current. Since the data indicate that we may ignore the contribution from surface generation, then the temperature dependence of the saturation current should yield information on the recombination-generation levels in the bulk.

By the Shockley-Read (6) theory for the bulk lifetime of a semiconductor, it can be shown for the bulk diffusion current that

$$i \propto T^2 e^{\frac{-E_g + \frac{1}{2}\Delta E}{kT}} \frac{\sqrt{p_o + n_o}}{n_o}$$

Here p_o is the hole, and n_o is the electron equilibrium concentrations, respectively. T is the absolute temperature, E_g is the energy gap width, and ΔE is the difference between the generation center energy level and either the lowest conduction band energy level or the highest valence band level. This ambiguity arises from uncertainties regarding the relative size of quantities in the expression for bulk lifetime.

Using this expression the limiting currents were measured on two anodes; one, 30 ohm-cm; the other, 18 ohm-cm over a range of temperatures.

The quantity log $(i/T^2)(n_o/\sqrt{n_o + p_o})$ was plotted against $(1/T)$. In this plot the slope should be equal to $(-E_g + \frac{1}{2}\Delta E)/2.3k$. These two samples yielded approximately the same value of the slope, i.e., -0.65 ev, from which a value of ΔE of 0.28 ev can be calculated (Fig. 7). This value is consistent with a Ni or Cu recombination level (7).

Five p-type Ge cathodes were studied next in 1.35N KOH. The currents tended to saturate but showed no well-defined saturation current. Ellis (8) has found that a Ge specimen shows an increased surface recombination velocity after having been made a cathode in dilute acid solution as the electrolyte. He attributes this increase to deposited hydrogen.

In our case since hydrogen is deposited, the surface recombination velocity (and hence, surface generation) may be increasing because of this hydrogen and, therefore, no distinct saturation is noted.

This hypothesis was tested by replacing the KOH solution with a 1.4M $(NH_4)_2S_2O_8$ solution. The hydrogen deposition is largely replaced in this case by the reduction of persulfate ions. A more distinct saturation is obtained with this electrolyte as seen in Fig. 8. The limiting currents in 1.4M $(NH_4)_2S_2O_8$ nevertheless were still too large to be due to bulk generation alone. This can be shown by a calculation from the measured lifetimes and resistivities. Rather a surface recombination velocity of $\sim 10^{+4}$ or higher is indicated in $(NH_4)_2S_2O_8$ solution.

Silicon

Five n-type Si anodes were used in 5% HF solutions; the currents tended to saturate fairly well and

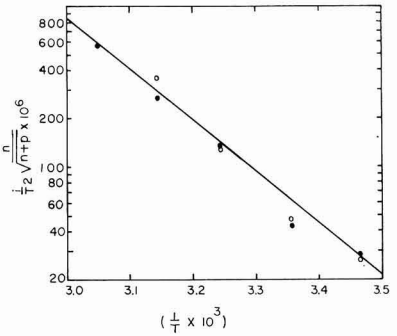

Fig. 7. Temperature variation of saturation current of two n-type Ge anodes in 1.35N KOH. O, 35 ohm-cm; •, 18 ohm-cm.

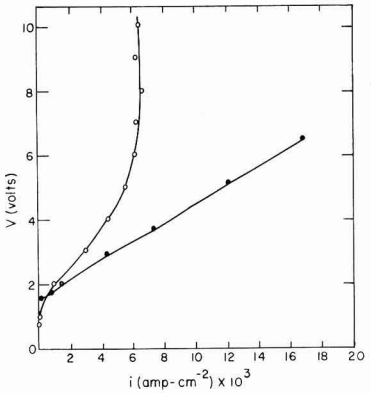

Fig. 8. Current density-voltage curve for one p-type Ge cathode at 25°C. O, 1.4M $(NH_4)_2S_2O_8$; •, 1.35N KOH.

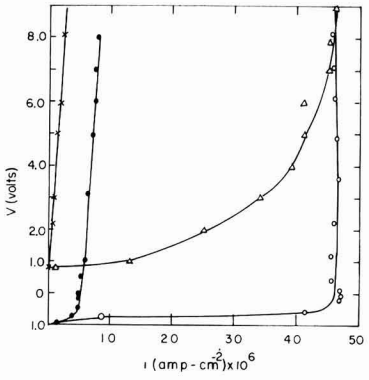

Fig. 9. Current density-voltage curves for one p-type Si cathode in dark X, and in diffuse light △, and one n-type Si anode in dark •, and in diffuse light O. In 5% HF at 25°C.

current densities in the range of 5-9 μamp-cm^{-2} were observed. For bulk generation, diffusion lengths of the order of $\sim 10^{-6}$ cm would be indicated for these samples. Recent work on Si indicates diffusion lengths of the order of 10^{-3} cm are the rule. Moreover, surface recombination velocities of the order of 10^{+6} or higher would be required if surface generation was the dominant process. However, this value seems improbably high.

From the work of Sah, *et al.* (11), the current due to generation in the space charge region for p-n Si junctions under large reverse bias is given as

$$i(\text{sp. ch.}) = \frac{q\, W\, n_i}{\tau_{po}\, e^{E_t - E_i/kT} + \tau_{no}\, e^{E_i - E_t/kT}}$$

In this expression q is the electronic charge, k is Boltzmann's constant, T is the absolute temperature, W is the width of the space charge region, n_i is the intrinsic carrier concentration in Si, and the quantities τ_{no}, τ_{po} are the reciprocal capture probabilities of electrons and holes, respectively. The quantity $E_t - E_i$ is the difference between the recombination generation center energy level and the intrinsic level.

Values found by these authors for the unknown quantities above are: $W = 10^{-4}$ cm; $E_t - E_i = 4.6\ kT$; $\tau_{po} = 1.2 \times 10^{-8}$ sec; $\tau_{no} = 4.3 \times 10^{-6}$ sec.

Using these values in the above expression for i(sp. ch.) we get

$$i(\text{sp. ch.}) = 0.6 \times 10^{-6} \text{ amp cm}^{-2}$$

While this value is somewhat lower than the values of current density found, it is still of the right order of magnitude to indicate the probability that in our n-type Si anodes the source of carriers is mainly due to generation in the space charge region.

One p-type Si cathode was studied in the same solution. The current is of the same order of magnitude and indicates generation of carriers in the space charge region.

In Fig. 9 is shown the current-voltage curves for one p-type Si cathode and one n-type Si anode in 5% HF solution. Two curves are shown for each electrode. Data for one curve was taken with light excluded from the electrode; data for the other was taken with the electrode exposed to the diffuse light from the surroundings.

Conclusion

1. Saturation currents in n-type Ge anodes in 1.35N KOH are due to the generation of holes in the bulk with negligible contribution from surface generation.
2. Furthermore a current multiplication of approximately 4, instead of a value of about 2 as found by others, is reported.
3. The failure of the p-type Ge cathode to saturate distinctly in 1.35N KOH can be attributed to deposited hydrogen.
4. It is probable that the limiting currents observed in Si electrodes in ~5% HF are due to generation of carriers in the space charge region of the electrode at the solution interface.

Acknowledgment

The author wishes to express his gratitude to Drs. G. Wallis, P. Wang, S. Wang, and S. Mayburg for valuable suggestions and criticisms. Thanks are also due to Mr. I. Feinberg for assistance with the lifetime and resistivity measurements.

Manuscript received May 13, 1958. This paper was prepared for delivery before the New York Meeting, April 27-May 1, 1958.

Any discussion of this paper will appear in a Discussion Section to be published in the June 1959 JOURNAL.

REFERENCES

1. C. G. B. Garrett and W. H. Brattain, *Bell Syst. Tech. J.*, **34**, 129 (1955).
2. A. Uhlir, Jr., *ibid.*, **35**, 333 (1956).
3. D. R. Turner, *This Journal*, **103**, 252 (1956).
4. W. E. Bradley, J. W. Tiley, R. A. Williams, J. B. Angell, F. P. Keiper, Jr., R. Kansas, R. F. Schwarz, and J. F. Walsh, *Proc. I.R.E.*, **41**, 1702 (1953).
5. S. G. Ellis, *Phys. Rev.*, **100**, 1140 (1955).
6. W. Shockley and W. Read, *ibid.*, **87**, 835 (1952).
7. J. A. Burton, G. W. Hull, F. J. Morin, and J. C. Severiens, *J. Phys. Chem.*, **57**, 853 (1953).
8. S. G. Ellis, *J. Appl. Phys.*, **28**, 1262 (1957).
9. S. Mayburg and L. Cohen, *Sylvania Tech. Rept. #57-03-7.*
10. C. A. Bittman and G. Bemski, *J. Appl. Phys.*, **28**, 1423 (1957).
11. C. T. Sah, R. N. Joyce, and W. Shockley, *Proc. I.R.E.*, **45**, 1228 (1957).

High-Pressure, High-Temperature Growth of Cadmium Sulfide Crystals

W. E. Medcalf and R. H. Fahrig

The Eagle-Picher Research Laboratories, Miami, Oklahoma

ABSTRACT

A process is described for growing cadmium sulfide crystals of uniform size, shape, and homogeneity from the melt. Structure and electrical characteristics of the crystals are discussed, and segregation data on several impurity species are given. A method is described for preparing high purity cadmium sulfide powder by the purification of cadmium and sulfur followed by direct combination of the elements.

Crystalline cadmium sulfide has risen to prominence in industry and research as a material which may be used in photovoltaic cells, radiation detection devices, infrared windows, and photosensitive elements.

The usual methods for the preparation of single crystals of cadmium sulfide have been confined to vapor phase or sublimation processes carried out at near atmospheric pressure. One such method was described by Frerichs (1, 2), in which hydrogen sulfide and a carrier gas are passed over heated cadmium metal. Crystals produced by this method are mostly ribbons or platelets. A second method described by Reynolds and Czyzak (3) is a static resublimation process in which a charge of cadmium sulfide is heated in an atmosphere of hydrogen sulfide in a sealed tube. Crystals in the form of prisms are formed directly on the charge as a result of local vaporization and crystallization. A modification of this method was reported by Reynolds and Greene (4) and involves vaporization of cadmium sulfide with recrystallization on a substrate in another part of the system. The vaporized cadmium sulfide crystallizes on the substrate in large grains, some of which weigh in excess of 50 g and are shown by x-ray measurement to be single crystals.

In the present work the development of a method of growing crystals from the melt was undertaken as another approach to the problem of growing cadmium sulfide crystals suitable for use in solar energy convertors. It was desired that the process would provide larger single crystals of cadmium sulfide with desirable photovoltaic properties and, specifically, that they would be homogeneous in respect to solute impurities and electrical characteristics.

Cadmium sulfide was first melted by Tiede and Schleede (5) and a melting point of 1750°C under 100 atm of nitrogen was reported. The experimental work was carried out in a small steel bomb containing an electrically heated graphite tube. The apparatus was operated for periods of a few minutes. Recently the melting of cadmium sulfide was carried out at the National Carbon Research Laboratories (6). This work was not published, but it is understood that a melting point of approximately 1500°C was obtained under a pressure of 200 atm of argon. More recently the melting point of cadmium sulfide was reported by Addamiano (7) to be 1475° ±15°C.

Equipment

The initial phase of the present study was the design and construction of a furnace capable of maintaining molten cadmium sulfide for a period of several hours without excessive vaporization. The basis for the design was the available information on temperature and pressure, a consideration of the results desired, and the corrosive effects of hot cadmium sulfide vapor on various materials of construction, determined experimentally. A schematic diagram of the furnace is shown in Fig. 1.

The pressure shell is a forged steel pot with cover. The inside dimensions are 10 in. in diameter by 20 in. deep. The wall is 3 in. thick and is jacketed for water cooling. The cover, which is held down by 20-1 in. alloy steel bolts, is fitted with sight glass opening, a central vertical opening, and a pipe con-

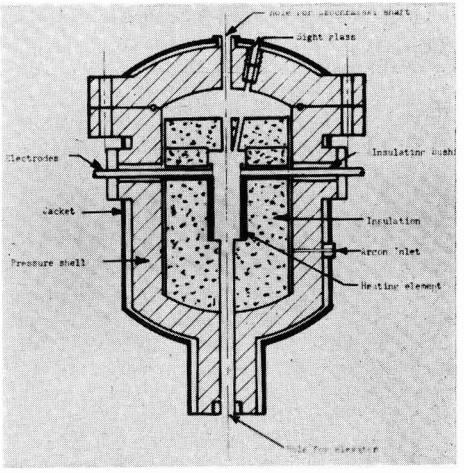

Fig. 1. Design of furnace used for growth of cadmium sulfide crystals from the melt.

nection to a gauge, safety rupture disk, and pressurizing line. The pot is equipped with insulating, pressure tight bushings around the electric power leads, and also a hydraulically operated elevator to vertically position the crucible inside the furnace. All pressure seals are Buna rubber "O" rings.

The purpose of providing the central top opening and the sight glass was for use in the Czochralski method of growing crystals, should this technique prove feasible. The elevator was provided for slow withdrawal of the melt from the hot zone.

The present method of protecting the walls of the pressure shell is by surrounding the heating element with fused stabilized zirconia brick lined with a porous carbon cylinder. The top section of the insulation is removed and replaced each time the furnace is opened for loading or unloading. The remainder of the insulation is packaged in a stainless steel container.

The heating element is a multiple split type graphite cylinder 3 in. OD x 2½ in. ID x 5 in. long. The thermal gradient along the length of the element is such that the temperature near the bottom is lower than that in the central and upper portions of the cylinder. The element is connected to the water-cooled molybdenum electrodes by threaded graphite studs.

Power for the furnace is furnished by a stepdown transformer with a variable autotransformer in the primary. The capacity of the power supply is 20 kw. Under 90% maximum heating load, the furnace draws 850 amp, at about 21.5 v. Control of the furnace temperature is by manual operation of the variable transformer.

Monitoring the temperature inside the furnace is made possible through the use of a boron graphite-graphite thermocouple (8). It is mounted on the end of a water-cooled elevator shaft. Output from the sensing device is fed to a strip chart recorder.

The p-type graphite was obtained from the National Carbon Research Laboratories.[1]

Experimental Procedure

The pressure furnace described above cannot be used readily for either the Czochralski method or for controlled withdrawal of the melt from the hot zone. Excessive vaporization of the charge and obscurement of the sight glass occur when an uncovered crucible, necessary for the Czochralski technique, is used. Convective currents caused by chimney effect result when the crucible is withdrawn from the hot zone.

The following procedure is used in growing single crystals: Approximately 150 g of crushed, densified cadmium sulfide is introduced into a high purity graphite crucible and placed inside the furnace heating element. The crucible is supported by the thermocouple and a porous carbon stool piece which are mounted on the top end of the elevator shaft. The crucible is covered by a loosely fitting graphite lid. The hot zone of the furnace is then capped by a porous carbon cover; and the top section of the furnace insulation, a cast ceramic disk 2½ in. thick, is laid on the top. The furnace cover is next bolted down and evacuation is begun. During evacuation the pressure lines and furnace are purged with argon. After evacuation, the furnace is filled with argon to a pressure of about 1000 psi and heating is started. The temperature of the bottom of the crucible is raised rapidly to about 1500°C. This measurement lacks precision since the "cold" junction of the thermocouple varies somewhat due to conduction of heat by the pressurized gas. After the temperature reaches this point, the furnace pressure, which has been rising with the temperature, is adjusted to 1500 psi and the heating is slowed down to level off the temperature for 1 hr. This assures complete melting of the charge. The power is then reduced slowly over a period of about 6 hr so that the temperature of the crucible bottom is brought down in a linear manner.

Controlled Solidification of the Melt

The thermal gradient along the heating element and conduction heat losses through the crucible support cause the lowest portion of the melt to solidify first. As the temperature is decreased by reduction of power to the element, progressive freezing of the melt takes place from the bottom upwards toward the top. A very slow advance of the solid-liquid interface encourages the formation of large crystals. Faster cooling results in smaller crystals arranged in a columnar formation.

Results

Some of the ingots are of good crystalline structure at the bottom but have a region or pocket at the top which is noncrystalline in nature. Minute particles of elemental cadmium and voids from which sulfur and cadmium have been volatilized are often present in this pocket. This indicates that a portion of the cadmium sulfide underwent thermal decomposition while in the molten state, and that the products of decomposition were rejected by the advancing growth of crystalline material. By carefully controlling the cooling rate the size of this noncrystalline area can be diminished.

Figure 2 is a photograph illustrating the crystalline and noncrystalline areas in three ingots which have been sectioned vertically.

Cadmium sulfide crystals grown under controlled conditions are single crystals. Several ingots have been obtained which are made up of only one large crystal weighing more than 100 g. Crystallization is

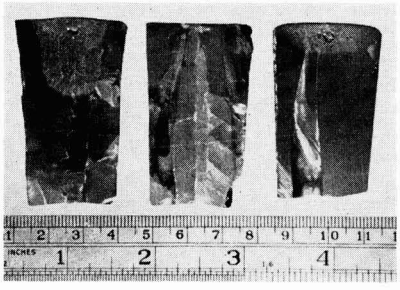

Fig. 2. Ingots of cadmium sulfide sectioned vertically

[1] Through the kindness of R. L. Shepard who, with his associates, developed the boron graphite-graphite thermocouple.

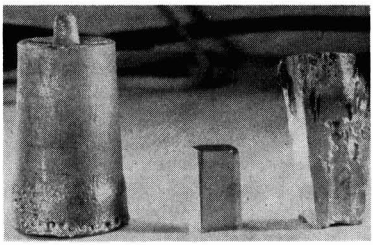

Fig. 3. Cadmium sulfide ingot with specimens cleaved and machined.

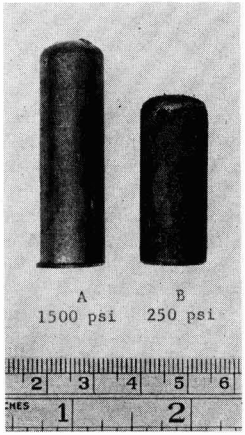

Fig. 4. Comparative size of cadmium sulfide ingots as a function of pressure.

in the hexagonal system and the vertical growth axis tends to coincide roughly with the C-axis to give an 0001 face at the top of the crystal, although in some cases the C-axis may be canted as much as 15° from the crucible axis. It is believed that this is due to unsymmetrical heat patterns existing in the hot zone of the furnace when seeding is begun in the bottom of the melt. The crystals may be cleaved, or may be machined to secure a specimen of any desired orientation.

Figure 3 is a photograph showing a single crystal ingot, a cleaved section of an ingot, and a specimen machined to a definite orientation.

Effect of Pressure on Crystal Growth

Several runs were carried out at pressures considerably lower than 1500 psi. With decreasing pressure the rate of volatilization of cadmium sulfide increased and the ingots were of poorer crystalline structure.

Identical weight of charge was used in the preparation of the ingots shown in Fig. 4. The charge was brought to the melting point in each case and then quick-cooled to decrease the amount of volatilization. The weight loss at 250 psi was 25.4% as compared to a 5% loss in weight at 1500 psi. There were more voids and noncrystalline areas in the ingots prepared at low pressures. Since our objective was to secure cadmium sulfide of good crystalline structure, the low pressure studies were discontinued. It is indicated, however, that low pressure melting may be used in zone-refining studies.

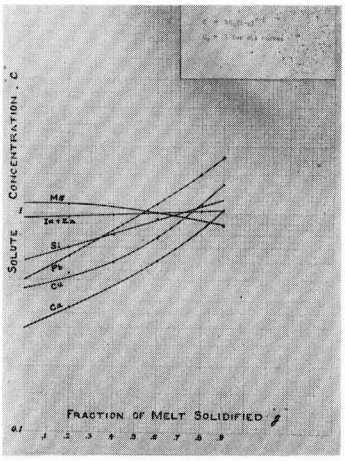

Fig. 5. Experimental concentration profiles for segregation of impurities in normal freezing of cadmium sulfide melt.

Segregation of Solute Impurities

Determination of effective segregation coefficients with normal freezing under a given set of experimental conditions was undertaken. Four crystals were grown under nearly identical conditions of charge, pressure, and cooling rate. The pressure was maintained at 1500 psi. The melts were caused to crystallize slowly over a period of 6 hr to provide a slowly advancing solid-liquid interface from the bottom to the top of the melt. Since the rate of movement of the interface could not be observed or precisely determined using the present equipment, the experimental coefficients obtained could not be considered as equilibrium values.

The four crystals produced were sectioned horizontally into five equal sections and analyzed spectrographically. The integrated concentration data were used to construct profiles depicting the concentration of impurities retained in the solid as a function of (g) the fraction of the melt solidified. The initial concentration C_o was taken as the average concentration of the five segments. By plotting the solute concentration C_s vs. (g) it is possible to determine the approximate K_{eff} from the intersection of the profile with the y-axis. Figure 5 represents the experimental profiles for several impurity species in the cadmium sulfide matrix.

The profiles indicate that silicon, calcium, copper, and lead tend to be rejected by the advancing solid-liquid interface and that zinc and indium are not segregated in the normal freezing process. The profile of the magnesium species indicates a distribution coefficient slightly greater than 1.0. More recent data, not shown in Fig. 5, provide information that manganese is not segregated during the crystallization process. This is shown in Table I.

The data indicate that (a) normal freezing or zone refining of cadmium sulfide may be used to remove such impurities as silicon, lead, calcium, and copper; and (b) that certain solute impurities such as indium, zinc, and manganese can be used as doping agents homogeneously distributed throughout the crystal.

Table I
CdS crystal No. 111, doping agent $MnCl_2$

Fraction solidified	Solute impurities, ppm Si	Mg	Cu	Ca	Mn
Top 0.9	500	5	1.0	50	50
0.8	20	5	0.5	10	50
0.6	20	5	0.5	10	50
0.4	10	5	*	10	50
0.2	10	5	*	10	50

CdS crystal No. 117, no doping agent

Fraction solidified	Solute impurities, ppm Si	Pb	Mg	Cu	Ca	Resistivity, ohm-cm
0.9	100	*	1	0.5	10	0.48
0.8	100	5	1	0.5	10	1.12
0.6	100	*	1	0.5	10	1.38
0.4	50	*	1	*	5	1.59
0.2	50	*	1	*	5	2.60

* Not detected.

Photovoltaic Cells

Small photovoltaic cells were prepared from crystals grown by (*a*) crystallization from the melt and (*b*) the vapor phase process (3). A comparison of photovoltaic properties is shown in Table II.

High Purity Cadmium Sulfide

Cadmium sulfide now available from commercial sources contains various impurities in concentrations of several parts per million. Such impurities include silicon, calcium, magnesium, zinc, lead, iron, aluminum, and copper. With the purpose of obtaining more effective control and evaluation of solute impurities in crystals grown from the melt, experimental work was carried out to provide cadmium sulfide feed material in which the impurity concentration would be not greater than 1 ppm. The procedure used in preparing cadmium sulfide of improved purity is described in the following paragraphs.

The procedure that was developed included the following steps: (*a*) purification of elemental cadmium, (*b*) purification of elemental sulfur, and (*c*) synthesis of cadmium sulfide from the purified elements. In the purification of elemental cadmium and sulfur it was found that the use of both distillation and zone melting processes was required to obtain the desired purity.

Commercial grade cadmium was given three distillations in a cast iron retort to effectively decrease the concentration of zinc and lead to approximately 20 ppm. These distillations proved to be necessary for subsequent removal of these elements to a concentration of less than 1 ppm by zone melting. The cadmium then was zone melted by the process described by Pfann (9). A graphite boat was used to provide an ingot 19 in. in length and weighing approximately 1 kg. After six molten zones of 1.0 in. length were passed horizontally through the solid ingot, the bar became monocrystalline over 90% of its length and the impurity concentration over a distance of 50% of its length was below the limits of spectrographic detection.

Four distillations of sulfur in a clear quartz unit removed iron, zinc, aluminum, and copper to near the limit of spectrographic detection. Silicon, calcium, and a trace of magnesium were still present in the sulfur after four distillations. To further purify the sulfur, zone melting techniques were investigated. These included (*a*) the conventional zone melting process in which a molten zone of approximately 1.0 in. in length was caused to traverse a horizontal solid ingot of sulfur and (*b*) a reversed zone melting procedure in which a small solid zone was caused to progress transversely through an elongated melt of sulfur. This technique of removing from a solid substance soluble impurities having a distribution coefficient greater than 1.0, was reported by Overby (10). The latter process proved to be effective in the removal of silicon and calcium from the sulfur. The zone melting procedures were carried out in a graphite boat 18 in. in length and purified ingots of sulfur weighing approximately 1 lb were produced.

The synthesis of cadmium sulfide was carried out by a vapor phase reaction in a quartz reactor. The purified sulfur and cadmium were volatilized from separate quartz boilers external to the reactor with helium used as the carrier gas. The reactor was

Table II. Comparison of photovoltaic properties of cadmium sulfide crystals grown from the melt and by a vapor phase process

Run No.	Method crystal growth	Resistivity, ohm-cm	Mobility, cm^2/v sec	Open circuit voltage, v	Conversion Efficiency*
HP-84	From melt	1.41	108	0.40	1.77%
HP 60	From melt	0.29	180	0.52	2.30†
HP-91(a)	From melt	1.62	175	0.36	2.22
HP-91(b)	From melt	1.62	171	0.44	2.42
HP-96	From melt	0.75	179	0.35	2.42
HP-57	From melt	0.13	300	0.475	6.11
	Vapor phase growth (average value)	—	—	—	2.05‡

* RFL-2 Lamp @ 1.5 g-cal/cm^2/min. (In sunlight the conversion efficiency is 30-50% greater.)
† Determined by the Research Laboratories of the Harshaw Chemical Co.
‡ This value was obtained from a recent and separate study of the conversion efficiencies of a large number of cadmium sulfide crystals grown by vapor phase deposition. It is included in the table for purposes of comparison.

Table III. Spectrographic analyses

		Impurities, ppm Si	Pb	Mg	Fe	Cu	Zn	Ca	Al
I	Cadmium								
	Triple distilled	10	10	1.0	1	3.0	20	2	2
	Zoned, 6 passes	1	*	1.0	*	*	*	*	*
II	Sulfur								
	Starting sulfur	20	*	1.0	4	4.0	*	80	3
	2X distilled	20	*	1.0	2	2.0	*	50	2
	4X distilled	10	*	0.5	*	1.0	*	30	*
	4X distilled and zone cooled	*	*	0.5	*	1.0	*	*	*
III	Cadmium sulfide (synthesized)	100	*	0.5	*	0.5	*	*	*

* Not detected.

maintained at a temperature of 900°C during the synthesis.

The cadmium sulfide formed as small crystals having a median radius of approximately 4μ. One pound of synthesized cadmium sulfide was produced per run representing a recovery of approximately 80% of theoretical based on the weight of cadmium used. The spectrographic data on the reactants and product are shown in Table III.

There was a significant increase in silicon during the synthesis due to introduction from the opaque quartz used in the reactor. There was no introduction of other impurities during the reaction.

Conclusions

Cadmium sulfide crystals of uniform size and shape can be grown from the melt in an argon atmosphere at 1500 psi. Controlled cooling to cause a solid-liquid interface to move from the bottom to the top of the vertical cylinder of molten cadmium sulfide at a slow and controlled rate results in the formation of single crystals weighing in excess of 100 g. At pressures as low as 250 psi only polycrystalline ingots are formed.

Ingots grown from the melt are homogeneous with respect to the orientation of certain solute impurities including indium, zinc, and manganese. Silicon, calcium, copper, and lead are segregated during the normal freezing of cadmium sulfide exhibiting an effective distribution coefficient of less than one. Solar cells prepared from melt grown crystals have photovoltaic conversion efficiencies equal to solar cells prepared from vapor grown cadmium sulfide crystals.

Synthesis of cadmium sulfide from elemental cadmium and sulfur which have been purified by distillation and zone melting techniques provides a material which has, with the exception of silicon, an impurity concentration not greater than 1 ppm as determined spectrographically.

Acknowledgment

Acknowledgment is given to the Aeronautical Research Laboratory for their sponsorship of this work and permission to publish the results. The authors also wish to express their appreciation to D. A. Hammond of Harshaw Chemical Company for check determinations on conversion efficiencies. The assistance of the following staff members of the Eagle-Picher Company in carrying out the work is also acknowledged: L. H. Garrison, J. E. Powderly, K. E. Bean, and N. H. Hemmat.

Manuscript received April 29, 1958. This paper was prepared for delivery before the New York Meeting, April 27 to May 1, 1958.

Any discussion of this paper will appear in a Discussion Section to be published in the June 1959 JOURNAL.

REFERENCES

1. R. Frerichs, *Naturwissenschaften*, **33**, 281 (1946).
2. R. Frerichs, *Phys. Rev.*, **72**, 594 (1947).
3. D. C. Reynolds and S. J. Czyzak, *ibid*, **79**, 543 (1950).
4. D. C. Reynolds and L. C. Greene, *J. Appl. Phys.*, **29**, 559 (1958).
5. E. Tiede and A. Schleede, *Ber.*, **53B**, 1717 (1920).
6. Information supplied in private communique by Dr. M. T. Jones of National Carbon Research Laboratories, Parma, Ohio
7. A. Addamiano, *J. Phys. & Colloid Chem.*, **61**, 1253 (1957).
8. R. L. Shepard, paper presented at Pittsburgh Meeting of the American Physical Society, March 15, 1956.
9. W. G. Pfann, *J. Metals*, **4**, 747 (1952).
10. S. L. Overby, U. S. Patent 2,801,192.

Some Semiconducting Properties of HgTe

J. Black, S. M. Ku, and H. T. Minden

Sylvania Research Laboratories, A Division of Sylvania Electric Products Inc., Bayside, New York

ABSTRACT

Mercuric telluride was synthesized and single crystals were prepared both in a horizontal capsule and by the Bridgman technique. The Hall coefficient R and the resistivity ρ were measured as a function of temperature and magnetic field. Above 250°K the material was intrinsic with an energy gap of around 0.02 ev and a mean density-of-states effective carrier mass of about 0.04 m_e. Hall effect and mangetoresistance data indicated that at 300°K $\mu_n \sim 16{,}000$ cm^2/v sec while $\mu_n/\mu_p \sim 10$. In the intrinsic temperature range, mobilities decreased with increasing temperature.

At low temperatures R decreased markedly with magnetic induction even though R measured at low fields was independent of temperature for one of the ingots. In addition, the magnetoresistance fell far below a B^2 dependence at low temperatures. This behavior is characteristic of p-type semiconductors in the transition temperature range between intrinsic and extrinsic conduction. In HgTe this transition temperature range is quite wide because of the low energy gap.

Since all material prepared from the melt was p-type, it seems that there is either a dominating acceptor impurity in all the samples or the maximum melting point of the compound does not occur at the stoichiometric composition.

Much work has been done in recent years in determining the electrical and optical properties of semiconducting compounds with the zinc blende structure. The main effort has been concentrated on the III-V series of compounds, which are especially interesting because of their high electron mobilities.

Table I

Crystal	Starting material	Trace impurities
Z21–35	99.8 + Te Triple Distilled Hg	Ag, Cu, Fe, Pb, Si No analysis
B51–1	99.999 Te 99.999 + Hg	Spectroscopically pure Spectroscopically pure

Comparatively little work has been done on the II-VI compounds, which have, in general, higher energy gaps but lower carrier mobilities than III-V semiconductors. Two of the compounds, however, HgSe and HgTe, have been reported to possess electron mobilities greater than 10,000 cm^2/v sec at room temperature (1). Previous investigations published have been made on thin films (2, 3), pressed powders (4), pressed and sintered powders (5), or fused ingots (5). Detailed measurements of the electrical properties of single-crystal HgTe have been reported recently by Harman and Logan (6).

It is the purpose of this paper to present the results of an investigation of the electrical properties of single-crystal HgTe. The Hall effect and resistivity of a number of samples have been measured from 80° to 650°K as a function of magnetic field strength.

Experimental Methods

Mercuric telluride was synthesized from the elements in sealed evacuated quartz capsules. The purity of the starting elements is shown in Table I. The capsule was slowly heated to 720°C, which is about 50° above the melting point of the compound; heating was done over a period of 24 hr to prevent the buildup of an excessive mercury vapor pressure. Once the capsule reached 720°C the melt was allowed to soak for an additional 2 hr with frequent agitation to insure mixing of the elements. After soaking, the material was slowly cooled to room temperature. Debye-Scherrer x-ray powder patterns of the synthesized HgTe agreed with data published previously by other investigators (7).

Two single-crystal ingots were prepared. One, Z21-35, received 35 zone refining passes and the single crystal was grown in the same boat that was used for zone refining. The other, B51-1, was grown as a single crystal by the Bridgman technique directly after synthesis.

Spectroscopic analysis of the zone-refined ingot, Z21-35, showed that all impurities observed segregated toward the last-to-freeze end. Sn, Bi, and Pb segregated rapidly while Ag, Fe, and Cu segregated slowly. The Cu and Fe concentration could not be reduced below ~5 ppm and ~50 ppm respectively in 35 passes.

Electrical measurements were made on single-crystal bars about 1 x 2 x 10 mm; samples were etched in aqua regia diluted with water. Stainless steel pressure contacts were used on some specimens; others were copper plated and soldered.

For low-temperature measurements the samples were cooled in a cryostat to about 80°K and then allowed to warm slowly to room temperature while their electrical properties were measured. Measurements above room temperature were made as the samples were being heated in a small nichrome furnace.

The Hall coefficient and resistivity were measured as a function of both temperature and magnetic field. The usual d-c technique was employed, and voltages were measured by means of a L&N Type K2 potentiometer. An Arthur D. Little 11-in. electromagnet was used. The voltage across the magnet current shunt was calibrated against the magnetic field which, in turn, was measured with a Rawson rotating coil gaussmeter.

Experimental Results

All samples studied had a negative Hall coefficient at all temperatures which were reached in this investigation.

Hall coefficient.—Figure 1 shows the effect of temperature on the Hall coefficient of a sample from B51-1, at various magnetic field strengths. At high temperatures the Hall coefficient, R, is nearly independent of magnetic induction B. At low temperatures R decreases with increasing magnetic field strength. In Fig. 2 data of Fig. 1 are replotted with temperature as a parameter instead of magnetic field strength to show the effect of B on R at various temperatures. At temperatures down to 160°K or so the Hall effect appears to be independent of B below

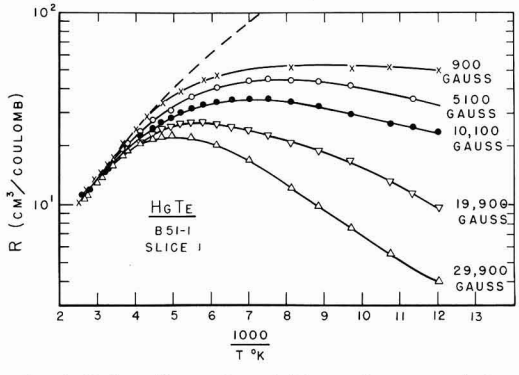

Fig. 1. Hall coefficient R vs. 1/T at various magnetic inductions for a sample cut from ingot B51-1.

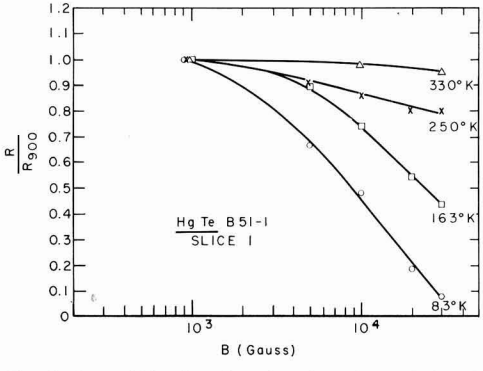

Fig. 2. Data of Fig. 1 replotted to show the variation of R (normalized to R at 900 gauss) with magnetic induction at constant temperature.

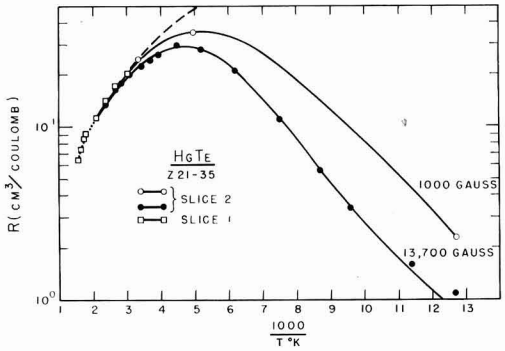

Fig. 3. Variation of R with 1/T at 1000 gauss and 13,700 gauss for two samples from ingot B51-1.

1000 gauss. At liquid nitrogen temperatures measurements below 1000 gauss are needed to determine whether R varies significantly with B at low field strengths.

Figure 3 shows the effect of temperature on the Hall coefficient of samples from Z21-35 at two magnetic field strengths. Irreversible changes in R occurred above 500°K. These changes were probably due to decomposition; in fact, the odor of Te was noticeable above 650°K. Because of this, data above about 500°K may be in error. The variation of R with magnetic field strength is shown in Fig. 4. Data for these curves were obtained from measurements of R as a function of B at 79°, 202°, and 296°K. It is clear that for ingot Z21-35 the Hall effect at liquid nitrogen temperatures is independent of magnetic field strength at values of B below 1000 gauss. The dependence of R on B at a given temperature is almost the same for both the B51-1 and the Z21-35 crystals.

Curves of the Hall effect at 900 gauss for two different samples from B51-1 are shown in Fig. 5. Slice No. 1, which has the higher Hall coefficient, was closer to the first-to-freeze end than was slice No. 3. Figure 5 also shows the Hall curves at 13,700 gauss for two samples from Z21-35. Again the sample (slice No. 3) that was closer to the first-to-freeze end has the higher Hall coefficient.

Resistivity.—Figure 6 shows the resistivity, ρ, as a function of inverse temperature for the various

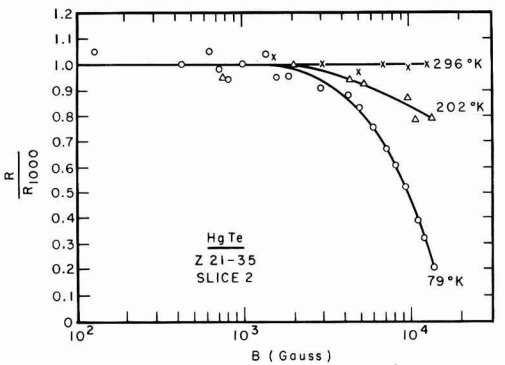

Fig. 4. Variation of R (normalized to R at 1000 gauss) with magnetic induction at various temperatures.

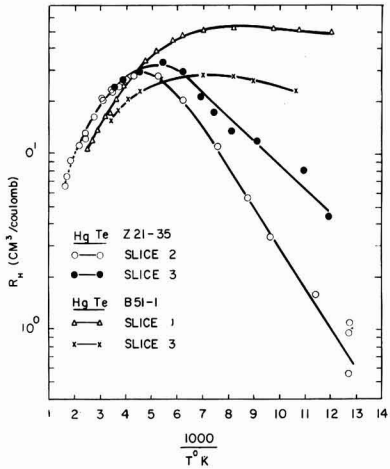

Fig. 5. Variation of R with 1/T (B=900 gauss) for two slices of ingot B51-1. Slice No. 1 was closer to the first-to-freeze end. Variation of R with 1/T (B=13,700 gauss) for two slices of ingot Z21-35. Slice No. 3 was closer to the first-to-freeze end.

samples of B51-1 and Z21-35. As with the Hall coefficient, irreversible changes in ρ were observed above 500°K, so that values of the resistivity may be in error in this temperature region.

The Hall mobility $\mu_H = R\sigma_o$ was calculated from the resistivity at zero magnetic field and the Hall coefficient at magnetic field strengths where R was independent of B. In Figure 7 log $R\sigma_o$ is plotted as a function of log T for samples from B51-1 and Z21-35. Room temperature values of Hall mobility are in agreement with those reported recently by other investigators (7).

Figure 8 shows the effect of temperature on the transverse magnetoresistance $\Delta\rho/\rho$ of two samples from B51-1 at various magnetic field strengths. These two samples were cut, side by side, from a thin disk obtained by slicing the ingot normal to its long axis. At 5000 gauss and at 10,000 gauss $\Delta\rho/\rho$ is the same for both samples over the whole range of temperature. At higher magnetic field strengths, however, the two samples showed differences in $\Delta\rho/\rho$ at temperatures below about 180°K.

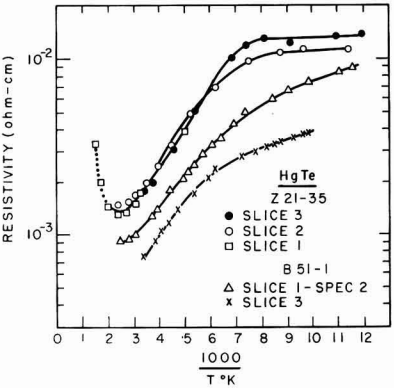

Fig. 6. Variation of the resistivity ρ with 1/T for various samples of HgTe.

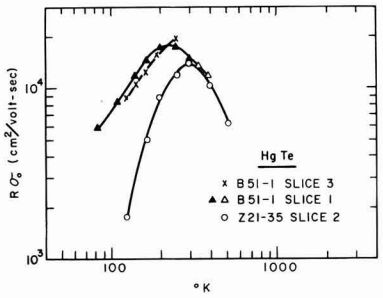

Fig. 7. Hall mobility vs. T for various HgTe samples

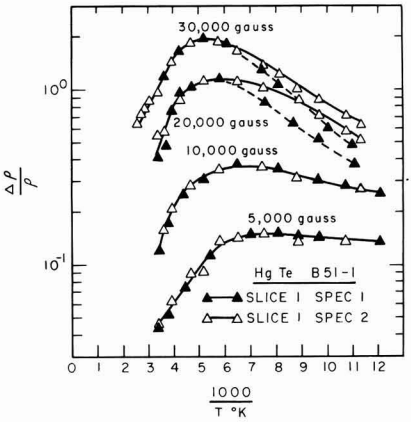

Fig. 8. Magnetoresistance $\Delta\rho/\rho$ vs. 1/T for two samples of ingot B51-1 at various magnetic inductions.

The effect of temperature on the magnetoresistance of three samples from Z21-35 at 13,700 gauss is plotted in Fig. 9. Slices 1 and 3 came from the first-to-freeze end of the ingot while slice 2 was cut from the center of the ingot. The slice nearer to the first-to-freeze end had the higher magnetoresistance at low temperatures. Above about 250°K the magnetoresistance of the three slices became equal.

A magnetoresistance mobility was calculated from the relation

$$\mu_m = \left(\frac{\Delta\rho}{\rho K B^2} \right)^{1/2} \qquad [1]$$

where

$$K = \frac{4-\pi}{\pi}\left(\frac{3\pi}{8}\right)^2 \qquad [2]$$

Figure 10 shows the effect of temperature on the magnetoresistance mobility, μ_m, of ingot B51-1 at various magnetic field strengths and of ingot Z21-35 at a field strength of 13,700 gauss. At low temperatures $\Delta\rho/\rho$ falls considerably below a B^2 dependence at high magnetic fields, while at high temperatures $\Delta\rho/\rho$ follows approximately a B^2 dependence. Furthermore, at high temperatures μ_m is the same for both B51-1 and Z21-35, and μ_m decreases with increasing temperature.

It should be mentioned that at room temperature a polycrystalline sample of HgTe showed a high transverse magnetoresistance ($\Delta\rho/\rho = 0.12$ at 10,000 gauss) while the longitudinal magnetoresistance was less than 10^{-3} at 10,000 gauss.

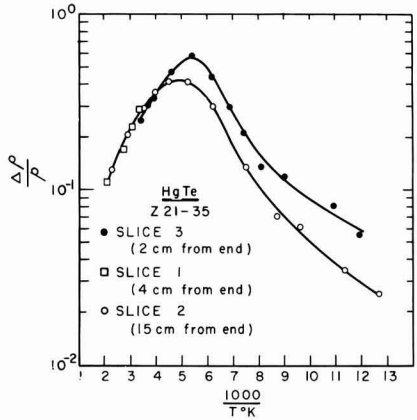

Fig. 9. Magnetoresistance, $\Delta\rho/\rho$, vs. 1/T for three slices of ingot Z21-35 at B=13,700 gauss.

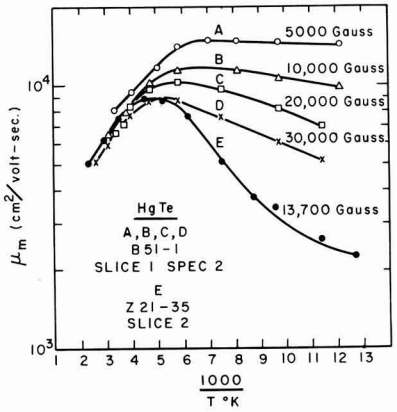

Fig. 10. Magnetoresistance mobility μ_m vs. 1/T at various magnetic inductions for two samples of HgTe.

Discussion

Energy gap.—The slopes of the log R and log ρ vs. $1/T$ curves (Fig. 1, 3, and 5) correspond to an energy gap of about 0.08 ev. This result is somewhat misleading because the $T^{3/2}$ dependence of the effective density of states must be taken into account for such a low energy gap. The dashed lines of Fig. 1 and 3 are calculated from the equation

$$R = -\left(\frac{3\pi}{8}\right)\left(\frac{b-1}{b+1}\right)\left(\frac{1}{\epsilon n_i}\right) \qquad [3]$$

where

$$n_i = 2\left(\frac{2\pi m^* kT}{h^2}\right)^{3/2} e^{-E_g/2kT} \qquad [4]$$

and

$$m^* = (m_n m_p)^{1/2} \qquad [5]$$

The energy gap assumed is 0.025 ev and the scale factor

$$\left(\frac{8}{3\pi}\right)\left(\frac{b+1}{b-1}\right)\left(\frac{m^*}{m_e}\right)^{3/2} = 0.023$$

If the first two factors are assumed to be unity, $m^*/m_e = 0.035$. The principal difficulty in the inter-

pretation is that for such a low energy gap the slope at room temperature is relatively insensitive to the value of the energy gap. If $E_g = 0$ is assumed, however, the slope of the calculated curve is definitely less than that of the experimental curve.

The use of Fermi-Dirac statistics instead of Maxwell-Boltzmann statistics increases the slope of the calculated log R vs. $1/T$ for a given energy gap.

Hall coefficient.—Since $R < 0$ in the intrinsic region, the mobility ratio $\mu_n/\mu_p = b > 1$. The log R vs. $1/T$ curve for ingot Z21-35 appears to be typical of p-type material (see Fig. 3). With a low energy gap the transition from intrinsic to extrinsic p-type behavior should take place over a wide range of temperature. This would account for the fact that even at 78°K R is still negative. At higher magnetic fields the Hall zero appears to shift to higher temperatures in a manner similar to that observed for InSb (8).

The Hall curve for ingot B51-1 at low magnetic fields appears to be typical of n-type material. On the other hand, at higher magnetic fields R decreases with lower temperatures as shown in Fig. 1. The most satisfactory explanation of this behavior is that ingot B51-1 is also p-type, but that it has a lower extrinsic hole concentration than ingot Z21-35. This would account for the fact that the Hall zeros for ingot B51-1 apparently occur at lower temperatures than they do for ingot Z21-35. In fact, Carlson has measured the Hall coefficient of apparently n-type HgTe at very low temperatures, and he found that R became positive near 20°K (9).

Mobility.—In the intrinsic region

$$R_o \sigma_o \propto \mu_n - \mu_p \qquad [6]$$

$$\Delta\rho/\rho B^2 \propto \mu_n \mu_p \qquad [7]$$

The constants of proportionality depend on the statistics used and on the scattering mechanism assumed. If Boltzmann statistics are used and if the mean free path is assumed independent of energy (lattice scattering), then at room temperature Eqs. [6] and [7] lead to $\mu_n = 15{,}800$ cm²/v sec, and $b = 5.27$. If the above assumptions are correct, μ_n and μ_p continually decrease with increasing temperature above 240°K. The validity of using Boltzmann statistics above room temperature may be questioned legitimately. For instance, using Boltzmann statistics at 300°K gives $b = 5.27$, while Fermi-Dirac statistics give $b = 14.50$. Nonetheless, it appears reasonable to conclude that in the neighborhood of room temperature $\mu_n \sim 16{,}000$ and $b \sim 10$ in contrast to a value of 100 reported by Harman and Logan (6) at low temperatures.

Harman and Logan and Carlson (10) have observed the large variation with magnetic field of the Hall coefficient in HgTe. This variation is large at low temperatures, but vanishes at room temperature. If the present interpretation of these results is correct, then truly n-type HgTe has not yet been reported. This leads one to suspect that HgTe might be "instrinsically" p-type. According to the theory of the zinc blende lattice, Te vacancies should act effectively as p-type impurities. On the other hand, Harman and Logan observed that the diffusion of Hg into HgTe lowers the intrinsic hole concentration. In order for Hg atoms to act as compensating donors, they would be expected to occupy interstitial positions. This raises the possibility that the acceptors in p-type HgTe are interstitial Te atoms. If this is so, the HgTe alloy having a maximum melting point would contain a slight stoichiometric excess of Te. This effect has been observed in Bi_2Te_3 (11) and PbSe (12). The result of extensively zone refining an ingot, e.g., our sample Z21-35, would be to bring the solid composition close to the (p-type) invariant point, while a single Bridgman pass (B51-1) would alter the starting (stoichiometric) composition less.

On the other hand, some correlation has been shown between the Hall coefficient and the segregation of impurities (Fig. 5). It is entirely possible that the same acceptor impurity occurs in all starting materials. Although ingot Z21-35 was extensively zone refined, it was made from less pure starting materials than ingot B51-1. The difference in purity of the starting materials might account for the fact that ingot Z21-35 apparently has a higher extrinsic hole concentration than ingot B51-1. Arsenic and antimony are common impurities in Te. They are not readily detectable by spectroscopic means so that spectroscopically pure Te might contain appreciable quantities of these impurities. If As or Sb atoms were to substitute in place of Te in the HgTe zinc blende lattice, they would act as acceptors. Because of the volatility of these impurities, zone refining the compound in a closed system (as was done for ingot Z21-35) would segregate them very slowly, so that the general level of impurity in the starting materials would be maintained.

Conclusion

Mercuric telluride has an extremely small but finite energy gap. It has high carrier mobilities characteristic of low energy gap compound semiconductors, and these high mobilities stem from low effective masses. Mercuric telluride also shares with most other semiconductors the fact that the electron mobility is higher than the hole mobility. As a result of the low energy gap, interpretation of the temperature variation of the Hall coefficient is not straightforward. Material which appears to be n-type may be in reality p-type. All HgTe synthesized by the authors appears to be p-type. The explanation could be in the p-type nature of the invariant solid composition of HgTe or in the presence of a dominating acceptor impurity.

Acknowledgment

The authors wish to acknowledge the help of Messrs. A. R. Liboff and L. Weaver who performed the measurements on ingot Z21-35. They also wish to thank Mr. D. Howell for assistance in preparing the manuscript.

Manuscript received April 14, 1958.

Any discussion of this paper will appear in a Discussion Section to be published in the June 1959 JOURNAL.

REFERENCES

1. C. H. L. Goodman, *Proc. Phys. Soc.*, **67B**, 258 (1954).
2. J. G. N. Braithwaite, *ibid.*, **64B**, 274 (1951).

3. O. D. Elpat'evskaya, R. A. Konikova, A. R. Regel, and I. V. Yavorskii, *Zhur. Tekh. Fiz.*, **26**, 2154 (1956); O. D. Elpat'evskaya, and A. R. Regel, *ibid.*, **26**, 2432 (1956); *ibid.*, **27**, 45 (1957).
4. A. I. Blum, and A. R. Regel, *ibid.*, **21**, 316 (1951).
5. E. Nikol'skaya, and A. R. Regel, *ibid.*, **25**, 1352 (1955).
6. T. C. Harman, and M. J. Logan, *Bull. Am. Phys. Soc.*, Series II, **3**, #1, Abstract E2, 15 (1958).
7. U. Zroll, *Z. Physik*, **138**, 167 (1954).
8. D. J. Howarth, R. H. Jones, and E. H. Putley, *Proc. Phys. Soc.*, **70B**, 124 (1957).
9. R. O. Carlson, Private communication.
10. R. O. Carlson, *Bull. Am. Phys. Soc.*, Series II, **2**, #7, Abstract L7, 347 (1957).
11. C. B. Satterthwaite, and R. W. Ure, Jr., *Phys. Rev.*, **108**, 1164 (1957).
12. A. F. Goldberg, and G. R. Mitchel, *J. Chem Phys.*, **22**, 220 (1954).

Electron Mobility in InP

M. Glicksman and K. Weiser[1]

RCA Laboratories, Princeton, New Jersey

ABSTRACT

The Hall mobility of electrons in InP has been observed as a function of temperature and of carrier concentration. A lattice mobility of 5000 cm²/v-sec at 290°K is calculated from these results, varying with temperature at least as rapidly as T^{-2}. The observations can be interpreted by assuming a combination of lattice and ionized impurity scattering with an effective mass of the order of 0.05 m_o or less.

The properties of the III-V compound indium phosphide are of interest because of its relatively large forbidden band-gap [1.25 ev (1)] and yet high electron mobility, with measured values as high as 4500 cm²/v-sec at 290°K. As yet little is known about the band structure or the scattering processes in this material. The study of the temperature dependence and the effect of impurities on the mobility reported in this paper indicate that the electrons in InP have a small effective mass (probably less than 0.05 m_o); concurrent investigations reported elsewhere (2) show that the lowest conduction band is spherically symmetric. In the purest of the crystals investigated in this study, the mobility varies as rapidly as T^{-2} in the temperature range 200°-300°K, indicating that scattering by the acoustic phonons of the lattice (which would give a mobility $\alpha\ T^{-1.5}$) is not the only scattering mechanism present.

Crystal Properties

The crystals used in this study were cut from polycrystalline ingots grown in sealed quartz vials, under a phosphorus pressure of about 10 atm. From data (3) on the system In-InP, we estimate that the melt consists of approximately 10% In and 90% InP. In general, the slabs were of a single crystal or at most contained one grain boundary. The homogeneity was investigated by a continuous scan of the variation of resistivity over the length of the bars measured, and only those which indicated a uniform resistivity, with at most perhaps 10% smooth variation over the section employed, are included.

The problem of compensation is an important one. Of course if the lattice mobility is known, the amount of compensation can be estimated from the measured values. However, if this is not the case, other, less precise means are employed. The homogeneity requirement is applied to this end, since it is expected that materials of large compensation will vary more radically in resistivity as a function of position in the crystal. The variation of mobility at a given temperature as a function of carrier concentration also should be considered, since of course anomalous results will appear for a crystal heavily compensated. One of these latter crystals (S67) is included in the group reported, as an example. Finally, the mobility should become essentially independent of the impurity concentration as the crystal purity improves. This is apparent for the purest samples investigated in the temperature range 200°-300°K (Fig. 1).

Procedure

A number of geometrical arrangements for the contacts to the crystals has been used. With the samples reported, the shape of the part measured is rectangular, with two sets of side probes for measuring potentials affixed in addition to the current contacts. Two sets are used so that the variation of the Hall coefficient along the length can be observed. The side probes in some cases were arms of the material itself, the whole bridge sample being cut with an ultrasonic tool; in other cases, the side contacts were soldered; and for some crystals they were 0.002 in. diameter wires welded to the indium phosphide. The last approached closest to the ideal situation, in which one wants no perturbation to the condition of the crystal itself from the contacts.

In all cases the contacts were ohmic in the region employed, i.e., the current-voltage relationship was a linear one. The region of contact usually was prepared for soldering by plating with copper, indium, or nickel. No appreciable difference was noted, and copper was used for most of the crystals with soldered contacts.

No special precautions were taken with the surfaces in this study. Most of the crystals had sand-blasted surfaces. However, several of the samples were acid-etched to leave a shiny surface. No dif-

[1] Present address: IBM Laboratories, Poughkeepsie, N. Y.

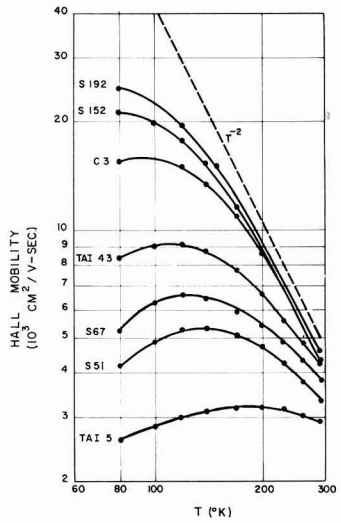

Fig. 1. Measured Hall mobilities $R_H\sigma$ as a function of temperature for n-type indium phosphide. Values for C3 have been adjusted to give 4300 cm^2/v-sec at 290°K.

ference in the results of the measurements was found due to the different surface treatments.

The Hall effect and the conductivity were measured as a function of temperature using a d-c system for the electrical measurements and a thermally isolated system for the temperature stabilization. The Hall voltage was measured, in all cases, as a function of the magnetic field, and the values quoted are those applicable in the limit of zero fields. Only the purest specimens showed any appreciable variation with magnetic field.

Observations

The values of the mobility as a function of temperature are shown in Fig. 1. Some of the electrical properties of the crystals are included in Table I. The crystals are listed in the sequence of increasing mobility at 77°K, which is also the sequence of decreasing electron concentration, except for the highly compensated crystal S67. The last three crystals have almost the same values of mobility in the temperature range 200°-300°K, indicating that in this region the mobility is dominated by lattice scattering. The slope of the mobility curves in this temperature range indicates a lattice mobility varying at least as T^{-2}. A dependence of T^{-2} was assumed in the analysis that follows.

Table I. Properties of n-type indium phosphide crystals

Crystal	Concentration of electrons at 290°K, 10^{16}cm^{-3}	Mobility at 290°K, cm^2/v-sec	Mobility at 77°K, cm^2/v-sec
TAI5	54	2910	2600
S51	7.4	3400	4170
S67	0.37	3800	4170
TAI43	4.3	4200	8300
C3	2.6	3800	13,500
S152	0.83	4300	21,000
S192*	0.63	4500	23,400

* These values represent the results for a number of samples, while the curve S-192 in Fig. 1 is for one which happened to have the largest mobility.

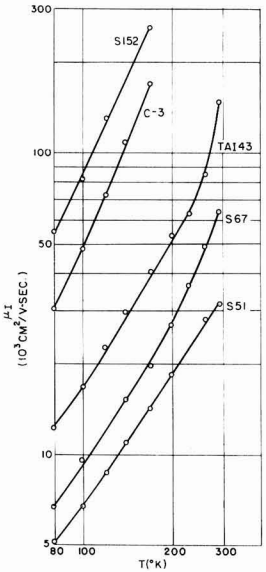

Fig. 2. Mobilities for scattering by ionized impurities in n-type InP as a function of temperature. Values were calculated from the observations of Fig. 1, assuming a lattice mobility $\mu_L = 4.2 \times 10^8\ T^{-2}$ cm^2/v-sec.

Discussion and Analysis

The data were analyzed in terms of a combination of lattice and ionized impurity scattering. The lattice scattering was assumed to be proportional to T^{-2}, as required by the observed variation of the mobilities of the purest crystals. The magnitude of the mobility at room temperature, even in the purest crystals, is still affected by the presence of ionized impurities. This contribution was estimated from an extrapolation of the low-temperature values of the impurity scattering mobility, which involved a reiterative procedure. The resulting lattice mobility is $4.2 \times 10^8\ T^{-2}$ cm^2/v-sec, giving a value of 5000 cm^2/v-sec at 290°K. The impurity mobilities for most of the crystals shown in Fig. 1 were obtained by using the expression for the combination of impurity and lattice mobilities given by Conwell (4). This expression assumes two conditions not actually present in our case. First, it refers to conductivity mobilities, whereas the measured values here are Hall mobilities. However, the ratio of Hall to drift mobility is unknown, and we have assumed it to be 1. This assumption is likely to be poorest for the crystals with largest impurity scattering.

Second, the Conwell expression assumes that the lattice scattering relaxation time is inversely proportional to the square root of the energy. If, as is likely, the scattering in indium phosphide is much like that thought to be the case in indium antimonide (5), i.e., dominantly polar scattering by the optical modes, the relaxation time approximation does not hold. The polar scattering is not strongly dependent (6) on the energy, however, for the examples under discussion here, and the error made in this assumption should not have a significant effect on the conclusions which can be drawn.

The resulting impurity scattering mobilities, calculated from the data by the subtraction technique discussed above, are given in Fig. 2 as a function of temperature. These are now believed to be in order of impurity content, so that it is clear that crystal S67 does have an impurity concentration between that of TAI43 and S51, at least ten times its net electron concentration. The mobilities have a strong positive temperature dependence, varying as $T^{3/2}$ below about 40,000 cm²/v-sec, and as T^{2} for mobilities larger than this value. This $T^{3/2}$ temperature dependence is in good qualitative agreement with that calculated by Brooks (7) and Herring (8). The change in slope observed may be due to the assumptions noted above. The greater slope is also in the region of reduced accuracy of the subtraction procedure because the mobility is dominated by the scattering by the lattice. We note the qualitative behavior as in strong support of our assumptions about the lattice mobility and wish to look further now into the direct behavior of the measured mobilities on the concentration of impurity centers present.

With the assumed lattice mobility, it is possible to calculate the mobility as a function of ionized impurity concentration, making use of the expression given by Brooks (7) and Herring (8) for the scattering by charged impurities.

$$\mu_I = \frac{4K^2}{e^3(m^*)^{1/2}N_I}\left(\frac{2kT}{\pi}\right)^{3/2}\frac{1}{\ln(1+b)-b/(1+b)}$$

$$\text{with } b = \frac{6Km^*(kT)^2}{\pi n h^2 e^2}$$

where K, the dielectric constant, was taken (9) as 10.8, and N_I and n are the densities of ionized impurities and electrons, respectively. The effective mass was retained as a parameter, and the results of the calculations at the three temperatures 80°, 120°, and 200°K are shown in Fig. 3(a), (b), and (c), respectively. The values 1, 0.1, 0.04, and 0.01 were used for the effective mass ratio m^*/m_o.

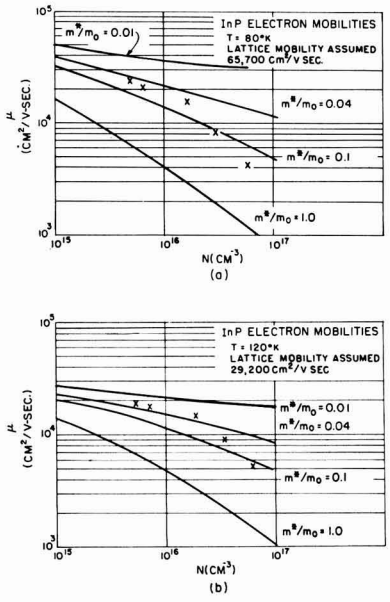

Fig. 3 a and b. Mobilities of electrons in indium phosphide as a function of ionized impurity concentration at (a) 80°K, and (b) 120°K. Curves are calculated.

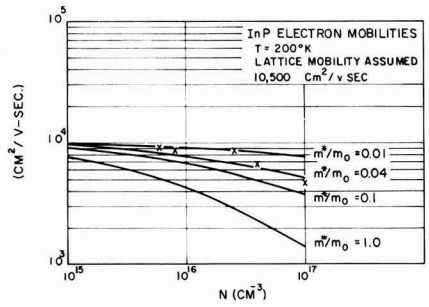

Fig. 3c. Same as Fig. 3a and b except at 200°K

Plotted in these figures are five points representing, in increasing impurity concentration, the crystals S192, S152, C3, TAI43, and S51. The values are plotted at the measured electron concentrations, while the calculated curves are for impurity concentrations. There are two obvious features of these curves. The first is that the three purest crystals do appear to lie along a consistent effective mass curve as a function of concentration, indicating that the electron density and the ionized impurity density are about the same. This is not the case for crystals TAI43 and S51. We conclude that these latter crystals are compensated appreciably. This is borne out by the observation that another sample of S51, cut close by the crystal described here, had an electron concentration 50% larger, i.e., 12×10^{16} cm^{-3}.

The second feature of interest is that the effective mass value giving the best fit to the curves is different for the different temperatures. Thus a value for m^*/m_o of about 0.05 is appropriate at 80°K, while about 0.02 is better at 120° and 200°K. Of course these values depend on the lattice mobility assumed. The values for the lattice mobility are extrapolated from high-temperature measurements using a power law dependence of T^{-2}. It is possible that the mobility deviates from a power law, especially if dominated by polar optical mode scattering. The value at 80°K is thus less certain than the values at higher temperatures.

Conclusions

The measurements of mobilities reported indicate that the electrons in indium phosphide have a lattice mobility varying with temperature at least as rapidly as T^{-2}. The observations, if interpreted as involving, in the purest crystals, essentially uncompensated samples, would indicate that the dependence is just this in the temperature range 200° to 300°K. Crystals of concentration 6×10^{15} electrons per cm³ have a mobility of 23,400 cm²/v-sec at liquid nitrogen temperatures, with the maximum in the mobility occurring at still lower temperatures. This would indicate that previous observations of Harman and Stambaugh (10) of a maximum mobility of 14,000 cm²/v-sec at 110°K for a crystal with an electron

concentration of 4×10^{15} cm^{-3} involved considerable compensation, perhaps of a factor five or more. An even larger amount of compensation is indicated for crystal A_n of Folberth and Weiss (11), which has a maximum mobility of about 8000 cm^2/v-sec, for an electron concentration of about 4×10^{15} cm^{-3}. Our observations indicate a lattice mobility at 290°K of 5000 cm^2/v-sec.

The mobility observations have been fitted by a mixture of lattice scattering and ionized impurity scattering. This fit involves the electron effective mass as a parameter, and values for m^*/m_o of 0.05 or less are found to give a fit to the data. Our conclusion as to the effective mass values is conservative because the analysis involves a number of assumptions of only approximate validity. Certainly a very small value is indicated, and the results are in good agreement with the approximate value 0.02 recently deduced from optical measurements by Reynolds, Lilburne, and Dell (12).

Acknowledgment

The authors wish to thank Ronald Guire, Benjamin Seabury, and Robert Vannozzi for their aid in the growth of these crystals and the measurements.

Manuscript received May 13, 1958. This paper was prepared for delivery before the New York Meeting, April 27-May 1, 1958. Work supported in part by the U. S. Air Force.

Any discussion of this paper will appear in a Discussion Section to be published in the June 1959 JOURNAL.

REFERENCES

1. F. Oswald, *Z. Naturforsch.*, **9a**, 181 (1954).
2. M. Glicksman, *Bull. Am. Phys. Soc.*, **II 3**, 120 (1958).
3. (a) J. v. d. Boomgaard and K. Schol, *Philips Research Repts.*, **12**, 127 (1957); (b) K. Weiser, *J. Phys. & Colloid Chem.*, **61**, 513 (1957); (c) M. Shafer and K. Weiser, *ibid.*, **61**, 1424 (1957).
4. P. P. Debye and E. M. Conwell, *Phys. Rev.*, **93**, 693 (1954).
5. H. Ehrenreich, *J. Phys. Chem. Solids*, **2**, 131 (1957).
6. D. J. Howarth and E. H. Sondheimer, *Proc. Roy. Soc.*, **A 219**, 53 (1953).
7. H. Brooks, *Phys. Rev.*, **83**, 879 (1951).
8. C. Herring, Unpublished results.
9. F. Oswald and R. Schade, *Z. Naturforsch.*, **9a**, 611 (1954).
10. T. C. Harman and E. P. Stambaugh, Recent News Paper, Semiconductor Symposium, Electrochem. Soc. Meeting, May 1957.
11. O. G. Folberth and H. Weiss, *Z. Naturforsch.*, **10a**, 615 (1955).
12. W. N. Reynolds, M. T. Lilburne, and R. M. Dell, *Proc. Phys. Soc.*, **71**, 416 (1958).

Preparation and Some Characteristics of Single-Crystal Indium Phosphide

T. C. Harman, J. I. Genco, W. P. Allred, and H. L. Goering

Battelle Memorial Institute, Columbus, Ohio

ABSTRACT

A technique for purifying phosphorus, reacting elemental indium and phosphorus, purifying the compound, indium phosphide, by a directional recrystallization, and growing large crystals all in one glass tube is described. A crystal puller for decomposable solids is described in detail and results for indium phosphide discussed. The electron mobility as a function of temperature is given for two single-crystal specimens. An electron mobility of 4000 cm^2/v-sec at 300°K for a specimen containing a carrier concentration of 1×10^{17}/cm^3 was achieved. Lifetime measurements by the photoconductivity-decay method are discussed. The optical-transmission characteristics of specimens containing electron concentrations of 10^{16}/cm^3 and 10^{15}/cm^3 are presented.

At the present time, there is considerable interest in semiconducting compounds for their numerous potential applications. Substantial effort is being expended upon methods (1, 2) for preparation of pure crystals of sufficient size for use in solid-state devices. Indium phosphide is particularly attractive for use in such solid-state devices as solar batteries, transistors, and rectifiers because of its energy gap of 1.25 ev and high electron mobility. It is the purpose of this paper to present two methods for the preparation of pure, large crystals of indium phosphide and to describe some characteristics of those crystals.

Crystal Growth of Indium Phosphide by Control of Liquid Indium-Phosphorus Vapor Reaction

Since indium is extremely insoluble in solid indium phosphide, pure crystals of the compound can be grown from an indium-indium phosphide solution. The technique of reacting the elements, purifying the compound by a directional recrystallization, and growing crystals all in one operation is now described. A diagram of the apparatus is shown in Fig. 1. A quartz boat containing indium and pure phosphorus is sealed in a quartz tube under a vacuum of approximately 10^{-6} mm Hg. The quartz tube is then placed in a three-furnace arrangement, as shown in Fig. 1. A temperature gradient of 60°C (1000°-1060°C) is maintained along the boat containing the indium by proper positioning of the furnaces. The temperature of the third furnace, which controls the phosphorus pressure in the tube, is increased slowly to 485°C. The phosphorus vapor then reacts with the liquid indium. As the reaction proceeds, the solubility of InP in liquid indium is exceeded and InP crystallizes at the cooler end of

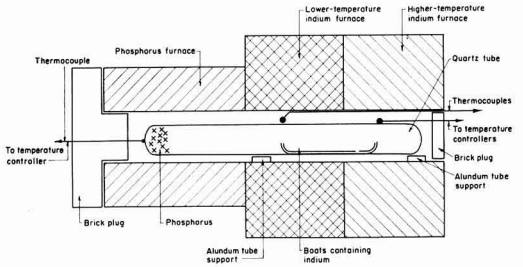

Fig. 1. Diagram of apparatus used for preparing InP

the boat. As the reaction proceeds, the solid-liquid interface slowly moves from the cooler end of the boat toward the hot end. Of the ingots prepared by this technique, at least five single-crystal dumbbell-shaped specimens (15 x 5 x 2 mm) were obtained. Some of the ingots were almost entirely one crystal.

This method of obtaining InP from indium solution has the advantage over the solution-growth method suggested by Wolff (1) in that large-bulk, single-phase ingots of the compound are obtained. Thus, no chemical techniques are required to separate the indium from the compound crystals.

Another possible advantage of the method over the usual crystal-growing processes is that the intrinsic number of lattice imperfections, that is, vacancies and interstitials, should be lower because the compound is crystallized at a temperature below its melting point. However, since the single crystals prepared by this technique are in contact with the quartz boat and, usually, with other crystals, gross imperfections (2) are probably introduced as a result of thermal stresses incurred on cooling. One crystal-growing technique that eliminates contact of the solidified crystal with container materials is the Czochralski technique. However, conventional germanium and silicon crystal pullers cannot be used for compounds, such as InP, that have a high vapor or dissociation pressure (3, 4).

Crystal Puller for Decomposable Solids

The crystal puller described in this paper is a modified version of the one described by Gremmelmaier (5) for the pulling of InAs and GaAs. It is believed that, with this system, the pulling of large, single-crystal ingots of InP, InAs, and GaAs can be reduced to a technique as standard as that for silicon. The over-all pulling system is illustrated in Fig. 2. The pulling system is variable, with pulling speeds as low as 1 mm/hr. Two Alnico V magnetron magnets which are coupled to a nonsymmetrical Permendur sleeve are used to pull and rotate the seed. The Permendur sleeve is housed in a Vycor jacket to protect it from phosphorus vapors.

The entire pulling chamber is heated to the desired temperature by resistance heaters. A voltage regulator on the resistance furnaces is necessary to obtain the required temperature control. The furnace around the lower part of the pulling chamber is constructed from a 10-cm-diameter Vycor tube, with the spiraled heating elements of 22-gauge Chromel wire, providing good visibility of the molten surface and seed crystal.

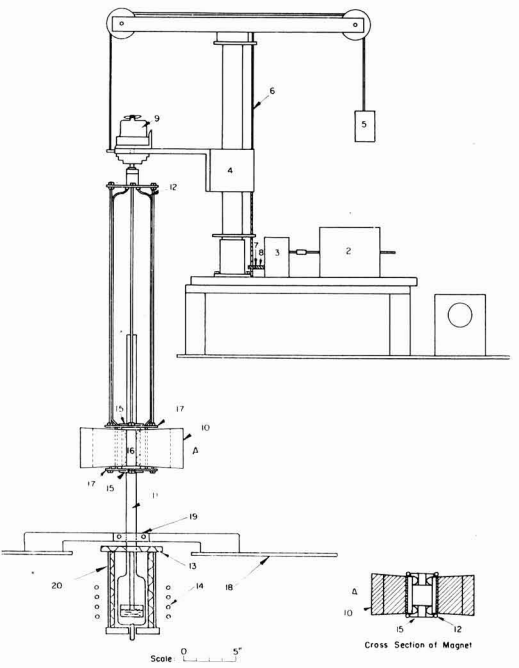

Fig. 2. Diagram of magnetic crystal puller. 1, Variac speed control for 1/15-hp, 115-v, d-c motor; 2, 1/15-hp, 115-v, d-c motor; 3, Boston gear reductor, ratio, 200:1; 4, mechanism for raising and lowering crystal, over-all traversing length, 18.5 in.; 5, counterbalance weight; 6, threaded rod; 7, spur gear; 8, worm gear; 9, clock motor (6 rpm); 10, Alnico V magnetron magnets; 11, stainless steel tube used as upper furnace housing, dimensions, 1.5-in. OD, 1⅜-in. ID, 23-in. length; 12, water lines for cooling magnet; 13, Chromel heating element to maintain desired ambient temperature at top of pulling chamber to control vapor pressure; 14, induction heating coil for melting InP; 15, Transite bearings; 16, Permendur spacers, dimensions, 2⅞-in. length, 1-in. width, 1⅞-in. depth; 17, upper and lower base plates to support magnet; 18, table top; 19, support for upper furnace housing; 20, transparent Vycor furnace, using Chromel heating element to maintain vapor pressure.

A diagram of the pulling chamber is shown in Fig. 3. The pulling chamber is a sealed Vycor envelope evacuated to a pressure of 2×10^{-6} mm Hg. A double-wound furnace of 22-gauge Chromel wire covered with porcelain beads is used as the upper furnace. The double winding is necessary to eliminate 60-cycle vibration of the winding inside the magnetic field.

The seed rod has bearings of AUC graphite, with a clearance of 6 mils at room temperature. It was found that graphite bearings are necessary for smooth rotation and withdrawal of the growing crystal. An induction heater which couples directly to the material is used to heat the melt. The temperature of the melt is controlled by a Pt-Pt, Rh thermocouple which feeds into a L&N temperature controller.

The first ingots pulled in this system were InAs, and single crystals were obtained. Later, InP crystals were pulled in this system, and Fig. 4 shows one of these. The InP was pulled at a rate of 5 mm/hr and a rotational rate of 6 rpm. The lowest tempera-

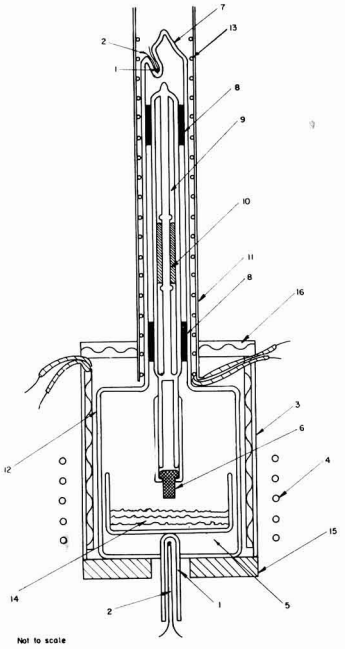

Fig. 3. Diagram of magnetic crystal puller reaction chamber. 1, thermocouple well; 2, Pt, Pt-Rh thermocouple; 3, Vycor-walled furnace wound with Chromel resistance wire; 4, induction heating coil; 5, quartz crucible, dimensions 1 15/16-in. OD, 1 13/16-in. ID, 2-in. height; 6, InP seed held in place with a Vycor seed holder; 7, Vycor tube, dimensions 25-mm OD, 21-in. length; 8, graphite bearings, 1.2-in. length; 9, Vycor tube to protect Permendur, dimensions 19-mm OD, 2⅝-in. length; 10, Permendur core, dimensions 2½-in. length, 15-mm OD, 8-mm ID; 11, stainless steel furnace housing; 12, Vycor tube, 64-mm OD; 13, upper furnace, 22-gauge, double-wound Chromel wire covered with porcelain beads; 14, InP melt; 15, Transite base plate; 16, Transite cover plate with Chromel heating element.

ture in the system was controlled at 485°C by the thermocouple at the top of Fig. 3. At this temperature the pressure of phosphorus is 5 atm. According to Boomgaard and Schol (4), a phosphorus pressure of 5 atm corresponds to a melt composition of InP-In at equilibrium of approximately 60 at. % In. The low solubility of indium in solid InP is illustrated by the relatively low carrier concentration, $10^{17}/cm^3$, and high electron mobility, 3000 $cm^2/v\text{-}sec$, of a polycrystalline n-type specimen cut from the ingot.

The polycrystalline seed used was obtained from a zone-melted ingot of InP. From Fig. 4, it can be seen that the crystal grew rapidly into large crystallites. The crystal in the front is a large single portion with the characteristic flats running the length of the crystal. The crystals on the right edge of the photograph start from the seed and run the entire length of the ingot. These results suggest that, with a single-crystal seed, large single-crystal ingots of InP can be grown easily.

Purification of Phosphorus

Several possible techniques were investigated for the purification of phosphorus. These techniques included sublimation of red phosphorus in a hydrogen stream, zone melting of white phosphorus, and vacuum distillation of white phosphorus. However, the results are believed inconclusive concerning the effectiveness of each technique because of the effects of oxygen impurities. Resistivities at room temperature ranged from 10 ohm-cm to 10^{-2} ohm-cm. Carrier concentrations ranged from $10^{19}/cm^3$ to $10^{17}/cm^3$. As discussed in the next section, oxygen is believed to produce deep-lying levels in InP which effectively trap out electrons originating from shallow donor levels. Thus, extremely low carrier concentrations can occur.

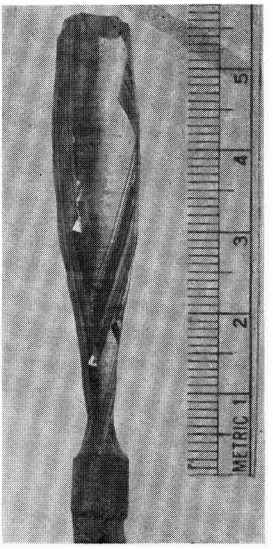

Fig. 4. Pulled ingot of InP

A technique has been developed that minimizes the contamination from oxygen and other impurities. In this method, a Vycor apparatus is used to purify phosphorus, to prepare the compound from the elements, and to grow crystals of the compound. As shown in Fig. 5, this system consists of a reservoir for red phosphorus, a primary condenser, a connection to a high-vacuum line, and a secondary condenser. A quartz reaction tube containing indium in a double quartz boat is attached to the secondary condenser. Although the oxide on the indium is carefully removed by scraping and cutting, an oxide film on the indium usually occurs upon melting. To remove the oxide film, two boats are used, as shown in Fig. 5. The inner boat possesses a small orifice which allows the molten indium to flow from the outer boat into the inner boat. The indium oxide floats on the surface of the outer boat

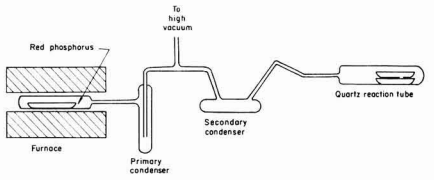

Fig. 5. Diagram of the phosphorus purification system

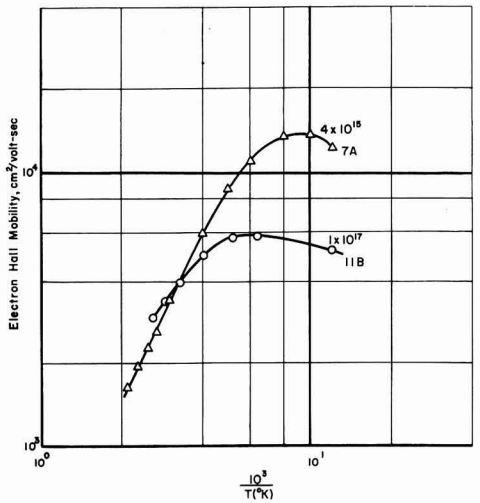

Fig. 6. Electron Hall mobility as a function of reciprocal temperature for two single-crystal specimens of InP.

and does not enter the inner boat, thus providing a clean surface for reaction.

The procedure for the purification of phosphorus is as follows. The system is thoroughly outgassed and evacuated to a pressure of about 4×10^{-5} mm Hg. The red phosphorus is heated to temperatures ranging from 300° to 380°C and sublimed into the primary condenser. When a sufficient amount of white phosphorus has collected in the primary condenser, the reservoir and the vacuum line are sealed off. Thereafter, the white phosphorus is distilled from the primary reservoir at 150°C into the secondary condenser and from the secondary condenser at 140°C into the quartz reaction tube. Each preceding section is sealed from the remaining part of the system after a distillation is carried out to prevent back distillation. The amount of white phosphorus admitted to the reaction tube is measured volumetrically. The reaction tube then is placed in the three-furnace arrangement shown in Fig. 1. To prevent oxygen from diffusing through the quartz reaction tube, the reaction tube is enclosed in a quartz protection tube containing approximately 2/3 atm of argon and some titanium chips. The titanium chips act as an effective getter of oxygen at the higher temperatures. In experiments in which titanium chips and a protection tube were not used in the preparation, deep-lying levels were always found. On the other hand, in experiments in which titanium chips and a protection tube were used, no evidence of deep-lying levels was obtained from the electrical and photoconductivity measurements.

Electrical Properties of Single-Crystal Indium Phosphide

Measurements of the Hall coefficient and the resistivity of a number of single-crystal specimens of InP showed that electron-carrier concentrations have been achieved in the 10^{16}/cm³ to 10^{17}/cm³ range at room temperature. However, the temperature dependence of the Hall coefficient of the lower carrier-concentration samples indicates the presence of multiple impurity or defect levels which effectively trap out electrons from shallow donor levels. By using the preparation techniques discussed in the previous sections, a carrier concentration of 1×10^{17}/cm³ is obtained. This relatively high carrier concentration is believed due to a low concentration of compensating acceptor impurities. As Fig. 6 shows, the uncompensated Specimen 11B has the same electron Hall mobility at room temperature as the low carrier-concentration Specimen 7A. Why the mobility curve of Specimen 11B rises above that of Specimen 7A cannot be explained on the basis of the usual lattice and impurity scattering concepts. The unusual mobility behavior of the specimen containing deep-lying levels (Specimen 7A) and the uncompensated Specimen 11B is being investigated further.

Lifetime Measurements

Lifetime measurements by the photoconductivity-decay method were carried out on several specimens. For the specimens of lower carrier concentration ($<10^{16}$/cm³), a long time constant of about 600μ sec was observed. By a pulse method, it was found that the long time constant was probably due to trapping of majority carriers. For the higher carrier-concentration samples, the photoresponse was too small to measure. The photoconductivity results suggest that the large photoresponse-time constant is due to nonequilibrium carriers which are trapped by deep-lying levels. Presumably, the source of the deep-lying levels is the oxygen impurity.

Optical Properties

Results of transmission measurements on two samples are given in Fig. 7. The thickness of the two specimens was the same, 4.5 mm. The specimens were shown to be optically homogeneous by masking various regions and measuring the percentage transmission of the unmasked areas. The variation

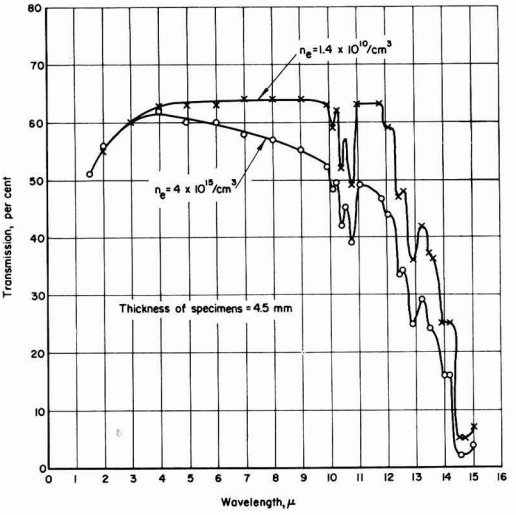

Fig. 7. Transmission characteristics of two N-type single-crystal specimens of InP at 300°K.

in percentage transmission was a few per cent. As shown in the figure, the percentage transmission was determined between 1.5μ and 15μ. At the short wave length, the transmission decreases from a maximum of 63% at 4μ to 51% at 1.5μ. In the intermediate wave length range, the transmission of the 10^{15} sample decreases from a maximum of 61% to 52% at 10μ, but the transmission of the 10^{10} sample is constant at 63%. The observed difference is probably due to free-carrier absorption. In the 10-15μ region, structure is observed in both specimens. Transmission minima appeared in three sets of three. Oswald (6) has observed two absorption bands in the 13-15μ region which correspond to the large transmission minima. The structure obtained in the 10-15μ range is similar to the lattice-absorption bands observed in germanium and silicon (7); however, there is more regularity.

Acknowledgments

The authors are indebted to E. P. Stambaugh for carrying out some of the preparation experiments, to E. B. Dale and R. Bray for the photoconductivity results, and to R. K. Willardson and A. C. Beer for many valuable discussions.

The research was supported jointly by the Army, Navy, and Air Force under contract with the Massachusetts Institute of Technology and performed under subcontract with the Massachusetts Institute of Technology.

Manuscript received April 25, 1958. A preliminary account of this paper was prepared for delivery at the Washington Meeting, May 13-16, 1957.

Any discussion of this paper will appear in a Discussion Section to be published in the June 1959 JOURNAL.

REFERENCES

1. G. Wolff, P. H. Keck, and J. D. Broder, *Phys. Rev.*, **94**, 1410 (1954).
2. R. E. Maringer and J. J. Duga, To be published.
3. J. van den Boomgaard and K. Schol, *Philips Research Repts.*, **12**, 127 (1957).
4. K. Weiser, *J. Phys. & Colloid Chem.*, **61**, 513 (1957).
5. R. Gremmelmaier, *Z. Naturforsch.*, **11a**, 511 (1956).
6. F. Oswald, *ibid.*, **9a**, 181 (1954).
7. R. S. Collins and H. Y. Fan, *Phys. Rev.*, **93**, 674 (1954).

Preparation of Crystals of Pure Hexagonal SiC

D. R. Hamilton

Research Laboratories, Westinghouse Electric Corporation, Pittsburgh, Pennsylvania

ABSTRACT

The mode of growth of SiC crystals in laboratory furnaces is examined. It is shown that the crystals grow in an environment dominated by radiation, and that this environment may be responsible for the specific orientation and possibly the habit of the crystals. It is demonstrated that, under normal experimental conditions, crystal growth is unlikely to proceed by a two-dimensional nucleation mechanism. The means of producing relatively pure crystals are discussed.

It has been known that large crystals of the semiconductor SiC occasionally grow during the operation of commercial SiC furnaces. Lely (1) recently succeeded in synthesizing crystals of this material on a laboratory scale. Pieces of SiC, formed into a hollow cylinder in a graphite crucible, were heated in a graphite tube furnace to about 2500°C. The temperatures were arranged so that the center of this cylinder of SiC was cooler than the exterior. Silicon carbide vapor diffusing inward thus became supersaturated and condensed in the center of the cylinder in the form of single crystals. The composition of the growing crystals was altered by addition of certain impurities to the atmosphere of preparation.

It is the purpose of this paper to examine in some detail the nature, habit, and orientation of crystals grown in this fashion. We shall deal exclusively with the preparation of crystals of relatively high purity.

Experimental

The furnace used in the present work is based on a design of Kroll (2) and is similar to that of Lely. It is shown in section in Fig. 1. The equipment

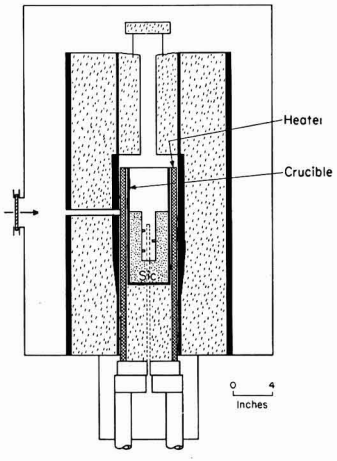

Fig. 1. High temperature graphite furnace. Planar SiC crystals are shown growing in the center of the furnace. All internal components are made of graphite or carbon, and the furnace is insulated with lampblack. The outer tank, of stainless steel, is water cooled and vacuum tight.

differs from that of Lely in that a precise temperature control is provided. Radiation from a selected area of the heater is sensed by a thermopile which is arranged to adjust the power input to the furnace by means of a saturable core reactor. The initial operating point is set by an optical pyrometer. Short-term control is about $\pm 1°C$, which is more than adequate for the present work. This system also maintains the furnace for many hours at what appears to be a constant temperature, within the reproducibility of optical pyrometer settings.

The furnace may be operated in high vacuum at temperatures up to about 2000°C. Above this temperature an inert atmosphere must be provided to suppress evaporation of the graphite furnace components. Although helium and hydrogen may be used, argon is most satisfactory. In the subsequent discussion operation at atmospheric pressure in one of these gases is presumed.

Crystal Growth and Habit

The crystals prepared by Lely deposited in the form of hexagonal pyramids, having one good face and irregular or rounded faces on the reverse. Occasionally planar crystals were grown. For physical measurements and device work the planar crystals are desirable.

Realizing that Lely's practice of using lump SiC did not lead to uniform thermal conditions, Chang and Kroko (3) carried out experiments with more homogeneous charges. These consisted of either commercial grain SiC or of silicon and carbon mixtures of various compositions. The central cavity or well, essential for crystal growth, was maintained by the use of a supporting spacer made of graphite (4). This configuration has been used extensively in the present work and is not only advantageous experimentally but also leads to a simplification that is important in estimates concerning the environment. Use of these more homogeneous charges led to a significantly higher yield of plates.

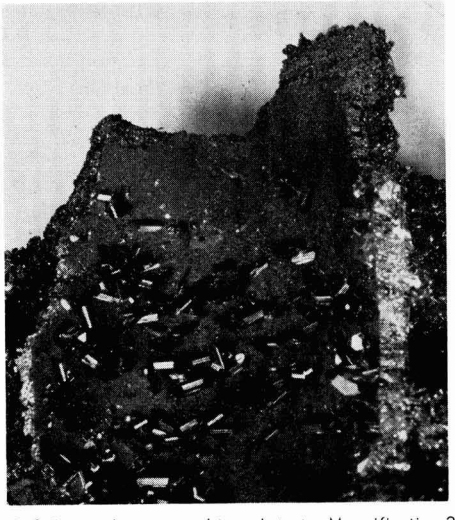

Fig. 2. SiC crystals on a graphite substrate. Magnification 2X.

Figure 2 shows part of such a charge of this configuration and the growth of crystals. The entire contents of a crucible were removed and split open to reveal the details. The majority of the crystals are planar, and, as may be seen, have a tendency toward horizontal orientation. Crystals of other orientations are present but have grown at lower rates. This behavior is found among crystals nucleated on graphite as well as on pieces of SiC, so it would appear that the behavior described is independent of the nature of the substrate.

It might be thought that convection currents within the well could supply vapor preferentially to the horizontal crystals. There is, however, some recent work that suggests that the atmosphere may be static. Lighthill (5) has examined theoretically the situation in which a hollow vertical cylinder is closed at the lower end, but is open at the upper end to a body of fluid at a lower temperature. Generally, convection occurs within the cylinder, but under certain conditions the fluid in the lower portion of the cylinder reaches the temperature of the walls and becomes stagnant. Martin (6) and others have shown that this feature is, in fact, found experimentally. We have therefore used Lighthill's work to examine the situation within the central well of the SiC furnace. To do so, we have assumed an argon ambient and have taken the Prandtl number as unity rather than $\mathrm{Pr} \sim 0.66$. This is necessary since Lighthill has solved the boundary value problem only for $\mathrm{Pr} = 1$ and ∞; the solutions vary but little with Pr. It is found that stagnation should commence at the bottom of the well for temperatures as low as 200°C. According to the theory, almost the entire tube should become stagnant at the high temperatures existing in the SiC furnace. It is probable then that the atmosphere in the central well will be static or nearly so, and we conclude that crystal growth is therefore not apt to be influenced by convection currents.

A possible explanation of the observed growth of large horizontal crystals may be found on examination of the thermal conditions about the growing crystals. A relationship between radiation cooling and crystal orientation is suggested in the following section. This relationship was early recognized by Patrick as well as by Kroko and Chang, and has been developed in discussions between these workers and the author.

Crystals receive heat from the walls of the central cavity by direct radiation and by thermal conductivity through the contact between the crystal and the well. A growing crystal also is heated by the heat of crystallization of the impinging material. This last term cannot affect orientation. The energy involved is estimated, from the data of Inghram, *et al.* (7), to be of the order of two calories an hour for a typical crystal and will be neglected in the following discussion. We will now consider the remaining terms and their possible influence on orientation.

It has been stated that crystal orientation is independent of the nature of the substrate. Thus thermal conditions at the contact cannot effect the ob-

served results. The actual magnitude of the heat flux through the contact may be estimated from the known thermal conductivity of SiC and average data for the area of contact. If the temperature gradient at the contact is 10 to 100°C/cm, then the corresponding heat flows are 0.004-0.04 w.

The heating due to radiation may be calculated if the emissivity of the crystal is known. Brugel (8) has measured the emissivity ϵ of SiC "Globar" elements at temperatures up to 1800°K. He has found ϵ to be about 0.9 and not strongly dependent on wave length or temperature. This result is not entirely unexpected, for the surface of such Globar elements is very rough. Pure single crystals, on the other hand, might be expected to show a slow decrease in emissivity at photon energies less than the energy gap. The gap is about 2 ev at 2500°C, corresponding to a photon wave length of 0.7 μ. We will assume, in the absence of other information, that the ϵ for pure single crystals is relatively low. The value used is 0.1. Now it is known experimentally that the well is essentially isothermal. Since the walls of the well may be formed of graphite, we may take $\epsilon = 0.9$ as a reasonable working figure. The energy flux into a typical crystal 1 mm^2 area is then found to be about 0.6 w.

The radiation field within the well is, however, plainly asymmetrical due to losses through the open upper end of the well. For a crystal at the midpoint of the well, this end occupies 5% of the total solid angle. The net heat loss through this end will depend on the emissivity and temperature of the area "seen." These figures are known from experimental data. It may then be estimated that a crystal of 1 mm^2 area will radiate about 10^{-2} w to this sink. Should the emissivity of SiC be greater than 0.1, then this energy loss and the effects to be ascribed to it would be correspondingly greater. The assumed low value of emissivity is unfavorable to the present arguments. This loss is sensitive to crystal orientation, for the effective radiating area depends on the cosine of the angle between the vertical (the direction of the sink) and the normal to the face of the crystal. Thus it is probable that crystals with the favored horizontal orientation will be coolest and consequently will grow most rapidly, provided that this radiative loss is the only orienting factor.

The only other heat flow is that due to the thermal conductivity of the atmosphere, which we shall assume to be argon. It has been suggested that the gas in the central well is stagnant and is isothermal with the well walls. In this event, the heat flow will be from the argon to the crystals and will be exceedingly small. If the argon is cooler than the crystals and is not isothermal with the well walls, then it may be estimated that a typical crystal would transfer, by conduction and convection, about 10^{-3} w, for a gradient of 100°/cm in the argon. This flow is so small that any orienting effects will be masked by those due to radiation. Therefore, it is concluded that orientation is governed largely by the direction and magnitude of the radiation losses.

These order of magnitude calculations indicate that the net energy losses of a growing crystal are small relative to the ambient radiation field. Consequently the temperature of the crystal should closely approach that of the walls of the well. We have measured the temperature of growing crystals and have found that this is indeed the case. The crystals, seen through an optical pyrometer, are barely distinguishable against the uniform background radiation of the surrounding well. The apparent temperature difference between a crystal and the adjacent wall is certainly not greater than 20°. This result must be examined with great care, for it is easy to be misled. As mentioned earlier, the energy gap of SiC at these temperatures is about 0.7 μ. The measurement is made at 0.65 μ in a region of high absorption and emissivity. Thus there need be no correction for energy transmitted through the crystal. The geometry of the experiment was such that direct reflection from a crystal face could not occur. Finally, examination of the crystals after the experiment showed that extensive diffuse reflection was unlikely. It is thus concluded that the temperature of the growing crystal is indeed within 20° of the temperature of the well. It should, of course, be noted that the act of measurement itself must increase this difference by increasing the radiation losses somewhat.

This temperature difference, together with the constants of the system, may be used to make calculations concerning the growth mechanism. We have estimated by the method of Harkins (9) that the surface free energy of SiC is about 3000 ergs/cm^2; it is certainly not lower than 1000 ergs/cm^2. It may then be shown that the nucleation rate of new growth layers is insufficient to explain the known growth rate. For growth to proceed by nucleation of new layers either the surface free energy would have to fall below 1000 ergs/cm^2, or the above-mentioned temperature difference would have to be greater than 50°. Since the 20° figure represents an upper limit only, it would appear that nucleation of new layers should not take place under normal conditions. Since screw dislocations are frequently found, it is probable that growth proceeds by means of a screw dislocation mechanism. There is also evidence that growth may be promoted at the crystal to substrate junction.

It has thus been shown that crystals of SiC of a particular orientation may be grown if the thermal environment is relatively isotropic and if the principal means of heat dissipation from a crystal is a directed radiative loss. Such an environment in all likelihood also influences habit, insofar as growth of crystals with large surface to volume ratios is favored. The actual growth mechanism may involve screw dislocations, but is not apt to proceed by nucleation of new layers.

Preparation of Pure SiC

Impurities present in crystals of SiC have three possible origins. They may be introduced in the starting materials, whether SiC or Si and C mixtures. Impurities may find their way from the internal fittings of the furnace into the growing crystals. Finally, contamination may originate in the atmosphere introduced into the furnace. The princi-

Table I. Spectrographic analysis of various samples of SiC, in ppm

Element Sample	Al	Fe	Ag*	Cu	Mg	Mn
Commercial green SiC†	100	10	10	30	50	15
Crystals grown from the above†	30	3	5	15	25	3
Purest SiC crystals	<10	<10			Trace	Trace

* No standards available.
† Geometric mean of the limits of concentration are quoted.

pal impurity in the argon atmosphere usually used is nitrogen, which is, as Lely and Kroger (10) have shown, a donor in SiC. Since they have described in some detail the behavior of nitrogen in SiC as well as the means of removing it from argon, we shall not discuss this point further.

Commercial green SiC is among the possible choices of starting material for the preparation of crystals of pure SiC. Its principal virtue is the low cost. On the other hand, it is known to contain a wide spectrum of impurities, as is shown in Table I.

An analysis of typical crystals grown from this SiC is shown in the second row of the table. It can be seen that a reduction in the concentration of a given element has taken place during crystal growth. Several mechanisms are involved in this purification. First, fractional sublimation takes place, since the distribution coefficient of many of the impurities is undoubtedly small. Second, the actual concentration of impurities in the atmosphere about the growing crystal is greatly reduced by two gas diffusion mechanisms. The impurities are present in the vapor phase as either the element proper or as compounds. In general these components are more volatile than SiC, and consequently may condense in a liquid or solid phase in cooler parts of the furnace. Concentration gradients are thus established which remove material from the immediate vicinity of the crystals. Thermal diffusion may also account for a certain separation. In general, large or heavy molecules diffuse down a temperature gradient to cooler regions. Finally, experiments have shown that impurities do diffuse through the SiC lattice at high temperatures. Thus impurities may diffuse out of the starting materials during the course of a run. The surface layers of the crystals may thus be less contaminated than the interior material, although diffusion naturally tends to level out these differences within the growing crystal.

Now, it is plain that the purity of the starting material may be greatly improved by the use of zone-refined silicon and high-purity carbon in place of commercial SiC. Zone-refined silicon is more than adequate for preparations of this sort, and high purity carbon may be prepared by heat treating carbon under vacuum and at high temperatures. Present results indicate that crystals grown from these materials are considerably purer than those grown from commercial SiC. Unfortunately the improvement is not as great as might be expected. One is forced to conclude that the furnace fittings are maintaining relatively high levels of contamination.

All high temperature fittings within the furnace are fabricated from graphite or carbon. Although certain of the smaller parts may be purified by heating to highest temperatures in the present furnace, the majority are too large to be accommodated in the hot zone and must be heated *in situ*. They do not reach sufficiently high temperatures for adequate purification. They remain, therefore, a pernicious source of contamination, even after many hours of purification heating.

A number of arrangements have been tried to overcome this problem without a major change in the design of the furnace. These have involved the use of double crucibles, similar to those of Lely, and systems of tightly sealed lids and baffles. The results have not been especially noteworthy.

An analysis of the purest material so far prepared is shown in the third line of Table I. This material was prepared from du Pont "Solar Cell" grade silicon and purified carbon. The crystals themselves are from 0.5 to 1.5 mm in thickness, and up to 4 mm across the hexagonal face. They are transparent in the visible region. The room temperature resistivity lies in the vicinity of 10^5 to 10^6 ohm-cm. If it is assumed that the electron mobility is not less than that found by Lely and Kroger for heavily doped samples, then the estimated room temperature carrier concentration must be of the order of $10^{18}/cm^3$. Since the electrical characteristics of the dominant impurities are not known, few firm conclusions can be drawn from this sort of information. We cannot, for example, rule out the possibility that the high resistivity is due, in part at least, to charge compensation.

Conclusions

It has been shown that SiC crystals grow in laboratory furnaces in an environment dominated by a radiative exchange of energy. The orientation and possibly the habit of the crystals is greatly affected by the nature of the radiative losses in such a system. Crystals of relatively high purity may be prepared provided care is taken in the choice of the materials used and in the maintenance of a high purity environment about the growing crystals.

Acknowledgment

The author acknowledges with great pleasure many stimulating discussions with L. Patrick, C. Cess, and L. Kroko. Thanks are also due to R. Longini for constructive criticisms of the manuscript, and to J. A. Lely and F. A. Kroger for providing us with preprints of their recent publications.

Manuscript received May 28, 1958. This paper was prepared for delivery before the New York Meeting, April 27-May 1, 1958.

Any discussion of this paper will appear in a Discussion Section to be published in the June 1959 JOURNAL.

REFERENCES

1. J. A. Lely, *Ber. deut. keram. Ges.*, **32**, 229 (1955).
2. W. J. Kroll, A. W. Schlechten, and L. A. Yerkes, *Trans. Electrochem. Soc.*, **89**, 317 (1946).
3. H. C. Chang and L. J. Kroko, Conference Paper

57-1131, American Institute of Electrical Engineers, Chicago, 1957.
4. H. C. Chang, R. E. Davis, and L. J. Kroko, International Conference on Semiconductors, Brussels, 1958.
5. M. J. Lighthill, *Quart. J. Mechanics and Applied Mathematics*, Oxford at the Clarendon Press, **6**, 398 (1953).
6. B. W. Martin, *Proc. Roy. Soc. (London)*, **A230**, 502 (1955).
7. G. De Maria, J. Growart, and M. G. Inghram, Meeting of American Physical Society, Chicago, 1958.
8. W. Brugel, *Z. Physik*, **127**, 400 (1950).
9. W. D. Harkins, *J. Chem. Phys.*, **10**, 268 (1942).
10. J. A. Lely and F. A. Kroger, Proceedings of the Garmisch Conference, 1956.

Technical Notes

Use of Bismuth as a Donor-Type Impurity in Germanium Single Crystals

George Mortimer

Clevite Transistor Products, Waltham, Massachusetts

Segregation Coefficient

The use of a doping impurity requires knowledge of its effective segregation coefficient for various conditions of growth. Bismuth was studied using considerable variations in both the concentration and the rate of advance of the solid-liquid interface.

Figure 1 shows the experimental curves obtained by growing horizontal crystals and averaging the resistivity obtained over the first 10 in. of length. The concentration of Bi in the solidified crystal can be seen to be quite dependent on the rate of growth. Following the pattern set by many other impurities, the amount of Bi introduced into the crystal per unit volume increases as the growth rate becomes more rapid (1).

Insufficient data are presently available for growth rates faster or slower than those shown at wide ranges of impurity concentration in the liquid zone. Sufficient information was gathered at one concentration, however, (approximately 50 mg Bi/100 g Ge) to show that even at the rate for the upper

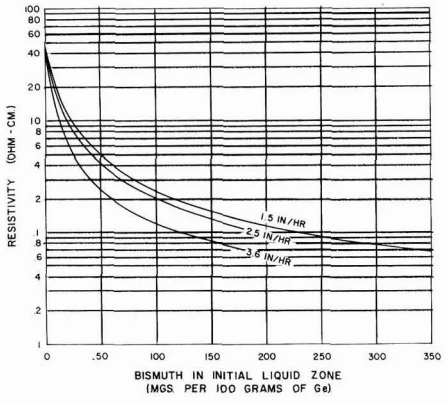

Fig. 1. Resistivity vs. quantity of Bi added to initial liquid zone (horizontally grown crystals).

curve (1½ in./hr) equilibrium had not been attained. At a growth rate of 0.67 in./hr and the doping level cited above, the resistivity averaged approximately 6.0 ohm-cm for a sample of five crystals. Data were also obtained using this concentration in the liquid at faster growth rates than those shown. The resistivity under these conditions continued to decrease, but a considerable scatter in the data made it difficult to obtain meaningful averages above 5 in./hr. At 6-7 in./hr, the liquid zone was difficult to maintain and the horizontally grown ingots generally became polycrystalline.

The segregation coefficient, computed from the data shown in Fig. 1, indicated an effective value of $K \cong 5 \times 10^{-5}$. This value was obtained using a resistivity of 4.0 ohm-cm, a mobility of 3600 cm²/v-sec, and a growth rate of 1½ in./hr.

Controlled Doping

The very small segregation coefficient cited above makes Bi an ideal impurity for growing long horizontal single crystals of Ge without observing any drop in resistivity along the length of the ingot. The concentration of impurity atoms, C, as a function of distance along the crystal, X, is given for all but the last zone by $C = KC_i e^{-K(X/l)}$, where l is the molten zone width and C_i the initial concentration in the molten zone (2).

It is assumed that initially the impurity atoms are all located in the first zone, and the remainder of the charge is intrinsic. Since K is approximately 5×10^{-5}, a total growth distance of approximately 2000 zone lengths would be necessary before the resistivity would increase by 10%. It is not normally practical to grow crystals with over-all lengths exceeding 25 zone lengths. Therefore, the end of one crystal may be used to dope the next crystal for many successive runs without the resistivity noticeably increasing and without accumulating much heavily doped end scrap.

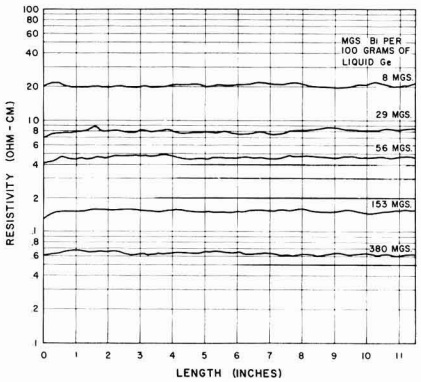

Fig. 2. Resistivity plots along the length of actual horizontally grown single crystals of Ge. The amount of Bi used to dope each of these crystals is noted just above its respective resistivity plot.

Fig. 2 shows actual resistivity plots of horizontally grown single crystals of Ge doped with Bi. The quantity of bismuth used per 100 g of liquid zone is noted on the graph above its respective resistivity plot. The liquid zone, crystal cross section, and growth rate were kept constant for all the crystals shown. This graph shows that the quantities of doping impurity necessary may easily be handled even in close to intrinsic resistivity ranges.

This procedure can be seen to allow for direct and accurate weighing of the Bi on an analytical balance for almost any liquid volume and resistivity desired. Most other Group III and V impurities, due to larger segregation coefficients and also in some cases to high vapor pressures, require the preparation and use of "master doping alloys."[1] The inconvenience of preparing these "master melts" and the difficulties involved in making them homogeneous without contamination are often considerable.

Maximum Concentration

The maximum amount of Bi that it is feasible to introduce into Ge during growth from the melt was investigated. A number of vertically pulled crystals were prepared which were heavily doped with up to 2 g of Bi per 250 g of Ge in the initial melt. These crystals were grown at relatively slow growth rates and with relatively uniform cross sections in order that equilibrium conditions might be approached.

The maximum quantity of Bi that could be introduced into these crystals during growth without adversely affecting their structural perfection was found to be of the order of 0.00005 at. % (0.1-0.2 ohm-cm). Figure 3 shows a cross section along the axis of a heavily doped crystal (0.8% Bi in the initial melt). The crystal was grown by the Czochralski technique at a rate of ¾ in./hr. The change from single to polycrystalline structure may be observed. Noticeable flaws start to appear in the crystal at a position about 40% down from the top (≅ 1.3% Bi in the melt), and the ingot became a

[1] Indium as a p-type impurity most nearly has the advantages discussed for Bi. However, even In, when used directly, must be added in quantities which are less than 1/10 of the Bi used under comparable conditions.

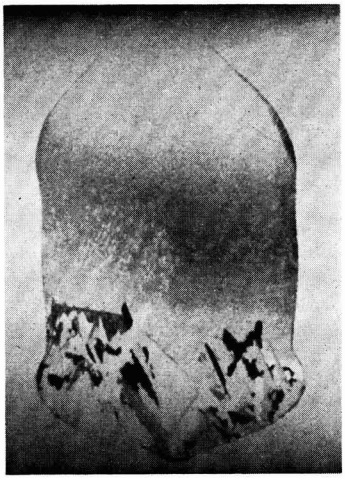

Fig. 3. Cross section from top to bottom of a vertically pulled ingot of Ge. The quantity of doping impurity added to the initial melt was so chosen that it would increase sufficiently in concentration to affect noticeably the perfection when approximately half the crystal was pulled. The gross imperfections in the center region and the polycrystal bottom were brought out by etching in silver etch.

randomly oriented polycrystal at approximately the 75% point (≅ 3.2% Bi in the melt). The resistivity was found to be 0.23 ohm-cm at the 40% point and 0.11 ohm-cm at the 75% point. Data on other crystals studied gave results very similar to those described above with polycrystal development again occurring when the resistivity had decreased to the 0.2 to 0.1 ohm-cm range.

Figure 4 shows a cross section of a heavily doped Bi crystal. This surface is cut perpendicular to the growth axis in a region between the 40 and 75% points of Fig. 3. This is the region where noticeable flaws start to appear but is prior to the randomly oriented polycrystal bottom section. The surface of

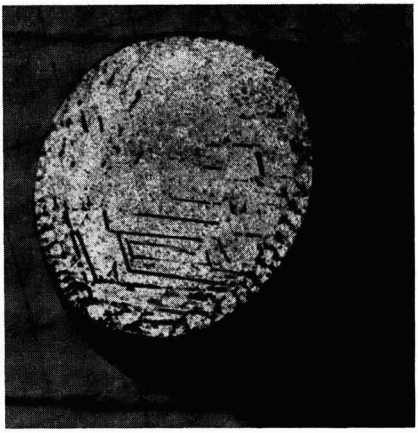

Fig. 4. Surface cut perpendicular to the growth axis from a heavily doped vertical crystal similar to that shown in Fig. 3. The surface was cut just above the region where randomly oriented polycrystal development starts. Note how the excess Bi was deposited along (1,1,1) planes in this region during growth and has been removed in the subsequent etching of this surface.

the crystal shown in Fig. 4 has been etched in silver nitrate etch.[2] It shows an anisotropic segregation of the Bi. The deep grooves indicate regions where excess Bi was deposited along (1,1,1) planes and later dissolved out during the etching process.

Bismuth was found to be most useful for controlling the resistivity of Ge crystals in the range above 1.0 ohm-cm but can be used successfully from 0.4 ohm-cm to intrinsic.

Crystal Quality

The quality of crystals produced using Bi as a doping impurity appeared comparable to that obtained using other Group III and Group V impurities.

A sample of 50 crystals produced during one period was checked for perfection. These crystals were all in a resistivity range between 1 and 10 ohm-cm. The highest dislocation density observed on any of these crystals was $6.4 \times 10^3/cm^2$ with the exception of three that had a slight amount of lineage present. Forty-four of the crystals had no readings above $3.0 \times 10^3/cm^2$, and many individual readings below $1.0 \times 10^3/cm^2$ were observed.

Bulk measurements of minority carrier lifetime on 13 samples in the 6-10 ohm-cm resistivity range produced an average value of 145 μsec. Only one reading was below 100 μsec, and the highest reading was 308 μsec.

Figure 5 shows the resistivity variation along the length of five horizontally grown single crystals produced consecutively. The same amount of Bi was used for each run. The high degree of reproducibility is indicative of the type of resistivity control that can be obtained using this doping procedure if proper care is taken of the other variables involved such as charge cross section, growth rate, and temperature control.

It is not implied that the quality of all crystals produced under all conditions was as good as these described in the preceding paragraphs. Degradation in quality, when it occurred, could be traced to other problems, however. The results definitely indicated that there are no major difficulties inherent in the use of Bi as a satisfactory doping impurity for Ge.

[2] Composition of etch: 2 parts 5% $AgNO_3$, 1 part HNO_3, 2 parts HF.

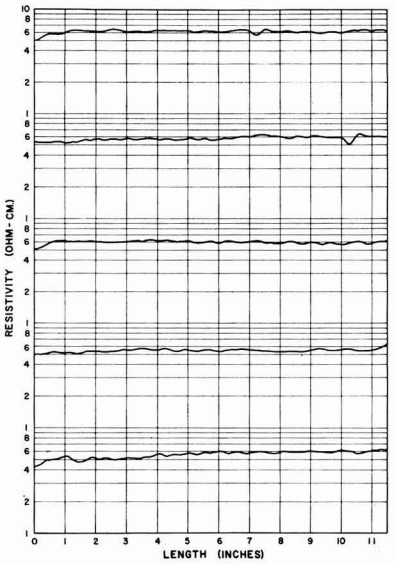

Fig. 5. Resistivity plots along the length of five consecutively grown horizontal single crystals of Ge. The same quantity of Bi was used to dope each crystal.

Acknowledgment

The author wishes particularly to thank Mr. C. C. Silva, Mr. A. A. Dulac, Mr. C. C. Wang, and Dr. J. F. Battey for their encouragement and helpful comments on this work.

Manuscript received May 29, 1958. This paper was prepared for delivery before the Ottawa Meeting, September 28-October 2, 1958.

Any discussion of this paper will appear in a Discussion Section to be published in the June 1959 JOURNAL.

REFERENCES

1. R. N. Hall, *J. Phys. Chem.*, **57**, 836 (1953).
2. W. G. Pfann, *Trans. A.I.M.E.*, **194**, 747 (1952).

Properties of Some Germanium Single Crystals Grown from Solutions of Molten Metals

H. F. John

Research Laboratories, Westinghouse Electric Corporation, Pittsburgh, Pennsylvania

Distribution coefficients and solid solubilities have been reported for a number of solutes at temperatures ranging from the melting point of germanium down to 400°C (1, 2). The data available in the lower temperature ranges for some of the more frequently used doping impurities have not always been consistent, however. The work reported here was undertaken in an attempt to obtain single-crystal material, grown under equilibrium conditions at a known, constant temperature, which would be similar to that found in the highly doped side of a p-n junction produced by an alloy fusion technique.

Under certain conditions a modified Czochralski technique can be used to grow single crystals of Ge from solutions of molten metals saturated with germanium. Germanium grown from melts containing as high as 5 at. % Sn has been described (3). The essential condition for growing crystals

from such metal solutions is the use of very slow pull rates. Slow pull rates are required because the crystal cannot be withdrawn at a rate faster than Ge can be transported by diffusion across the immobile layer which separates the growing crystal front from the main body of turbulent solution. The diffusion of material across this immobile layer can be increased if the thickness of the layer is kept to a minimum by rapidly rotating the seed crystal, and if the thermal gradient across the immobile layer is made large.

Crystal Growing

Highly doped single crystals of Ge 6 mm in diameter and a few mm thick have been grown from In, Ga, Al, and Sn-Sb solutions[1] using pull rates of 0.7-2.0 mm/hr, rotation rates of 75 rpm, and a conventional seed clamp which allowed reasonably good thermal conduction through the pull rod. Melts of known composition, whose liquidus temperatures were determined from phase diagrams, were held a few degrees above the liquidus temperature. The temperature at which crystallization takes place is then this liquidus temperature, provided crystallization takes place slowly and provided the amount of Ge removed is kept small compared to the total amount dissolved. Crystals can be grown from melts of constant composition if a reservoir of Ge is present which can go into solution as crystallization takes place onto the seed. Using the latter technique, however, it is more difficult to initiate proper crystal growth. When the seed is lowered into the melt, cooling takes place in the vicinity of the seed to a degree which can be sufficient to cause initially fast and nonuniform growth. Also the temperature at the growth interface may differ slightly from the measured pot temperature. All material discussed below was grown without using a reservoir of Ge.

Characteristics of Material

Some properties of the crystals grown in the manner described above are given in Table I. The composition of the melt is given in the first column. The crystallization temperature (second column) is the liquidus temperature for this composition as determined from available phase diagrams [In (4), Ga (4), Al (5), Sn (5)]. Resistivities (column 3) were determined by a two-probe technique. Impurity concentrations (column 4) were determined by conventional Hall measurements. The mobilities (column 5) were calculated from the resistivity and concentration of carriers. The distribution coefficient of the doping impurity between the solid and liquid phase is given in the sixth column. Hall voltages obtained on the Ga-doped sample were so small as to be near the detection limit of the apparatus used; consequently, the concentration of carriers could be determined only as being greater than 5×10^{19} cm^{-3} by these measurements. No Hall measurements were made on the Al-doped crystal. If a mobility of 100 cm^2/v-sec is assumed, the concentration of carriers in the Ga-doped sample would be about 2×10^{20} cm^{-3} and in the Al-doped sample about 7×10^{19} cm^{-3}. The respective distribution coefficients at the liquidus temperature would then be about 7×10^{-3} and 3×10^{-3}. An etch pit count on the In-doped crystals showed the concentration of dislocations to be about 5×10^4 cm^{-2}. The minority carrier lifetime of the In-doped crystals was found to be below the detection limit of the apparatus used, which was about 2 μsec. Microscopic examination of etched crystals showed no metal inclusions in the main body of any of the crystals; however, in the Ga-doped and Sn-Sb-doped crystals a few very small inclusions were noted at the extreme edge of the crystal.

The distribution coefficients given in Table I for In are lower by about a factor of 3 than those given by Thurmond, Trumbore, and Kowalchik (1). Although there is considerable uncertainty about the distribution coefficients for Al and Ga as calculated from the data in Table I, these are also lower than those reported in the above reference and in the case of Al very much lower. The values for In appear to be more in line with those recently reported by Hall (2), who has suggested that metal inclusions contained in crystals grown at low temperatures may be responsible for some of the high distribution coefficients reported by Thurmond, Trumbore, and Kowalchik (1). The value obtained for the distribution coefficient of Sb is less than a factor of two higher than that reported by Thurmond, Trumbore, and Kowalchik (1) and is, therefore, within experimental error. If their value is too high, as has been suggested by Hall (2), then our high value of distribution coefficient would lend support to the idea that the expansion of the Ge lattice caused by the Sn (3) can enhance the solubility of the Sb. It should be noted that determination of impurity concentrations from Hall effect measurements is subject to some uncertainty, particularly when used on the above materials which are neither strictly semiconductors nor metals. Hall effect measurements, while indirect, are not, how-

[1] The In used was the Indium Corporation's 99.97 grade. The Ga was Eagle-Picher "electronic grade." The Al was a specially purified Alcoa product believed to be better than 99.999%. The Sn was a Baker product containing 0.00005% As. The Sb was a Fisher C.P. product.

Table I. Properties of highly doped Ge crystals

Composition of melt, molar units	Crystallization temp, °C	ρ ohm-cm	N (Hall) cm^{-3}	μ_H cm^2/v-sec	$\frac{N_{solid}}{N_{liquid}}$
$In_{.79}Ge_{.21}$	600	5.7×10^{-3}	5.4×10^{18}	200	2.5×10^{-4}
$In_{.65}Ge_{.35}$	685	7.0×10^{-3}	3.8×10^{18}	230	2.1×10^{-4}
$Ga_{.63}Ge_{.37}$	630	3.3×10^{-4}	(2×10^{20}) *	(100)	(7×10^{-3}) *
$Al_{.55}Ge_{.45}$	615	8.2×10^{-4}	(7×10^{19}) *	(100)	(3×10^{-3}) *
$Sn_{.70}Sb_{.07}Ge_{.23}$	~610	2.0×10^{-3}	6.9×10^{18}	450	3.8×10^{-3}

* Determined using the resistivity and a mobility of 100 cm^2/v-sec.

ever, so sensitive to metallic inclusions as direct chemical analysis and are, furthermore, nondestructive and adaptable to small samples.

Manuscript received June 2, 1958. The main part of this paper was prepared for delivery before the Cleveland Meeting, Sept. 30-Oct. 4, 1956.

Any discussion of this paper will appear in a Discussion Section to be published in the June 1959 JOURNAL.

REFERENCES

1. C. D. Thurmond, F. A. Trumbore, and M. Kowalchik, *J. Chem. Phys.*, **25**, 799 (1956).
2. R. N. Hall, *J. Phys. Chem. Solids*, **3**, 63 (1957).
3. F. A. Trumbore, *This Journal*, **103**, 597 (1956).
4. W. Klemm, L. Klemm, E. Hohmann, H. Volk, E. Orlamünder, and H. Klein, *Z. anorg. u. allgem. Chem.*, **256**, 244 (1948).
5. H. Stöhr and W. Klemm, *ibid.*, **241**, 312 (1939).

Technical Review

Semiconducting Compounds—A Challenge in Applied and Basic Research

A. C. Beer

Battelle Memorial Institute, Columbus, Ohio

ABSTRACT

The use of a number of semiconducting compounds in device applications is discussed for categories defined by the external field which produces a modulation of the carrier density or mobility. Included are applications based on response to electric fields, magnetic fields, thermal fields, photon energy, and thermal energy. The implications of recent investigations as regards band structure, states densities, charge carrier mobilities, crystal imperfections, and other basic characteristics are presented.

The domain of semiconducting compounds encompasses so large an area that, in order to give coherence to a discussion of these materials, it is necessary to devise methods of classification. The scheme which is adopted here is to define categories on the basis of the external fields which produce a modulation of the charge-carrier density or its mobility. After all, the principal applications of semiconductors stem from the fact that the electrical properties are strongly influenced by environmental factors which can be controlled in a certain arbitrary manner and which are defined by the particular application.

To be more specific, consider the factors contributing to the electrical conductivity, namely, the charge-carrier density and the mobility. Modulation of the equilibrium charge-carrier density by an electric field, the so-called carrier injection, is the basis of semiconductor rectifiers and transistors. On the other hand, a modulation occurring by means of optical absorption leads to devices such as infrared detectors, phototransistors, or solar batteries.

It is possible, also, to modulate the mobility by means of external fields. Since mobility is the tensor component of the conductivity, a very effective way of accomplishing such a modulation is by a magnetic field. Examples of practical applications involve Hall-effect devices, magnetoresistance devices, magnetic rectifiers, and PEM infrared detectors. The last device actually encompasses two of the categories just discussed, since electron-hole separation is effected by means of the photon energy.

A list of some of the categories resulting from this classification system is presented in Table I. Examples of specific devices are given for each classification.

The major part of this paper is concerned with a number of the compound semiconductors having unique properties which permit applications in some of the categories shown. In addition, some of the inroads to our fundamental understanding of transport processes in semiconductors, which are coming about through studies on some of these compounds having unusual characteristics, are discussed.

Carrier-Density Modulations

Application of Electric Fields

Evidence indicates that the materials which are being studied most actively with regard to transistor applications are some of the higher band separation III-V compounds such as InP, GaAs, AlSb, and GaP. Recently the compound SiC also has received considerable attention. In addition, some work is being done on the low-gap material indium antimonide for use in transistor applications below −50°C and for use in microwave circuitry (1).

Some of the advantages of the III-V compounds are the diamond-type lattice, which insures a reasonably good thermal conductivity and a high elec-

Table I. Operational classification of semiconductors

Carrier-density modulations	Mobility modulations
Electric field (a) Moderate Transistors, rectifiers (b) Strong Avalanche phenomena, Zener currents, varistors, surge arrestors	Thermal energy (temperature) Nonlinear elements Electric field Hot-electron phenomena
Photon energy Photoconductors, infrared detectors, infrared filters and windows Solar batteries	Force field Elastoresistance
Thermal energy (temperature) Thermistors	
Thermal field Thermoelectric power generation Peltier cooling	Magnetic field Hall effect, magnetoresistance (many applications)
Force field Piezoelectric effects	
Crystallographic modifications (a) Phase-change phenomena Control circuits (b) Impurity effects Chemical analysis (c) Dislocations or other physical imperfections Strain gauges, nuclear particle flux indicators	
Crystallographic modifications—magnetic field Magnetic rectifier based on asymmetrical surface recombinations	
Photon energy—magnetic field Photoelectromagnetic detectors	

tron mobility. A most important consideration is the fact that deviations from stoichiometry apparently are controlled readily by crystal-pulling and zone-melting techniques.

Much information can be found on the III-V compounds in the literature (2, 3) and will not be repeated here. However, some rather recent data are presented to show that steady improvements are

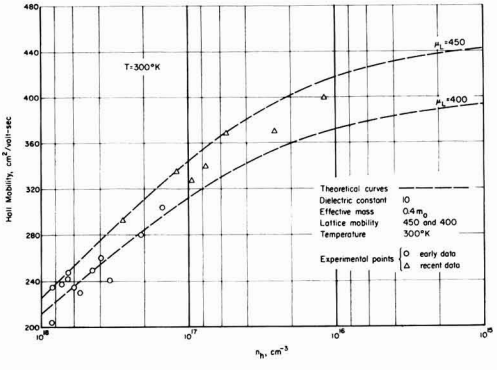

Fig. 1. Hole mobility as a function of carrier concentration for aluminum antimonide.

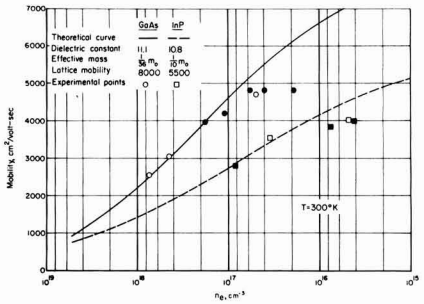

Fig. 2. Earlier data on electron mobility in GaAs and InP

being made in these materials and to suggest that perhaps one is not being unduly rash in thinking that in several years some of these compounds may pre-empt the position of germanium and silicon in certain applications.

In evaluating a given specimen of material for device application, I am going to compare its characteristic on a curve of the Hall mobility as a function of the extrinsic carrier concentration for the material in question. This procedure is more trustworthy than the consideration of either resistivity or Hall coefficient when the degree of compensation of donors and acceptors is not directly known. Figure 1 shows such data for aluminum antimonide. The circles represent data prior to 1958. The triangles show the results of improvements which were achieved less than six months ago (4).

The data in Fig. 2 indicate the earlier state of affairs for gallium arsenide and indium phosphide. The theoretical curves were drawn using simple theory to account for scattering by lattice vibrations and ionized impurities. At the time, it appeared that we may have been overly optimistic in our choice of lattice mobilities. However, let us replot the theoretical curves and include some later data, as is shown in Fig. 3.

It now becomes apparent that the earlier material was significantly compensated, even though the net excess of donors over acceptors was quite high. The characteristics of the better material are quite striking. Theoretical curves through these points suggest that the lattice mobility in indium phosphide may

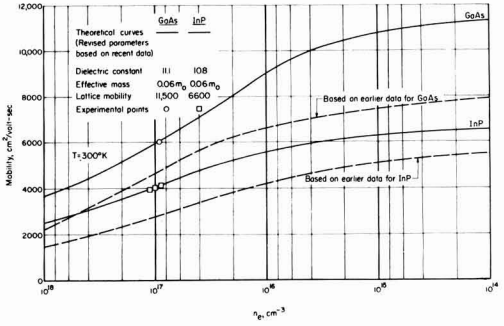

Fig. 3. More recent data on mobility in GaAs and InP. GaAs point is from Whelan and Wheatley (5); data for InP were taken at Battelle (4).

Table II. Mobilities at 300°K and ionized impurity contents for the best AlSb, InP, and GaAs prior to February 1958

	AlSb	InP	GaAs	GaSb	InAs	InSb*
Approximate μ^{L}_{e} (cm²/v-sec)	—	6600	11,500	—	40,000	1,200,000
Highest measured μ_e ($R\,\sigma$)	—	4600	6000	4000	30,000	620,000
Approximate N_i (impurities/cm³)	—	5×10^{15}	1×10^{17}	7×10^{17}	1.7×10^{16}	1.7×10^{14}
Approximate μ^{L}_{h}	450	150	650	—	—	—
Highest measured μ_h ($R\,\sigma$)	400	100	400	785	—	10,000
Approximate N_i (impurities/cm³)	3×10^{16}	3×10^{17}	3×10^{17}	2×10^{17}	—	1×10^{15}

* Values given at 77°K.

be as high as 6500 cm²/v-sec, and in gallium arsenide 11,500. To those who recall in Shockley's book the famous presentation of the historical data on mobility in germanium (6), the progression of measured mobility values in the III-V compounds has a familiar appearance. We are still in the region where significant improvements in materials developments are possible. Nevertheless, in the compounds just discussed, it does appear that we are now getting sufficiently good information to permit us to make reliable predictions about the lattice mobility. A brief résumé of the present state of affairs on the major III-V compounds is given in Table II.

Photon Energy

An important application for compound semiconductors is infrared detection. Probably the most widely used materials are lead sulfide, selenide, and telluride. These compounds cover a range from 1 to 7 μ (7). They are prepared in the form of deposited films on suitable substrates and must be cooled.

Magnesium stannide (8) (Mg_2Sn) and two of the III-V compounds also have interesting photoproperties in the 3 to 7½-μ range. The latter compounds are indium arsenide (9) and indium antimonide (10). These materials show considerable sensitivity in devices utilizing the photoelectromagnetic effect.[1] Such operation permits better sensitivity at higher temperatures than does the usual type of detector. It has been pointed out that InSb detectors now can be made which are more sensitive than any other uncooled detector throughout the range from 3 to 7½ μ (11). Another special property of InSb and InAs is the small effective electron mass. Thus, the density of states at the bottom of the conduction band is low, and the transmission edge can be shifted to higher energies, i.e., shorter wave lengths, by increasing the concentration of ionized carriers in the conduction band (9, 12-14). This behavior is of interest in connection with infrared filters and windows.

Because of transparency into the relatively far infrared, certain compound semiconductors may find numerous applications as window materials. An example of this is given by the transmission characteristics of cadmium telluride as shown in Fig. 4.

Photoconductive response in semiconducting compounds is, of course, not limited to the infrared region. Many applications range through the visible spectrum to that of x-rays and γ-rays. There are also α- and β-particle counters. Examples of compounds which find uses in these areas are sulfides, selenides, and tellurides of cadmium or zinc (15).

[1] A discussion of PEM phenomena will be given in a subsequent section.

Thermal Energy (Temperature)

The most common device for which the electrical characteristics are strongly temperature dependent is the thermally sensitive resistor or thermistor. These are usually made from mixtures of metal oxides. However, a crystal semiconductor in the intrinsic region will have a resistivity varying as exp $W/2kT$, provided that the mobility is reasonably well-behaved and does not differ appreciably from the classic $T^{-3/2}$ temperature dependence. With this exponential behavior, the temperature coefficient of resistance is proportional to the band separation, so that large-band-separation intrinsic materials are highly temperature sensitive. The practical difficulty in most cases is that such intrinsic semiconductors are almost insulators. In certain III-V compounds, however, the intrinsic resistivity is lowered as a result of unusually large mobilities, and some of these materials, therefore, can be used to advantage in thermistor circuits. In Fig. 5 is shown the measured resistivity as a function of temperature for a specimen of indium phosphide. It is calculated that at 350°K the temperature coefficient is approximately 6.3%/°K. This is somewhat larger than the figure of 4% quoted for the powder-process thermistors (16).

Thermal Fields

Probably the most widely studied application of the interaction of electrons and thermal fields is thermoelectric power generation and Peltier cooling. Good efficiencies in either of these processes obviously require the same kinds of characteristics for the materials. To illustrate the concepts involved, consider the Peltier effect, as exemplified by the heat transport between two junctions.

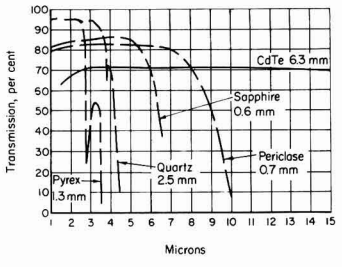

Fig. 4. Transmission of CdTe and other window materials as function of wave length. Solid line is from Battelle data, dashed lines are after Moss (7).

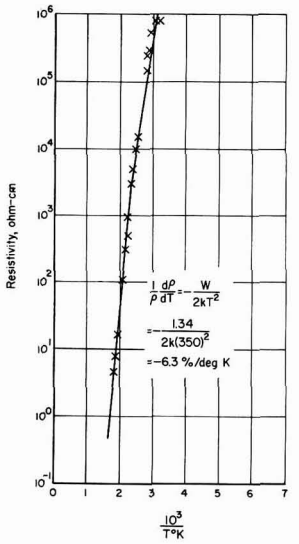

Fig. 5. Resistivity as function of temperature for intrinsic specimen of InP.

In Fig. 6 is presented the maximum temperature differential as a function of a parameter proportional to the current in the circuit. The Peltier transport is directly proportional to the current, as can be seen at low currents. However, the achievement of an arbitrary ΔT is limited by opposing effects due to thermal transport and to Joule heating. The first process is proportional to ΔT, and the second to I^2. Hence, they both become predominant at higher currents, so that ΔT reaches a maximum. It turns out that the efficiency of thermoelectric processes can be described by a parameter which characterizes the material. The so-called "figure of merit" is commonly written as $\alpha^2/K\rho$.[2] Knowing this ratio, one can calculate quite accurately the temperature difference resulting in a Peltier couple (17). The basic problem is, therefore, to develop materials with highest values of the figure of merit.

The present theory of thermal transport processes is not sufficiently developed to permit one to make quantitative predictions regarding the figure of merit. The more obvious difficulties are associated with the treatment of the scattering mechanism and with the contribution of the lattice to the thermal conductivity. However, certain guideposts are available for selecting thermoelectric materials. Some of these are:

1. The material must not be intrinsic—since holes and electrons produce opposite thermal emfs.
2. The carrier concentration should be high, but not at the expense of degeneracy. Therefore, a large effective mass is desirable, but not at the sacrifice of mobility.
3. The charge-carrier scattering mechanism is important; processes involving ionized impurities or optical modes of the lattice are preferred to some extent over those by acoustic phonons.
4. The lattice thermal conductivity should be low so that K does not deviate too greatly from the Wiedemann-Franz value. This latter consideration is probably one of the reasons why compounds with the zinc blende crystal structure have exhibited too large a thermal conductivity to have promising thermoelectric properties.
5. Another desirable feature is that the compound have a large lattice constant and a low dissociation energy, both of which tend to reduce the lattice thermal transport (18). However, a low dissociation energy implies a small energy gap, and, as was indicated before, the gap must not be so small that intrinsic conduction predominates at the temperatures of operation.
6. The mean atomic weight of the elements of the compound should be high, since mobility (in the case of impurity scattering) or the ratio of mobility to thermal conductivity (in the case of lattice scattering) increases with mean atomic weight (19).

The materials which are the subject of much current investigation, namely, the selenides and tellurides of lead and bismuth and derived compounds and alloys, satisfy the criteria which were just outlined. Further insight into some of the materials may be gained from Fig. 7, which shows the thermoelectric properties of p-type bismuth telluride, doped with excess bismuth.

A technique for reducing the lattice thermal conductivity without disturbing too seriously the elec-

[2] The thermoelectric power in v/°C is designated by α; the thermal conductivity in w/cm °C, by K; and the resistivity in ohm-cm, by ρ.

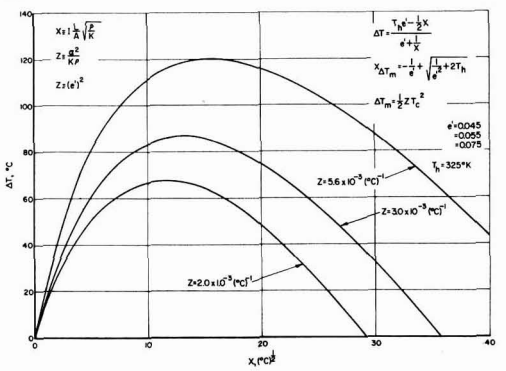

Fig. 6. Maximum temperature differential in Peltier couple. Abscissae are proportional to current.

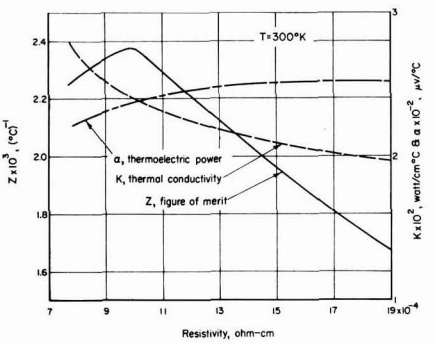

Fig. 7. Thermoelectric data on p-type specimen of Bi_2Te_3

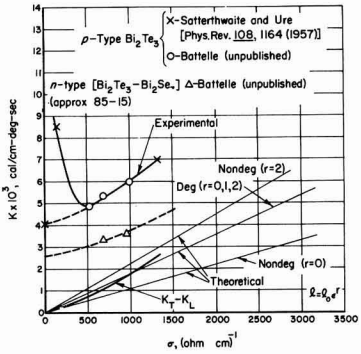

Fig. 8. Thermal conductivities for Bi_2Te_3 and an alloy

trical properties is the alloying of similar compounds. It was pointed out by Joffe (20) that the lattice distortions produced in each case are relatively small and, therefore, affect principally the lattice transport, since the wave length of the thermal oscillations at ordinary temperatures is the order of a lattice constant. The wave length of the electrons of the Fermi energy, on the other hand, is considerably greater than the lattice constant, and, therefore, the carrier mobility is reduced only a small amount. Figure 8 illustrates some results of alloying bismuth telluride with bismuth selenide. Here the measured thermal conductivity is plotted as a function of the electrical conductivity of the specimen. The lattice thermal conductivity is given by extrapolation of the data to $\sigma = 0$. Measurements on low-conductivity specimens cannot provide this information, since in nearly intrinsic material additional transport effects become important, such as ambipolar diffusion and ionization energy transport. This is evidenced by the point from Satterthwaite and Ure's (21) data for σ less than 250 (ohm-cm)$^{-1}$. These investigators determined K_L from the temperature dependence of the extrinsic data, and the result is in good agreement with the extrapolation of the Battelle data.

An interesting check of the applicability of present theory can be made by determining $K_T - K_L$, i.e., the difference between the total conductivity and the lattice contribution, as a function of the electrical conductivity. In the extrinsic region this difference is essentially $K_{\text{electronic}}$. The result is plotted on the graph, flanked by several theoretical lines representative of different scattering mechanisms. It is seen that results are consistent with expectations.

A similar lowering of lattice thermal conductivity with alloying has been shown by Joffe and co-workers to occur with lead telluride. The value decreases by a factor of two as approximately 20% lead selenide is added (22).

Many more illustrations could be given of thermoelectric materials, although the field is still only partially explored. This is especially true when one considers materials which might be operable at higher temperatures, say, above 600°C. It is clear that this area of research is still in its infancy and that much work needs to be done, both in materials preparation and in basic theoretical developments.

Combination-Carrier Density and Mobility Modulations

Crystallographic Modifications

A number of interesting properties are included in this category. Take, for example, the change in phase or crystallographic structure which occurs in a number of compounds. Illustrations are silver sulfide (23) and barium titanate (24). At approximately 175°C the resistivity of silver sulfide drops discontinuously by three orders of magnitude. The use of such type of materials in alarm systems is obvious. Also, it is apparent that the current-voltage characteristic of such an element can be controlled rather widely by the thermal characteristics of its mounting.

If impurities capable of producing donor or acceptor levels are added to high-purity semiconductors, changes in carrier densities and in low-temperature mobilities result. After appropriate "calibration" experiments are done with known impurity additions, electrical measurements can be used to supply sometimes both quantitative and qualitative information on chemical impurities. Figure 9 illustrates the principle involved in the identification and quantitative determination of tellurium content in InSb through the use of Hall measurements (25). The distributions of tellurium and of the unknown impurity along standard InSb ingots are seen to coincide. A similar procedure has been used to identify sulfur in indium arsenide.

Since very high-purity indium and antimony are now available, such techniques can be used to check the purity of other elements used in making III-V compounds, such as gallium and arsenic, through the preparation of a test specimen of gallium antimonide with the use of very pure antimony, and of indium arsenide, using the pure indium.

A novel application of the effects of foreign impurities has recently been discussed by investigators at the Physikalischen Institut at Bonn (26). They found that they could use cuprous oxide films, and to a less satisfactory extent, cadmium sulfide single crystals, as a quantitative detector of neutral atoms of sulfur or selenium in a molecular beam.

Crystallographic Modification Combined with Magnetic Field

An interesting application of the use of surface treatments to produce a crystal asymmetry which, in combination with an applied magnetic field, leads to nonlinear conduction (27) has been investigated by Weisshaar, Welker, and associates. During one

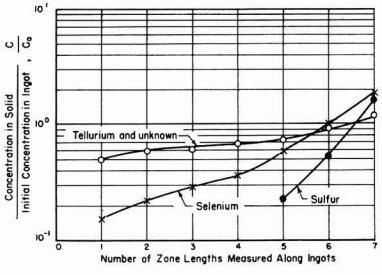

Fig. 9. Relative distribution of some group VI impurities in InSb after five zone-melt passes, after Harman (25).

direction of the current, the holes and electrons in an intrinsic semiconductor are deflected by the magnetic field to a face which, say, has been sandblasted to produce a high surface recombination. During the other cycle, the carriers are deflected to an etched surface of low recombination velocity. Experiments were carried out on germanium, and at zero magnetic field the current-voltage characteristic was linear. At 8000 gauss, however, substantial asymmetry was introduced. Moss has calculated that, for use with indium antimonide, an optimum specimen thickness would be in the order of 30 μ, and that back-to-front ratios of 1000 to 1 are potentially possible (28).

Joint Modulations by Photon Energy and Magnetic Field

This process is the basis of the PEM effect which, when used with indium antimonide, has provided one of the most sensitive infrared detectors for operation at room temperature (11). In addition, it is a very useful tool for studying recombination processes and surface states (29, 30).

Consider a slab of semiconductor of thickness t along the x-direction, large in the other directions, and illuminated on the yz-face by light of appropriate wave length directed along the x-axis. These photons release electron-hole pairs which will diffuse in the x-direction. If now a magnetic field is directed along the z-axis, the electrons and holes will be accelerated oppositely along the y-direction and a potential difference will appear along the y-axis in the specimen. This is the PEM voltage.

When using the technique to measure bulk lifetimes, one usually determines both PEM and photoconductive responses for the same illumination. In this way it is not necessary to have an independent knowledge of the photon flux density or the surface recombination velocities. The method is especially suited to the measurement of lifetimes of 10^{-7} sec and lower in high-mobility materials such as InSb.

Mobility Modulations

The only examples discussed in this grouping are the galvanomagnetic effects, which are extremely large in high-mobility materials.

When a magnetic field is applied normal to the current direction in a conductor, an initial lateral deflection of charge carriers results, as shown in Fig. 10. This charge accumulation produces a transverse potential gradient, called the Hall field. The Hall field assumes such a value that the force on a charge carrier of "average" velocity is zero in the crossed electric and magnetic fields.

If all the charge carriers had the same velocity, then the Hall-field force would cancel exactly the force due to the magnetic field on the moving charge, and no charge carriers would be deflected. Hence, there would be no magnetoresistance. Actually, however, a distribution of velocities exists in semiconductors so that those carriers with velocities larger or smaller than the "average" will be caused to traverse larger paths, thus increasing the resistance of the conductor.

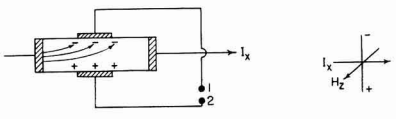

Fig. 10. Initial deflection of charge carriers by magnetic field to create Hall field.

Table III. Relation between mobility and Hall angle

$$E_y = Rj_xH_z,\ V_H = 10^{-8}\frac{RIH}{d} = 10^{-8}\frac{\rho I\mu H}{d}$$

Hall angle:

$$\text{Tan}\ \theta \equiv E_y/E_x = 10^{-8}R\sigma H = 10^{-8}\mu H$$

Semiconductor	T, °K	Tan θ (For H = 5000 gauss)
Germanium, electrons	300	0.2
InAs, electrons	300	2.0
InSb, electrons	300	4.0
InSb, electrons	77	25.0

From the preceding discussion it is apparent that any arrangement for decreasing the Hall field will augment the magnetoresistance. For example, if in Fig. 10, terminals 1 and 2 are connected through a low impedance, a current will exist in this circuit. In the case of certain semiconductors, such as indium antimonide, this secondary current can be relatively large. Since this transverse current across the semiconductor is still normal to the magnetic field, one may regard it as creating another Hall voltage which opposes the electric field causing the primary current. Thus it follows that the primary current may be modulated by varying either the magnetic field or the secondary load. The pertinent equations describing the Hall effect along with typical values of certain parameters for several semiconductors are given in Table III.

Because of these large transverse phenomena in semiconductors such as indium antimonide and indium arsenide, a series of applications has been developed in Germany (31) and in England (32) as well as in America (33-35). In such devices, the individual element is the so-called "Hall generator," which may be considered as a square slab of high-mobility semiconductor having contacts on each of the four sides. A few applications of such units are fluxmeters, d-c to a-c converters, and devices to multiply all quantities which can be made to depend on current and on magnetic field: for example, product operations in an analog computer, and measurements of torque of an electric motor. Factors important in the performance of Hall generators are listed in Table IV.

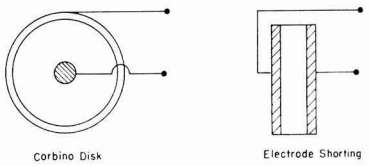

Fig. 11. Mechanisms to produce shorting of Hall voltage

Table IV. Performance of Hall generators

Max. power to load: $W_o = V_H^2/4Z_i$; efficiency $\eta \equiv W_o/W_i \sim 10^{-16}H^2\,(R/\rho)^2$, $\mu H << 1$
No load: $V_H \sim 10^{-8}W_i^{1/2}\,HR/\rho^{1/2}$, $\mu H << 1$

Material	T, °K	R (cm³/coulomb)	ρ (ohm-cm)	R/ρ (cm²/v-sec)	$\left[\frac{R}{\rho}\right]^2$	$\frac{R}{\rho^{1/2}}$
Bismuth	300	1.5	0.00012	12,500	1.56×10^8	0.14×10^3
Ge (intrinsic)	300	60,000	45	1300	0.02	8.9
Ge (medium)	300	8000	2	4000	0.16	5.7
Ge (low Tc)	300	10	0.01	1000	0.01	0.1
InSb (intrinsic)	300	360	0.006	60,000	36	4.6
InSb (low Tc)	300	20	0.0008	25,000	6	0.7
InAs (intrinsic)	300	10,000	0.25	40,000	16	20
InAs (low Tc)	300	500	0.015	30,000	9	4.1
InSb (high purity)	77	37,300	0.06	620,000	3840	152

Returning now to the magnetoresistance effects, it was seen how results could be augmented by shorting the Hall voltage. This is done most effectively by the disk geometry shown in Fig. 11. The arrangement is known as the Corbino disk.[3] A somewhat simpler design for producing shorting is the use of large end contacts, as is seen at the right (37). Characteristics of these types of InSb elements are presented in Fig. 12.

It is seen that rectangular geometries approach quite closely the results for the disk. One difficulty with the simple units as circuit elements is their low impedance, less than 0.1 ohm for the specimens representing the curves on the slide. To improve this, one can resort to very thin rectangular wafers with shorting bars deposited thereon. A commercial specimen of this type has a zero-magnetic-field resistance of ½ ohm.[4] The data are indicated by the solid circles. It is seen that such a fabrication technique has increased appreciably the impedance of the unit and yet provided a good magnetoresistance ratio.

The applications of such units are again myriad. Examples are contactless switches and potentiometers, d-c to a-c converters, synchronous rectifiers, and voltage regulators (38).

[3] After O. M. Corbino who investigated the circulating secondary currents in a bismuth disk carrying a primary electric current in a magnetic field (36).

[4] Supplied us by courtesy of K. Eggleston of Ohio Semiconductors, Inc.

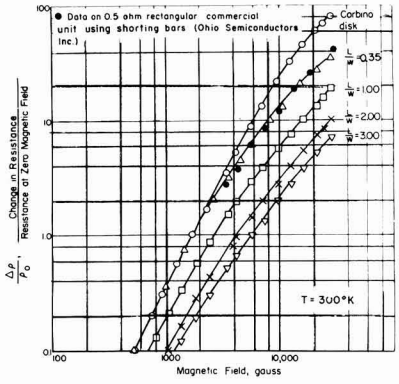

Fig. 12. Magnetoresistance in n-type InSb for Corbino disk and for several ratios of sample length to width (full area contacts at ends).

Research on Semiconducting Compounds as a Means for Advancing Solid-State Theory

In addition to yielding materials with unique properties which are potentially valuable for device applications, the field of semiconducting compounds has provided much interesting research for the basic scientist and has given us a means for testing some of our theoretical predictions concerning the solid state. In this respect, indium antimonide has received the lion's share of attention. Because of its high electron mobility, one can study with ordinary laboratory magnets phenomena which would require fantastic magnetic field strengths to observe in other materials. Figure 13 shows magnetoresistance measurements (39) extending into the region where electron-orbit quantization must be considered (40-42). For the point on the extreme right, the energy of an electron in its cyclotron orbit is 2.6 that of its thermal energy—and this at 77°K!

A further consideration is that the conduction band is reasonably isotropic, having one energy minimum at the zero of the electron wave number (43). Such a simple structure is always a boon to the theorist, since it reduces the complexities entering into the interpretation of the experimental data.

Another interesting feature is the large ratio of electron-to-hole mobility. As a result, it is possible to study in one single instrinsic sample certain characteristics of electrons and of holes. This is illus-

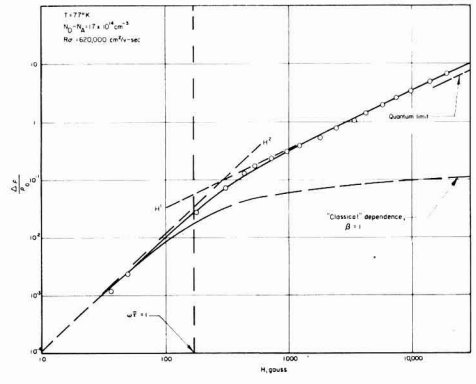

Fig. 13. Magnetoresistance of n-type InSb as function of magnetic field (after Bate, Willardson, and Beer [to appear in "J. Phys. Chem. Solids]).

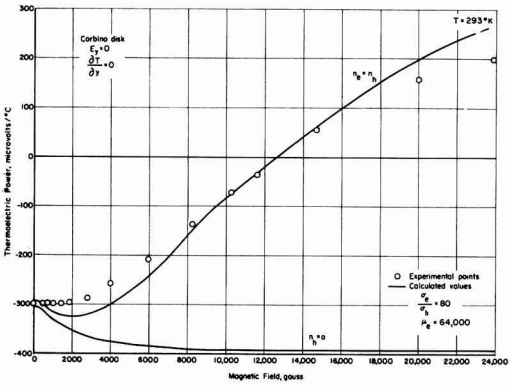

Fig. 14. Thermoelectric power of intrinsic InSb for Corbino disk geometry as function of magnetic field.

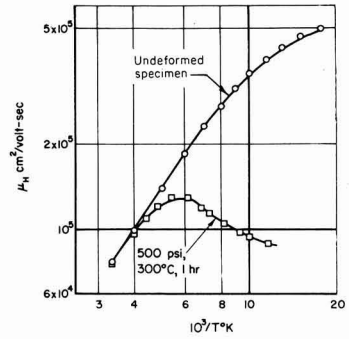

Fig. 15. Effect of plastic deformation on electron mobility in high-purity InSb sample with 1×10^{14} extrinsic carriers/cm³.

trated by the thermoelectric measurements shown in Fig. 14 (44, 45). Because of their high mobility, the electron transport effects predominate in intrinsic material. However, this contribution is strongly magnetic-field dependent, so that at above 12 kilogauss the holes take over. The theoretical curve was based on a single charge-carrier scattering mechanism. If electron-hole scattering is also taken into account, the minimum tends to disappear (45).

The unusual mobility at low temperatures renders InSb a sensitive material for registering effects of deformation. This is illustrated in Fig. 15, which shows the change in temperature dependence of mobility after one hour's compression at 300°C (46).

Other features of interest to theorists include the overlapping of donor levels with the conduction band even in relatively pure indium antimonide and indium arsenide, nonparabolic heavy-mass bands (43, 47). an anomalous negative magnetoresistance in indium antimonide (48), and anomalies in Hall coefficient, such as double reversals, in certain specimens of indium arsenide (49).

In indium phosphide, recent magnetoresistance measurements by Glicksman on oriented crystals suggest that the conduction band is fairly isotropic (50). Preliminary results at Battelle indicate the same situation may exist for mercury telluride inasmuch as the ratio of longitudinal and transverse magnetoresistance was found to be quite small, that is, approximately 2%.

Summary

I have tried to give some indication of the tremendous breadth encompassed by the field of semiconducting compounds and to show that progress is being achieved on a great variety of fronts. It seems clear that, already at the present stage of materials development, a variety of useful devices can be perfected by ingenious experimenters, and if improvements in materials perfection should follow the usual course, a number of very promising developments should accrue. Also, it has been seen that a number of compounds have rather unique characteristics, and these are providing challenging areas of investigation, both for the experimentalist and for the theorist.

Acknowledgment

The author is indebted to his associates at Battelle for use of unpublished data and for assistance with the manuscript. In particular, he desires to mention R. Bate, J. Duga, T. Harman, E. Lougher, B. Paris, C. Peet, F. Reid, T. Shilliday, and R. Willardson.

Manuscript received April 30, 1958. This paper was prepared for delivery before the New York Meeting, April 27-May 1, 1958.

Any discussion of this paper will appear in a Discussion Section to be published in the June 1959 JOURNAL.

REFERENCES

1. C. T. McCoy, *Proc. Inst. Radio Engrs.*, **46**, 61 (1958).
2. H. Welker and H. Weiss, "Solid State Physics," Vol. 3, p. 1, Academic Press, Inc., New York (1956).
3. F. A. Cunnell and E. W. Saker, "Progress in Semiconductors," Vol. 2, p. 37, John Wiley & Sons, Inc., New York (1957).
4. F. J. Reid and R. K. Willardson, *J. Electronics and Control*, **5**, 54 (1958).
5. J. M. Whelan and G. H. Wheatley, To appear in *J. Phys. Chem. Solids.*
6. W. Shockley, "Electrons and Holes in Semiconductors," p. 338, D. Van Nostrand Co., Inc., New York (1950).
7. T. S. Moss, *Proc. Inst. Radio Engrs.*, **43**, 1869 (1955).
8. H. P. R. Frederikse and R. F. Blunt, *ibid.*, **43**, 1828 (1955).
9. R. M. Talley and D. P. Enright, *Phys. Rev.*, **95**, 1092 (1954).
10. T. S. Moss, "Photoconductivity Conference," p. 427, John Wiley & Sons, Inc., New York (1956).
11. T. S. Moss, "Solid State Phenomena in Electric Circuits," p. 123, Interscience Publishers, New York (1957).
12. M. Tanenbaum and H. B. Briggs, *Phys. Rev.*, **91**, 1561 (1953).
13. A. C. Beer, R. K. Willardson, and A. E. Middleton, *ibid.*, **93**, 912 (1954).
14. E. Burstein, *ibid.*, **93**, 632 (1954).
15. R. H. Bube, *Proc. Inst. Radio Engrs.*, **43**, 1836 (1955).
16. E. M. Conwell and W. J. Leivo, "The Science of Engineering Materials," p. 418, John Wiley & Sons, Inc., New York (1957).
17. T. S. Shilliday, *J. Appl. Phys.*, **28**, 1035 (1957).
18. T. A. Kontorova, *Soviet Physics-Technical Physics*, **1**, No. 9 (1959).
19. H. J. Goldsmid and R. W. Douglas, *Brit. J. Appl. Phys.*, **5**, 386 (1954).
20. A. F. Joffe, *et al, Dokl. Akad, Nauk. SSSR*, **106**, 981 (1956).

21. C. B. Satterthwaite and R. W. Ure, Jr., *Phys. Rev.*, **108**, 1164 (1957).
22. A. F. Joffe, *Can. J. Phys.*, **34**, No. 12A, 1342 (1956).
23. F. R. Quinn, U.S. Pat. 2,609,470, Sept. 2, 1952.
24. H. A. Sauer and S. S. Flaschen, *Proc. 1956 Electronic Components Symposium at Washington, D. C.*, p. 41, Engineering Publishers, New York (1956).
25. T. C. Harman, *This Journal*, **103**, 128 (1956).
26. W. Gebhardt and O. Osberghaus, *Z. Physik*, **150**, 33 (1958).
27. E. Weisshaar and H. Welker, *Z. Naturforsch.*, **8a**, 681 (1953).
28. T. S. Moss, *op. cit.*, p. 113.
29. O. Garreta and J. Grosvalet, "Progress in Semiconductors," Vol. 1, p. 165, John Wiley & Sons, New York (1956).
30. S. W. Kurnick and R. N. Zitter, *J. Appl. Phys.*, **27**, 278 (1956).
31. F. Kuhrt, *et al, Siemens-Z.*, **28**, 299 [also 370, 376] (1954).
32. I. M. Ross and E. W. Saker, *J. Electronics*, **1**, 223 (1955).
33. W. C. Dunlap, Jr., U. S. Pat. 2,725,504, Nov. 29, 1955.
34. W. P. Mason, W. H. Hewitt, and R. F. Wick, *J. Appl. Phys.*, **24**, 166 (1953).
35. R. F. Wick, *ibid.*, **25**, 741 (1954).
36. E. P. Adams, *Proc. Am. Phil. Soc.*, **54**, 47 (1915).
37. O. Madelung, *Naturwissenschaften*, **42**, 406 (1955).
38. R. K. Willardson and A. C. Beer, *Elec. Mfg.*, **57**, 79 (1956).
39. R. T. Bate, R. K. Willardson, and A. C. Beer, *Bull. Am. Phys. Soc.*, **3**, 119 (1958) [complete article to appear in *J. Phys. Chem. Solids*].
40. R. K. Willardson, T. C. Harman, P. Choquard, and A. C. Beer, *Phys. Rev.*, **98**, 227 (1955).
41. P. N. Argyres and E. N. Adams, *ibid.*, **104**, 900 (1956).
42. P. N. Argyres, *ibid.*, **109**, 1115 (1958).
43. E. O. Kane, *J. Phys. Chem. Solids*, **1**, 249 (1957).
44. R. K. Willardson and A. C. Beer, *Bull. Am. Phys. Soc.*, **1**, 54 (1956).
45. A. C. Beer, J. A. Armstrong, and I. N. Greenberg, *Phys. Rev.*, **107**, 1506 (1957).
46. J. J. Duga, R. E. Maringer, and A. C. Beer, *Bull. Am. Phys. Soc.*, **3**, 106 (1958).
47. F. Stern, *ibid.*, **3**, 120 (1958).
48. H. P. R. Frederikse and W. R. Hosler, *Phys. Rev.*, **108**, 1136 (1957).
49. J. R. Dixon, *Bull. Am. Phys. Soc.*, **3**, 120 (1958).
50. M. Glicksman, *ibid.*, **3**, 120 (1958).

Correction

On page 544 (Vol. 105, September 1958) of the paper by M. J. Allen and V. J. Powell on the Oxidation of Various Indole Alkaloids, the sequence of formulas should be inserted after the sentence, ". . . in this instance we would have at the electrode surface due to adsorption of the alkaloid molecule:"

Discussion Section

This Discussion Section includes discussion of papers appearing in the JOURNAL of The Electrochemical Society, **104**, No. 3 (March 1957), and **105**, No. 1-6 (January-June 1958). Discussion not available for this issue will appear in the Discussion Section of the June 1959 JOURNAL.

Hydrogen Evolution Reaction on Copper, Gold, Molybdenum, Palladium, Rhodium, and Iron; Mechanism and Measurement Technique under High Purity Conditions

N. Pentland, J. O'M. Bockris, and E. Sheldon
(pp. 182-194, Vol. 104)

R. Piontelli, U. Bertocci, G. Poli, and G. Serravalle[1]: The following may be suggested as representing certain aspects of the views of Pentland, Bockris, and Sheldon (P., B., and S.), in reference to the technique of measurements in electrode kinetics, with which we are not in agreement.

1. The geometrical characteristics of the cell seem to be considered by P., B., and S. of rather secondary importance, if the electrodes to be investigated are employed in the form of a wire suspended in the solution.

2. As the possible "spurious components" of the measured overvoltages, P., B., and S. consider only the "ohmic drop" and the "concentration component." No "screening effects" are considered,[2] and the evaluation of the ohmic drop in the layer between capillary and electrode has to be effected, by assuming here the same current density distribution admitted to exist on the whole electrode surface.

3. The evaluation of the "concentration component," according to P., B., and S., may be effected following similar assumptions and adopting for the thickness of the diffusion layer the "appropriate value" of "approximately 0.005 cm."

4. Essential criteria for checking "a posteriori" the correctness of overvoltage measurements are: (*a*) correspondence to Tafel law; (*b*) practical absence of time variations.

I. The rather indefinite current distribution on the electrodes of a cell of the type used by P., B., and S. allows only for rough conclusions on the dependence of the measured overvoltages on current density (c.d.).

II. The P., B., and S. opinion on the screening effects may be rejected both on theoretical grounds and according to the experimental evidence.[3] As a matter of fact, the presence of an obstacle near the electrode surface involves a reduction of the effective specific rate of the electrode reaction and of the mass transfer processes and, thus, of the (absolute) local value of the corresponding overvoltages.

This value is influenced both directly (as a consequence of the reduction of c.d.) and indirectly (as a consequence of the anomalous chemical configuration of the interphase region).

In the case of electrode processes involving metal ion exchanges, the local reduction of the c.d. due to obstacles sufficiently near the electrode surface can be recognized easily by studying the distribution of the cathodic deposition or of the anodic attack.

Let us plunge, in a sulfuric acid solution, a nickel plate having a well-planed surface, and press a Luggin capillary (having a well-planed and sharp terminal contour) on the surface itself.

Let us place a second Luggin capillary (also connected with a reference electrode) at 1 or 2 mm from the electrode surface. Recording separately the anodic polarization of the Ni electrode, as given by the two tensiometric devices, one encounters conditions under which on the shielded area no passivity at all occurs, while on the rest of the surface complete passivity is met, the recorded overvoltages thus differing on the order of 1 v.

III. As far as the "concentration component" is concerned, the value of the diffusion layer thickness cannot be stated in general, and, following the P., B., and S. policy and thus renouncing to any imposed convection, it would be necessary to check this value in any particular case.

IV. In respect of the criteria (*a*) and (*b*) at point 4, the paper under discussion seems to leave choice only between two alternatives: either some of the present results of P., B., and S. (concerning, for instance, Rh) are also incorrect, or these criteria do not present the general validity, formerly attributed to it.

N. Pentland, J. O'M. Bockris, and E. Sheldon: We (P., B., and S.) are pleased to be able to elucidate those parts of the technique of the examination of slow electrode reactions which Piontelli, Bertocci, Poli, and Serravalle (P., B., P., and S.) appear to have misunderstood.

I. *Cell geometry.*—The secondary importance of the cell geometry under the conditions of our experiments is not associated with "wires suspended in solution." The principles of the effect of size and shape of electrolytic cells have been given most informatively in the literature by Hoar and Agar,[4] who show that the effect of these factors on cell measurements decreases with increasing concentra-

[1] Laboratorio di Chimica Fisica, Elettrochimica e Metallurgia, del Politecnico di Milano, Milan, Italy.

[2] J. O'M. Bockris, I. A. Ammar, and A. K. M. S. Huq, *J. Phys. Chem.*, **61**, 882 (1957).

[3(a)] R. Aletti, U. Bertocci, G. Bianchi, C. Guerci, R. Piontelli, G. Poli, and G. Serravalle, *Compt. Rend. CITCE, Berne*, **3**, 30 (1951); R. Piontelli, G. Bianchi, and R. Aletti, *Z. Elektrochem.*, **56**, 86 (1952); R. Piontelli, G. Bianchi, U. Bertocci, C. Guerci, and B. Rivolta, *ibid.*, **58**, 54 (1954); R. Piontelli, U. Bertocci, G. Bianchi, C. Guerci, and G. Poli, *ibid.*, **58**, 86 (1954).

[(b)] R. Piontelli and G. Bianchi, *Gazz. chim. ital.*, **79**, 646, 863, 867 (1949) and **80**, 581 (1950); R. Piontelli and G. Bianchi, *Compt. Rend. CITCE, Milan*, **2**, 379 (1950); R. Piontelli, *Gazz. chim. ital.*, **83**, 357, 370 (1953); R. Piontelli, *Trans. Inst. Metal Finishing*, **31**, 51 (1954); R. Piontelli, B. Rivolta, and G. Montanelli, *Z. Elektrochem.*, **59**, 64 (1955); R. Piontelli, *Rend. inst. lombardo sci.*, **88**, 51 (1955); R. Piontelli, G. Bianchi, U. Bertocci, and B. Rivolta, *Ricerca sci.*, **26**, 838 (1956).

[4] J. N. Agar and T. P. Hoar, *Discussions Faraday Soc.*, **1**, 158 (1947); T. P. Hoar and J. N. Agar, *ibid.*, **1**, 162 (1947).

tion and decreasing values of the exchange c.d. If the potential difference between points in the solution at extreme positions of the electrode is negligible (2-3 mv's), current distribution effects, i.e., results of cell geometry, can be neglected. That this was so in our experiments was established, e.g., by: (i) the observed independence of the overpotential values at a given c.d. with movement of the Luggin capillary (L.c.) vertically over the electrodes; (ii) the satisfactory agreement between the results of P., B., and S. on Cu in acid solutions with those repo.ted earlier by Bockris and Azzam[5]: in the latter workers' cell, a completely different geometry existed from that of the former.

Measurements utilizing cell geometry similar to that used by P., B., and S. have somewhat more than "roughly established" the shape of the overpotential-current density relation in the hydrogen evolution reaction (h.e.r.). For example, measurements by Kabanov and Jova,[6] Bockris and Parsons,[7] Post and Hiskey,[8] and Bockris and Azzam[5] have led to the establishment of a consistent relation for Hg in acid solutions over a c.d. range of about 12 powers of 10. Or, our own measurements on, e.g., Au in 0.01*N* HCl lead to Tafel parameters in which Conf. log i_o are 0.2, and Conf. $b \simeq 0.010$. Values of such parameters of a greater order of accuracy have not hitherto been reported in the literature for this type of system.[9]

II. *Corrections for screening and ohmic effects.*—Our attitude to these effects is that calculated corrections are difficult to carry out with meaningful accuracy,[10] so that conditions of c.d. and concentration, for a given i_o value, should be limited to values such that the effects of screening and ohmic errors are negligible. That this condition was achieved in the technique which we used is established (in respect to screening) by: (i) the observed independence of overpotential values at a given c.d. with shape and size of the L.c.; (ii) agreement in numerical values of parameters between a number of independent workers (*see* footnotes 9 and 10); chance coincidence of ohmic and screening errors, respectively, among the work of several workers in different laboratories would hardly have a high probability; (iii) agreement of the experimentally established overpotential-c.d. relation with that given by theory neglecting screening effects; (iv) agreement of values (on Fe electrodes in 0.1*N* HCl), obtained by a technique similar to that of P., B., and S., with those obtained on the same system but using an electronic commutator and with the L.c. far removed from the electrode;[11] (v) the detailed examination of screening effects in measurements of hydrogen electrode kinetics, recently described by Huq and Basak.[12] They report (for conditions of measurement similar to those used by P., B., and S.) that "no screening effect on the activation overpotential was observed (±1 mv)."

Points II, (ii), (iii), and (iv) establish freedom of the technique of measurement used by P., B., and S. from ohmic errors.

Theoretical calculations of the order of magnitude of the ohmic component[13] can only be used as a rough guide to what is to be expected for a given situation (or to explore, orderwise, the nature of a deviation from the normal overpotential-c.d. relation).

III. *Concentration overpotential.*—P., B., P., and S. have not understood the use to which a theoretical overpotential-c.d. relation for diffusion-controlled behavior was put in our work. Such calculations have not the numerical significance which would allow their use as corrections of experimental measurements of hydrogen overpotential: they were not so used by us. However, such calculations can be used, with those of ohmic overpotential, to obtain an indication of the order of the highest c.d. to which measurements of hydrogen overpotential would be expected to be free from an appreciable (2-3 mv) contribution of concentration overpotential (and the value of δ was used from the work of King,[14] which was carried out under conditions similar to ours and indicated little dependence of δ on gas evolution; change of c.d.; or variation of concentration).

In summary of I-III; the parameters of the hydrogen evolution reaction, which are recorded in the paper by P., B., and S., were established under experimental conditions chosen so that the effects I-III had been made negligible (the achievement of such a condition seems to us to belong to the proper design of experimental measurements in electrode kinetics). They do not contain calculated corrections. Hence, P., B., P., and S.'s statements in their I-III lack point.

IV. *Criteria of "correctness" of measurements.*—Applicability of Tafel's equation, and lack of sporadic time variation of overpotential at a given c.d., are frequently occurring (but not alone sufficient) characteristics of "correct" measurements of the kinetics of the h.e.r. They give evidence of the absence of competing redox processes, and nonactivation components of the hydrogen overpotential, and suggest that surface active materials are not undergoing adsorption or deposition on the electrode surface during measurement. However, on certain solid electrode materials a small ($\simeq 10\%$) reproducible variation of overpotential with time occurs during the initial states of polarization after which the overpotential remains constant for many hours. Such a variation is not removed by increasing the degree of purification of the solution. It may be due to the time required to set up steady-state surface concentrations of H atoms, which would depend for certain metals on diffusion process of H into the bulk

[5] J. O'M. Bockris and A. M. Azzam, *Trans. Faraday Soc.*, **48**, 145 (1952).
[6] B. Kabanov and I. Jova, *Acta Physiocochim.*, **10**, 617 (1939).
[7] J. O'M. Bockris and R. Parsons, *Trans. Faraday Soc.*, **45**, 916 (1949).
[8] B. Post and H. Hiskey, *J. Am. Chem. Soc.*, **72**, 4203 (1950); **73** 161 (1951).
[9] The cells used by P., B., and S. possessed a geometry similar to those used by a number of other workers in this field [cf., e.g., A. Lukovstev, B. Levina, and A. N. Frumkin, *Acta Physiocochim.*, **11**, 21 (1939); H. P. Stout, *Discussions Faraday Soc.*, **1**, 107 (1947); A. N. Frumkin and A. Aladjalowa, *Acta Physicochim.*, **19**, 1 (1944); B. Post and H. Hiskey, *loc. cit.*; I. A. Ammar and S. A. Awad, *J. Phys. Chem.*, **60**, 837 (1957); *idem, ibid.*, 1290; *idem, ibid.*, **62**, 805 (1958); *idem, ibid.*, **62**, 801 (1958); *idem, ibid.*, **62**, 660 (1958)].
[10] The inaccuracy of such a calculated correction has been stressed by one of us [J. O'M. Bockris, I. A. Ammar, and A. K. M. S. Huq, *J. Phys. Chem.*, **61**, 879 (1957)].
[11] J. O'M. Bockris and B. E. Conway, *J. Phys. Chem.*, **53**, 527 (1949).
[12] A. K. M. S. Huq and A. K. Basak, *Pakistan J. Sci. Research*, **10**, 71 (1958).
[13] J. O'M. Bockris, "Modern Aspects of Electrochemistry," p. 264, Academic Press, New York (1954).
[14] C. V. King, *This Journal*, **102**, 193 (1955).

of the metal. Such an effect could, in principle, cause the absence of a rectilineal section in the experimental Tafel plot. In fact, the behavior of Rh is not an example of this possibility: further examination of data for the system Rh in 0.01*N* HCl shows that a distinctly rectilineal section exists (5 experimental points on the Tafel plot), between log i values of about −3.10 and −2.7.

We submit that the above considerations are fairly simple and suggest that the apparent misunderstandings of P., B., P., and S. may arise from the fact that they have concentrated in their experimental work on the measurement of overpotential developed during metal deposition. In this type of electrode reaction, relatively high c.d.'s are often needed to give rise to measurable activation overpotentials. Under such conditions, errors due to screening, ohmic, and concentration effects would be much more difficult to avoid than with the highly polarizable hydrogen electrode reactions. These difficulties in measurements of the deposition of metals perhaps may not be unconnected with a lack of progress in the evaluation of specifically described mechanisms of metal deposition, which has been an unfortunate feature of certain postwar work in this field (conversely, cf. Mehl and Bockris,[15] Gerischer,[16] Lorenz,[17] Conway and Bockris[8]).

The Action of Lead Pigments and Lead Soaps on Aluminum

M. J. Pryor, R. J. Hogan, and F. B. Patten (pp. 9-17, Vol. 105)

D. A. Vermilyea[19]: In this paper the authors suggest that the field in the oxide film on Al is smaller when large rather than small ions are adsorbed on its surface. They state that for this reason the rate of corrosion is less when large ions are adsorbed.

Now, the electric field across a film of reaction product on a metal specimen immersed in an electrolytic solution is determined by the free energy change in the film-forming reaction and the polarizations accompanying the various electrode reactions involved. The adsorption of ions on the surface of a film will have a minor effect on the field within the film, although such adsorption will result in changes in the potentials within the electrical double layer in the solution outside the film. The charges on ions which become adsorbed as a result of chemical or dispersion forces only will be compensated by an excess of ions of opposite sign in the double layer near the electrode. There would be a large change in the field in that part of the double layer between the adsorbed ions and the compensating atmosphere of oppositely charged ions, but outside of this region the change in field would be small; in the limit of a uniform charge such penetration would be entirely absent. On the other hand, if the ions are adsorbed because of electrostatic forces only, that is, because of the charge of the electrode, then the same number of ions will be adsorbed regardless of their size, since they must compensate for the electrode charge. In any case, therefore, the field in the film is to a first approximation unchanged by the adsorption of ions on its surface.

Therefore, it appears doubtful whether the ideas concerning the effects of ions of different sizes on the corrosion of Al are correct. It is more likely that different ions change the corrosion rate by changing the electrode process, for example, by altering the structure of the reaction film.

M. J. Pryor: Dr. Vermilyea's interesting comments on our paper are sincerely appreciated.

It is agreed that the maximum value of a field across a film of reaction product will be a function of the total free energy change. However, we conclude that the field strengths must usually be less than the maximum values because the total free energy change is not generally related to the rate of formation of the reaction product.

Dr. Vermilyea suggests that the structure of the reaction product film is important in determining rates of corrosion of passive film formation. This is undoubtedly true and we have shown that variations in crystallographic and defect structure strongly influence the rate of ion and electron transport through thin films on Al.[20] However, this factor alone does not appear sufficient to explain the difference in reaction rates in different electrolytes. For instance, the crystallographic structure of passive films formed in neutral chromates and in Pb soaps is the same, i.e., γ-Al_2O_3. The defect concentration in these films appears to be similar as judged by dissipation factor and capacitance measurements. Rough calculation of the free energies of formation for the two film-forming reactions indicates that these are of similar magnitude. However, the equilibrium film thickness of γ-Al_2O_3 formed in chromate solutions is very much greater than that in formed Pb soaps. Clearly, some explanation other than free energy change and variation in crystallographic and defect structure is required to explain this factor.

These reasons lead us to consider the possible effect of different fields across the oxide film resulting from specific adsorption of ions. It is suggested by Dr. Vermilyea that, if ions are specifically adsorbed on the oxide surface, the resulting charge will be neutralized by oppositely charged ions in the double layer near the electrode. However, the total charge of the anions reacting on the oxide surface must be equal to the total charge on the cations reacting at the oxide surface in order to maintain electrical neutrality in the over-all reaction. Both anions and cations must therefore be adsorbed on the oxide. If this premise is accepted it is clearly not necessary to postulate equal and opposite charge in the solution double layers. This would be expected to be true during adsorption of long-chain fatty acid anions since our studies indicate that the nonpolar end of the carbon chain is presented to the solution. Even if cations were associated, in a diffuse double layer, with the adsorbed long-chain fatty acid anions, the field across the diffuse double layer would be low.

[15] W. Mehl and J. O'M. Bockris, *J. Chem. Phys.*, 27, 818 (1957).
[16] H. Gerischer, *Z. Elektrochem.*, Bonhoeffer Festband (1958).
[17] W. Lorenz, *Naturwiss.*, 22, 1 (1953).
[18] B. E. Conway and J. O'M. Bockris, *Proc. Roy. Soc.*, Nov. 1958.
[19] Research Lab., General Electric Co., Schenectady, N. Y.

[20] M. J. Pryor, *Z. Elektrochem.*, In press.

The Stern concept of a double layer shows the major potential change is across the specifically adsorbed ion with a smaller potential change across the diffuse double layer. We have difficulty in believing this concept is valid for long-chain fatty acid anions. Here the polar end of the chain is attached to the oxide surface. We have suggested that the major potential change in this case could well be transmitted across a thin dielectric film of γ-Al_2O_3. Since the specific resistance of passive films on Al is between 10^9 and 10^{12} ohms/cm^2/cm, we feel confident that high-resistance layers of this type may easily support potential gradients of the order of 10^6-10^7 v/cm.

If the above concept is combined with the influence of crystallographic and defect structure of the reaction product film, a satisfactory explanation of corrosion and inhibition of Al is obtained.

F. A. Champion[21]: I was interested to note that the results of Messrs. Pryor, Hogan, and Patten support the more practical work on this subject carried out from these laboratories.[22] The latter work cited showed red Pb pigment to be harmful in industrial and marine atmospheres, which are those which might be expected to provide electrolytes conducive to the galvanic effects demonstrated by Messrs, Pryor, Hogan, and Patten. In rural environments, with the much lower concentrations of electrolytes, no such *harmful* effects of practical importance were observed. The effects can be delayed by waterproofing coats, but under service conditions these cannot be relied on to exclude electrolytes from the primer: if they could, then inhibiting pigments would be unnecessary in primers.

M. J. Pryor: Dr. Champion's remarks on the correlation between the previous coating investigations of Rigg and Skerrey and our present work are indeed gratifying and are appreciated. Earlier, we rather doubted that such a clean-cut correlation would be observed because commercial pigments used in paints are usually of low purity and the Pb compounds used in our investigation were as pure as we could obtain. For instance, pigment grade red Pb may often contain as much as 4% litharge, which might be expected to modify results. It is evident from the information kindly supplied by Dr. Champion that the effect of pigment purity is of lesser magnitude than we had anticipated and that a more direct correlation may be drawn between our laboratory results and the performance of organic coatings pigmented with Pb compounds.

D. M. Brasher[23] **and C. P. De**[24]: The experimental results obtained by Pryor, Hogan, and Patten, indicating that of the various types of Pb-containing extracts tested only the Pb soaps are truly inhibitive toward Al, are of great interest.

We would agree with the suggestion that the primary cause of inhibition in the soap solutions is adsorption of the fatty acid anions. The greater efficiency of the more acid Pb soaps, as contrasted with the more alkaline Na and Ca soaps, may perhaps be correlated directly with the observations of Butler,[25] from electrocapillary studies, on the effect of *p*H on the relative degrees of adsorption of fatty acid anions at the metal/solution interface. Butler showed that potassium hydrogen phthalate depressed the electrocapillary maximum and shifted the positive branch of the electrocapillary curve more than did the neutral phthalate. A theoretical correlation between the inhibitive properties of anions and their electrocapillary behavior at different metal surfaces has been suggested by De.[26] It might also be possible that the lower rates of corrosion of Al in red Pb and basic $PbCO_3$ extracts, as compared with those in metallic Pb and litharge extracts, could be ascribed, in addition to the effect of *p*H, to the presence of the inhibitive anions plumbate and carbonate, respectively.

Regarding the mechanism of oxide film growth (assumed to occur only when corrosion is inhibited), it would be interesting to know if inhibition was found to be *maintained* in the fatty acid solutions in the complete absence of oxygen. It is claimed that the absence of oxygen caused only a slight lowering of potential, but owing to slight confusion in the text between "corrosion" and "oxide formation" (p. 16, col. 2, line 9 of discussed paper), the above point is not clear. In work on steel it has been established that inhibition cannot be obtained by nonoxidizing inhibitors in the absence of oxygen; for example, Lochte and Paul[27] and Mayne, *et al.*[28] obtained "corroding" potentials for steel in deaerated sodium phosphate or sodium hydroxide, respectively, and in this laboratory sodium benzoate was found not to inhibit in the absence of oxygen.[29] In radiotracer studies on steel, using K_2CrO_4 labeled with Cr^{51}, it has been shown that oxide films grow logarithmically with time in chromate solutions;[30] further, by an indirect method involving pre-exposure to air, or pre-immersion in aerated inhibitor solutions, film growth in air, sodium benzoate, phosphate, or hydroxide solutions was found to be logarithmic in each case, with a rate constant approximately the same in all environments.[31] This seems to be strong evidence that the mechanism of oxidation is the same in all cases, and is associated with oxygen as the oxidizing agent. Possibly, of course, the fatty acid anion can oxidize Al but not Fe. It is noteworthy that oxygen largely displaces even chromate as the oxidant for Fe in aerated chromate solutions.[32]

We would agree that oxide film formation probably augments the inhibitive properties of the adsorbed layer. Confirmatory evidence for this has been obtained in "potential decay" studies on steel,[33]

[21] Research Labs., The British Aluminium Co. Ltd., Chalfont Park, Gerrards Cross, Bucks., England.
[22] J. Rigg and W. W. Skerrey, *J. Inst. Metals*, **75**, 69 (1948); **81**, 481 (1953).
[23] National Chemical Lab., Teddington, Middlesex, England.
[24] Naval Chemical and Metallurgical Lab., Naval Dockyard, Bombay 1, India.
[25] J. A. V. Butler and C. Ockrent, *J. Phys. Chem.*, **34**, 2286 (1930).
[26] C. P. De, *Nature*, **180**, 803 (1957).
[27] H. L. Lochte and R. E. Paul, *Trans. Electrochem. Soc.*, **64**, 164 (1933).
[28] J. E. O. Mayne, J. W. Menter, and M. J. Pryor, *J. Chem. Soc.*, 1950, 3229.
[29] "Chemistry Research 1954," p. 12, Her Majesty's Stationery Office, London (1955).
[30] D. M. Brasher, A. H. Kingsbury, and A. D. Mercer, *Nature*, **180**, 27 (1957).
[31] Partially reported in "Chemistry Research 1957," p. 12, Her Majesty's Stationery Office, London (1958).
[32] D. M. Brasher and C. P. De, *Nature*, **180**, 28 (1957).
[33] "Chemistry Research 1951," p. 13, Her Majesty's Stationery Office, London (1952).

immersed in chromate solutions for various periods and then transferred to distilled water. The longer the period of pre-immersion in chromate, the slower the subsequent decay of potential in distilled water.

M. J. Pryor: The comments submitted by Brasher and De are most interesting and are appreciated. Certainly the past work by Butler[35] and Adam[34] strongly suggests that an acid soap should be more strongly adsorbed at an interface than a neutral soap. Consequently, a correlation between electrocapillarity behavior and adsorption of the fatty acid anion must exist. However, the correlation between electrocapillarity behavior and inhibition must be more complex because subsequent oxidation of the Al and reduction of the fatty acid anions occurred in the systems we were studying. These latter reactions do not appear to be primarily related to the degree of adsorption but rather to structural aspects of the particular fatty acid anions such as the number, position, and type of unsaturated bonds. Consequently, we would expect an accurate correlation between electrocapillarity behavior and inhibition only if subsequent oxidation was either absent or of significant importance.

Subsequent experimental study of this system, reported elsewhere,[35] provides in main part the answers to the additional questions raised by Brasher and De. In lead linoleate and lead laurate extracts, the presence of dissolved oxygen has virtually no effect in the potential of Al, nor on its passivity. Consequently, passivity may be generated and maintained in deaerated extracts. Here it is evident that oxidation is produced by the discharge of the fatty acid anions with dissolved oxygen playing a minor role. Since we believe that these fatty acid anions are sufficiently strongly adsorbed on the metal or oxide to displace hydroxyl ions from the surface, it is not unreasonable to postulate that they will also largely displace the higher concentration oxygen dissolved in the electrolyte. We have shown previously[36] that the potential of steel in deaerated nonoxidizing inhibitors is controlled accurately by the ferrous ion activity in equilibrium with $Fe(OH)_2$ (or, in the case of phosphate solutions, ferrous phosphate) at the particular pH under examination, provided the ferrous ion activity is greater than around 10^{-6} g ions/l. If Al behaved similarly, we would anticipate very active potentials and slow corrosion if the oxidizing action of lead linoleate and laurate was due to dissolved oxygen. The contrary results outlined above indicate that we must classify these extracts as oxidizing inhibitors.

Slightly different results are obtained in lead ricinoleate in that the potential is much more sensitive to the oxygen content of the electrolyte. Deaeration can shift the potential by as much as 250 mv in the active direction. However, the Al still behaves in a passive manner (or corrodes at an undetectable rate) for 4 days which is the maximum time for which experiments were performed on this system. We have attributed these results to weaker adsorption of the higher pH ricinoleate. The weaker adsorption of ricinoleate should permit more easy simultaneous adsorption of oxygen which would then be expected to contribute to the passivation process in solutions containing dissolved air. This contention is supported in Table I, published here, by measurement of the current efficiency of anodic oxidation of Al in Pb soap extracts saturated with dissolved air at very low current density and at potentials below that at which oxygen is evolved.

Table I. Current efficiency of oxide formation by anodic polarization in different lead soaps at 25°C

Electrolyte	Concentration	Initial pH	Current efficiency % at 0.5 $\mu a/cm^2$	Current efficiency % at 1.0 $\mu a/cm^2$
Lead linoleate	218 mg Pb/l	5.5	91	92
Lead ricinoleate	208 mg Pb/l	6.0	78	82
Lead laurate	296 mg Pb/l	5.5	87	88

The lowered efficiency of oxide formation in ricinoleate extracts is held to be evidence of its weaker adsorption on the Al specimens. In turn, this will lead to magnified effects of the simultaneous presence of oxygen in the solution. Probably some considerable similarity exists between the action of lead ricinoleate on Al and that of sodium tungstate and molybdate on Fe which we described earlier.[36]

[34] N. K. Adam, "The Physics and Chemistry of Surfaces," p. 128, Oxford University Press, Oxford (1941).
[35] M. J. Pryor, *Z. Elektrochem.*, In press.

Equilibria in the Niobium-Hydrogen System

W. M. Albrecht, M. W. Mallett, and W. D. Goode

(pp. 219-223, Vol. 105)

O. M. Katz and E. A. Gulbransen[37]**:** Recently we have again become greatly interested in the study of hydrogen in metals. One of the materials we have investigated is high-purity Nb of the following analysis:

Ta—590	ppm
Fe—330	ppm
Mo—54	ppm
H —2.3	ppm
O —31	ppm
N —131	ppm
C —59	ppm
Zr—0.79	wt %

For equilibrium studies the Nb strip sample (0.025 x 0.500 x 4.429 cm) was polished under purified kerosene through 4/0 emery paper and pretreated for 1 hr at ~ 850°C at $< 0.001\mu$ Hg. Mass spectrometer analysis of the H_2, obtained by diffusion through a palladium tube, showed it to be 99.99+% pure.

A vacuum microbalance incorporated in an entirely new type of enclosure that has been designed to compensate for any "buoyancy effects" was used. Pressure readings were taken with a metal diaphragm, null-indicator in conjunction with a 0.6313 in. ID, precision, Hg manometer. Reproducibility of readings was ±0.2 mm Hg. The temperature variation was ±3°C.

Pressure-composition isotherms were obtained by varying the H_2 pressure and reading the microbalance deflection after equilibrium was reached,

[36] M. J. Pryor and M. Cohen, *This Journal*, **100**, 203 (1953).
[37] Chemistry Dept., Westinghouse Electric Corp., Beulah Rd., Churchill Boro., Pittsburgh 35, Pa.

all at constant temperature. The results are shown in Fig. 1 published here. Close agreement with the

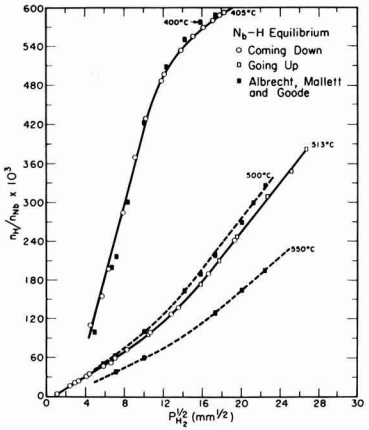

Fig. 1

work of Messrs. Albrecht, Mallett, and Goode in this temperature range was most interesting considering the completely different approach we used.

Data on the phase equilibrium below 300°C are also being collected and will soon be available.

W. M. Albrecht, M. W. Mallett, and W. D. Goode: It is gratifying that the data of Messrs. Katz and Gulbransen corroborate our findings, particularly in view of the difference in the Zr contents of the Nb. No Zr (< 50 ppm) was detected in spectrographic analyses of our material. Apparently, Zr up to about 1 wt % has no measurable effect on the Nb-H_2 equilibria.

Corrosion of Anodically and Cathodically Polarized Magnesium in Aqueous Media

G. R. Hoey and M. Cohen (pp. 245-250, Vol. 105)

W. E. Higgins[35]**:** It is most unfortunate that the authors should have prepared the Mg surfaces by abrasion with emery paper. This activates the surface and brings about a condition where parasitic corrosion is relatively vigorous. A specimen so treated and placed in dilute NaCl solution will evolve gas visibly, whereas a similar specimen rubbed with fine pumice powder is very much more inert.

The reason for this is apparently the pickup of microscopic cathodic particles from the emery (which is a good conductor and a very active cathode). Fine glass paper and clean pumice, on the other hand, are inert and do not bring about the effect described.

It follows that the results obtained by the authors may be very different from those which might be expected from a clean Mg surface.

Robinson's suggestion, that the defect of the current efficiency from 100% is largely due to the breakdown of a protective film, seems very probable for the following reasons: Clean Mg when placed in an electrolyte such as NaCl begins to dissolve slowly and in doing so brings about a condition of high alkalinity in the surface layers of liquid. The presence of such an alkaline layer provides the conditions for a protective film of $MgOH_2$ to form, and dissolution of the metal is slowed down. (It is a significant fact that Mg dissolves much more rapidly in running water than in static conditions.) If, however, the Mg is coupled to a more noble metal, the electrical tension is sufficient to push out Mg atoms into solution. By abstracting electrons, the atoms become positively charged and those in contact with an electrolyte form ions moving away from the metal surface. It seems obvious therefore that such ions passing into solution will interfere with the formation of a film, which involves the production of an insoluble, as distinct from a soluble, product, that is, a Mg compound which clings to the metal surface. If this is so, then it becomes clear why self-corrosion increases as the current drawn from the anode increases. This indeed can be verified by observation. An anode of 100% efficiency ought not to evolve hydrogen on its own surface; the hydrogen ought to be evolved only at the cathode. Yet a Mg anode evolves hydrogen, and the more so as the anode current increases. It would seem that the only explanation is that the H on the anode arises from *local* cathodes due to impurities—in other words, efficiency of the main reaction is being reduced by local reaction. The total efficiency, if it could be measured, would probably be 100% but only the efficiency of the main reaction—between the anode and the cathode—is subject to measurement.

Regarding the undercutting of the Mg grain, this certainly may occur, but it is not strictly by intergranular attack. The grain boundaries are usually cathodic to the grain interior, and therefore the grain is corroded principally at the edges where it adjoins the cathodic grain boundary. This is to be expected since the corrosion current takes the shortest path and the consequence is that the center portion of the grain becomes detached and drops out. By suitable techniques the remnants of the grain boundary constituents can be photographed still in situ. Fig. 1 (a Mg alloy) shows a partly consumed

Fig. 1

grain with the grain boundary constituent outlining the spaces where other grains have disappeared.

G. R. Hoey and M. Cohen: The Mg specimens used in all experiments were annealed at 300°C for 2 hr in an argon atmosphere, polished on 1/0 emery

[35] Magnesium Elektron Ltd., Lumm's Lane, Clifton Junction, Swinton, Manchester, England.

paper, degreased, and etched in 0.1*N* HCl for 1 min. The etchant, 0.1*N* HCl, gives a uniform etch and is sufficiently strong to expose for experimentation the Mg substrate rather than worked metal, emery grit, or, perhaps, as in Higgins' case, pumice powder. One of the objects of this research was to study the behavior of pure Mg.

Higgins states that the only explanation for evolution of hydrogen on Mg is that the hydrogen arises from local cathodes due to impurities. The concentration of cathodic impurities (Fe, Ni, and Cu) in the Mg used in this work was below their tolerance limits, i.e., further purification of Mg will not reduce the corrosion rate significantly. One of the explanations suggested in the paper probably explains hydrogen evolution on Mg.

Corrosion of Mg by undermining of metallic Mg which was demonstrated for experimental conditions favoring thick film formation was not suggested in the paper to be strictly intergranular attack. Intergranular attack was observed only on cathodically polarized Mg at elevated temperatures for which a hydrogen embrittlement theory was proposed. It is not clear from Higgins' discussion or Fig. 1 which of the two types of attack he is considering.

Polarographic Reduction of Delta⁴-3-Ketosteroids in Well-Buffered Media

Peter Kabasakalian and James McGlotten (pp. 261-264, Vol. 105)

Petr Zuman[39]: In solutions of Δ^4-3-ketosteroids, well buffered with usual buffers, principally two waves were observed by us[40] as well as by Lund[41] (the observed adsorption prewaves, which are not discussed by Kabasakalian and McGlotten, probably because they used high steroid concentrations, will be omitted in the present discussion). In the acid region only the more positive wave, in the alkaline only the more negative one, was observed. In the *p*H-region between *p*H 5 and 9 (dependent on the nature of the ketosteroid studied and on the drop-time used), both waves were developed and their ratio was put in the form of a dissociation curve (cf. Fig. 1-3 in footnote 40). When the more positive wave was less than 20% of the total wave-height, its height was independent of the Hg pressure; it follows that this is a current controlled by the rate of a chemical reaction.

The explanation of these facts was that the more positive wave corresponds to the reduction of a protonized form of the ketosteroid, the more negative one to the un-ionized steroid, stable at higher *p*H-values. The kinetic character was explained by the control of the more positive wave by the rate of recombination of the un-ionized steroid with an acid.

All the facts observed[40-42] are consistent with the mechanism:

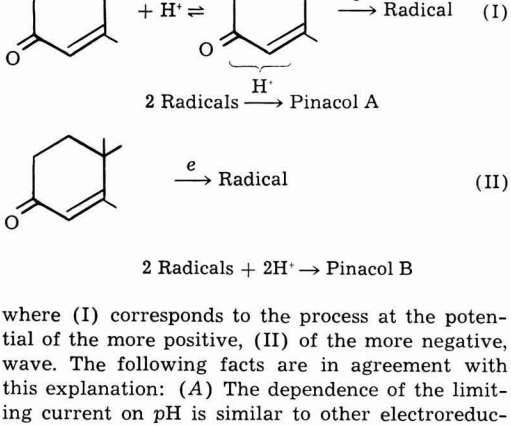

where (I) corresponds to the process at the potential of the more positive, (II) of the more negative, wave. The following facts are in agreement with this explanation: (*A*) The dependence of the limiting current on *p*H is similar to other electroreductions of weak acids and in accordance with the theory.[43, 44] (*B*) The dependence of the half-wave potential of the more positive wave on *p*H for *p*H-values smaller than pK, the change in slope of this dependence at *p*H = pK, as well as the practical independence observed for the more negative wave are similar to the dependence of the half-wave potentials of reducible acids and practical *p*H-independence of the wave for the corresponding base.[45-48] The form of the dependence of the wave of the cation is, moreover, in accordance with the approximate theory for the shifts of half-wave potentials of kinetic currents.[49] The half-wave potential of the un-ionized ketosteroid is practically *p*H-independent, in accordance with the fact that no proton is accepted in the potential-determining step (II). The smaller shifts observed in this case as well as for other anions are probably due to secondary effects like ionic strength, concentration of cations, etc. (*C*) Different isomers of pinacol (Pinacol A and Pinacol B) were isolated,[42] when a preparative reduction on a Hg pool electrode was carried out in acid or in alkaline solutions, respectively. This is a support of two different reduction mechanisms (I) and (II).

The findings of Lund[42] have shown that the rate of protonation preceding the electroreduction plays an important role even at the Hg pool electrode. So far as we know, this is the first case recorded where a rate (not an equilibrium) of a reaction preceding the electron-transfer changes the mechanism of a reduction on a Hg pool electrode.

The existence of the protonized form of Δ^4-3-ketosteroids has been proved by electropreparative[42] as well as polarographic[40] findings.

In their article, Kabasakalian and McGlotten try to explain the change of the wave-height with *p*H by the formation of: a "steroid-hydrogen ion complex, represented a reaction between a steroid and a

[39] Polarographic Institute of the Czechoslovak Academy of Science, Prague, Czechoslovakia.
[40] P. Zuman, J. Tenygl, and M. Brezina, *Chem. listy*, **47**, 1152 (1953); *Collection Czechoslov. Chem. Communs.*, **19**, 46 (1954).
[41] H. Lund, Personal communication.
[42] H. Lund, *Acta Chem. Scand.*, **11**, 283 (1957).
[43] R. Brdicka and K. Wiesner, *Collection Czechoslov. Chem. Communs.*, **12**, 138 (1947); R. Brdicka, *ibid.*, **19**, S41 (1954).
[44] J. Koutecky, *Chem. listy*, **47**, 323 (1953); *Collection Czechoslov. Chem. Communs.*, **18**, 597 (1953).
[45] R. Brdicka, *Collection Czechoslov. Chem. Communs.*, **12**, 212 (1947).
[46] V. Hanus, Thesis, Charles University, Prague (1949).
[47] J. Volke and V. Volková, *Chem. listy*, **49**, 490 (1954); *Collection Czechoslov. Chem. Communs.*, **20**, 1332 (1955).
[48] P. Zuman, J. Chodkowski, and F. Santavy, *Collection Czechoslov. Chem. Communs.*, In press.
[49] N. Tanaka and R. Tamumushi, Proc. First Intern. Polarographic Congr., Prague, 1951, Part I, p. 486, published by Prirodoved. vydav., Prague (1951).

specific buffer acid (rather than a generalized acid-base reaction)." In contradiction to this statement, Eq. (I) in the discussed paper corresponds to a general acid-base reaction. Even when not explicitly stated, the particle reduced in the more positive wave is supposed to be a complex of the steroid with the buffer acid. There is no experimental support for the reduction of such a particle. The observed independence of the first wave to the total current in changing the concentration of the steroid, as well as the *p*H-dependence of the wave height found in changing the ratio of primary and secondary phosphates (without holding ionic strength constant—Table IV), are better explained by the mechanism given by us. Also, the shape of the dependence of the half-wave potential on *p*H could hardly be explained by the reduction of a complex only.

On the other hand, to consider the ratio of the first and second waves as proportional to equilibrium concentrations is an error, which was early discerned by Brdicka.[45] The calculation of K in Table V of the discussed paper bears witness to misunderstanding of the principles of kinetic currents controlled by recombination, which here play the major role.

It is possible that, in the *rate of formation* of the protonized form, other proton donors besides the hydroxonium ion play a role,[50-55] and the rate constant becomes

$$k_r = k_{H_2O} + k_{H_3O^+}[H_3O^+] + \Sigma\, k_{HA}[HA]$$

Unfortunately, the quantitative treatment of the recombination rate constants (k_r) is impossible so far, because of lack of the thermodynamical equilibrium constants ($K = k_d/k_r$). But the small change of i_1/i_2 with the buffer concentration at *p*H = const (Tables IV and V of Kabasakalian and McGlotten) shows that the contributions of $k_{H_3BO_3}$ and $k_{H_2PO_4^-}$ are rather small, if the change in i_1/i_2 is not caused by the change in ionic strength[46, 56] at all.

An explanation of the observed two waves by inappropriate buffering is also improbable. In our experiments, the concentration of the acid buffer-component was always 50 times higher than the concentration of the depolarizer. Because at least a twentyfold excess of the buffer is necessary[56-58] for good buffering, the solutions with the lowest buffer concentrations in Table IV(c) are inappropriately buffered.

When in the *p*H-range, where recombination occurs, buffers with trialkylamine as basic component were used, only one wave was observed (paper by Kabasakalian and McGlotten, under discussion). This was interpreted as normal behavior and the curves in phosphate and borate buffers are supposed to be due to a specific action of buffer components.

Volková[59] has shown recently that the influence of acids of the type NR_3H^+ on recombinations is different from acids of the type H_2A_1, HA_1, or HA_1^-. For un-ionized acids or for anions with acid nature in reactions

$$HA_1 + A_2^- \rightleftharpoons HA_2 + A_1^- \qquad [1]$$

$$HA_1^- + A_2^- \rightleftharpoons HA_2 + A_1^{2-} \qquad [2]$$

(where HA_2 is the reducible acid) the concentration of the buffer has a small or often negligible influence on the ratio i_1/i_2. For acids of the type NR_3H^+ a remarkable effect was observed,[59] the nature of which is dependent on the type of the reducible acid involved. For a reaction of negatively charged particles of the type

$$NR_3H^+ + A_2^- \rightleftharpoons HA_2 + NR_3 \qquad [3]$$

the height of the wave of the acid form HA_2 increases with increasing concentration of NR_3H^+. On the other hand, for the first wave of phthalic acid, corresponding to a reduction of a cation,[58] where uncharged acid is reacting with protons, a decrease in the wave of $H_2A_2^+$ with increasing amine buffer concentration was observed.[59]

Similarly a decrease of the more positive wave of protonized testosterone with increasing concentration of NR_3H^+ was observed (Fig. 1 published here).

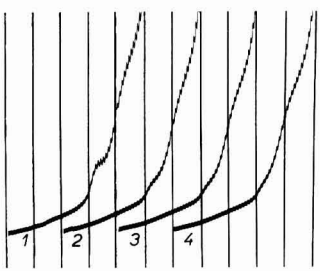

Fig. 1. Influence of concentration of trimethylamine buffer on the waves of methyltestosterone; 0.5 mM methyltestosterone in 50% ethanol with 0.05 M borate buffer pH 8.5 with different concentrations of a trimethylamine buffer pH 8.5 added. Concentration of trimethylamine buffer: 1, 0; 2, 1.0 mM; 3, 3.0 mM; 4, 5.0 mM. Ionic strength kept constant. Curves starting at —1.2 v, mercurous sulfate electrode, Kalousek's vessel, 200 mv/absc, t_1 = 3.2 sec, m = 1.93 mg/sec, full-scale sensitivity 1.3 μa.

Also, in this case a protonation of an uncharged particle takes place.

The effect of the small concentration of trimethylamine buffer in the presence of an excess of borate buffer of the same *p*H-value (Fig. 1) excludes the possibility of a *p*H-change on the surface of the electrode. Even the smallest concentration of trimethylamine buffer used is sufficient to change the whole character of the curve. This cannot be explained by complex formation with borate or phosphate, but rather by a specific effect of NR_3H^+-ions on the rate of recombination.

The behavior in different buffers containing 50% ethanol and of the same *p*H is given in Fig. 2 pub-

[50] K. Wiesner, M. Wheatley, and J. M. Los, *J. Am. Chem. Soc.*, 76, 4858 (1954); M. S. Wheatley, *Experientia*, 12, 339 (1956).
[51] J. H. Green and A. Walkley, *Austr. J. Chem.*, 8, 51 (1955).
[52] R. Zahradník, E. Svátek, and M. Chvapil, *Chem. listy*, 51, 2232 (1957).
[53] E. T. Bartel, Z. R. Grabowski, W. Kemula, and W. Turnowska-Rubaszewska, *Roczniki Chem.*, 31, 13 (1957).
[54] O. Hrdy, *Chem. listy*, 52, 1058 (1958).
[55] P. Zuman, Unpublished results on the polarography of periodic acid.
[56] V. Hanus, Proc. First Intern. Polarographic Congr., Prague, 1951, Part I, p. 811, published by Prirodoved. vydav., Prague (1951).
[57] J. Kuta, *Acta Chim. Acad. Sci. Hung.*, 9, 119 (1956); *Chem. listy*, 49, 1419 (1955); *Collection Czechoslov. Chem. Communs.*, 21, 697 (1956).
[58] A. Ryvolova and V. Hanus, *Chem. listy*, 50, 46 (1956).
[59] V. Volkova, Paper presented before the Second Czechoslovak-Hungarian Polarographic Conference, Prague (1958).

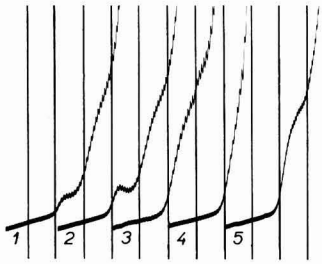

Fig. 2. Influence of buffer composition at pH 8.3 on the waves of methyltestosterone; 0.5 mM methyltestosterone in 50% ethanol in buffers of pH 8.3 of different composition: 1, borate buffer; 2, veronal buffer; 3, trimethylamine buffer; 4, triethanolamine buffer—the wave is obscured by catalytic hydrogen evolution; 5, ammonia-ammonium chloride buffer. Curves starting at —1.4 v, mercurous sulfate electrode, Kalousek's vessel, 200 mv/absc, t_1 = 3.2 sec, m = 1.93 mg/sec, full-scale sensitivity 1.3 μa.

lished here. The curve in the veronal buffer is practically the same as in borate and shows two waves. The curves in trimethylamine and NH_3 buffers[60] are similar to each other but different from the ones mentioned above in showing one wave only. Kabasakalian and McGlotten, in the discussed paper, supposed that one wave at higher *p*H's is observed in organic buffers only. The polarogram in Fig. 2 published here shows that an organic buffer like veronal can show the same normal behavior as borate and that even in an inorganic buffer like NH_3 the NH_4^+-ions can play the same role as NR_3H^+. The type of the buffer acid and not the origin is of primary importance.

The shift of half-wave potentials in buffers with NR_3H^+ as the acid component is complicated by the dependence of the half-wave potential on the concentration of NR_3H^+, similar to the influence of NH_4^+ and quaternary cations on other reduction processes.[61,62]

It can be concluded that the behavior of ketosteroids in phosphate, borate, veronal, and similar buffers is normal and in agreement with the theory. The influence of amine-containing buffers is exceptional in decreasing the first wave and in shifting the second wave to more positive potentials.

P. Kabasakalian: In an attempt to show that the wave splitting obtained during the polarographic reduction of steroids using phosphate and borate buffers was not due to the *p*H of the solution but to the specific buffer components, we had proposed the formation of a steroid-hydrogen ion complex after determining that these buffers did not contribute appreciably to any recombination rate. Although we were able to determine the value of the "equilibrium constants" for the phosphoric and boric acid interaction with the steroids, we must admit that this does not necessarily prove the existence of such an equilibrium.

Zuman's contention that the reaction is in essence identical to that of a reducible acid is based on the fact that the limiting current and half-wave potential behavior with *p*H is similar to that for a reducible acid and that the isolation of different stereoisomers from a large-scale reduction by Lund is supposed to indicate two different reaction mechanisms. Products of irreversible reactions are not good criteria of the potential-determining step mechanism. Bladon, Cornforth, and Jaeger[63] have questioned Lund's proof of structure and his mechanism which assumes that the radicals retain their configuration until they dimerize by a slow reaction.

Tanaka and Tamamushi have derived, from the standpoint of chemical kinetics, the limiting current-*p*H and half-wave potential-*p*H relationships of reducible organic acids. They considered the case where the dissociated anion, A^-, and undissociated molecule, HA, of an organic acid are kept in equilibrium in the body of the solution according to Eq. (I) and where the undissociated molecule is reduced at the more positive potential than the dissociated anion.

$$A^- + H^+ \rightleftharpoons HA \qquad (I)$$

The undissociated molecule combines with the electrons at the electrode surface and then the reduced ion, $R^=$, reacts with the hydrogen ions resulting in the reduced molecule, RH_2.

$$HA + 2e \rightleftharpoons R^= \qquad (II)$$

$$R^= + 2H^+ \rightleftharpoons RH_2 \qquad (III)$$

The derived relationships satisfactorily explained the behavior of pyruvic and phenylglyoxylic acids.

Zuman has proposed that steroids undergo the following type of reaction.

$$S + H^+ \rightleftharpoons SH^+ \qquad (IV)$$

$$SH^+ + e \rightleftharpoons SH\cdot \qquad (V)$$

followed by dimerization of $SH\cdot$.

There is a major difference between these two mechanisms. The hydrogen in the acid group in Eq. (I) is not the one that is involved in the reduction step while the hydrogen in the protonated steroid in Eq. (IV) is involved in the reduction. This difference should be enough to make questionable Zuman's contention that steroid reductions are identical to the acid reductions.

Steroid reductions using phosphate, borate, and veronal buffers have all the characteristics of a reducible acid but the following data conflict: different acid buffers which do not contribute appreciably to the recombination rate of the protonated reducible species fail to give the same wave splitting at identical *p*Hs as Table I published here indicates.

Table I

Buffer	*p*H	i/i'
Phosphate	7.84	2.02
Veronal	7.90	0.50
Borate	8.04	0.25
Phosphate	8.09	1.40

Buffer acid = 0.05M; ionic strength = 0.2.

[60] The concentration of ammonia in the buffer is so low that practically no condensation (*see* footnote 61) of the carbonyl group occurs.

[61] P. Zuman, *Collection Czechoslov. Chem. Communs.*, 15, 839 (1950).

[62] M. Ashworth, *Collection Czechoslov. Chem. Communs.*, 13, 229 (1948).

[63] P. Bladon, J. W. Cornforth, and R. H. Jaeger, *J. Chem. Soc.*, 1958, 863.

In order to explain the single wave we obtained with amine buffers, Zuman proposes that three things must happen:

(*A*) the height of the first wave is reduced presumably to zero; (*B*) the second wave has its half-wave potential moved an exact amount so that it now coincides with the former position of the first wave; (*C*) the half-wave potential of the new shifted second wave, which was formerly *p*H independent, is now *p*H dependent an exact amount which brings it into line with all the other good buffers which were used at the lower *p*Hs.

It would indeed be very fortuitous if these three things occurred simultaneously, together with the fact that in our study two different amines, trimethylamine and triethylamine, which were used would have to fulfill the above requirements.

We did not find that the half-wave potential shifted with amine buffer concentration as Table II published here indicates.

Table II

Buffer conc.	$-E_{1/2}$	k	pH
0.20M	1.59	2.0	8.8
0.10M	1.59	2.1	8.9
0.05M	1.60	2.1	8.9

Constant ionic strength.

It is our candid opinion that neither our nor Zuman's proposal satisfactorily explains the wave splitting obtained with phosphate, borate, and veronal buffers.

Silver, Cobalt, and Positive-Grid Corrosion in the Lead-Acid Battery

J. J. Lander (pp. 289-292, Vol. 105)

J. F. Schaefer and H. R. Karas[64]: A microscopic investigation of positive grid corrosion in lead-acid batteries has been in progress in the Globe-Union Labs. for the past year (1957). The mounting and polishing technique as developed by Simon and Jones of the Naval Research Labs. is being effectively employed. Data are obtained by measuring the cross-sectional areas of grid bars at various stages during life of batteries, with the remaining metal calculated as a percentage of the original grid bar area.

In the course of work on various alloys, several series of experiments with Co and Co and Ag additions to cells have been made. In concordance with ideas expressed over the past several years, and stated by Lander today, as to the importance of standing time during battery service, we have collected data on the occurrence of grid corrosion on open circuit standing.

Figure 1 shows the corrosion of a positive grid bar after two years' open-circuit stand at ambient temperature in an unheated garage in Detroit. About 55% of the grid metal has corroded away. Examination of the battery definitely showed positive grid failure and some years ago would have been classified as failure due to overcharging.

[64] Globe-Union Inc., Milwaukee 1, Wis.

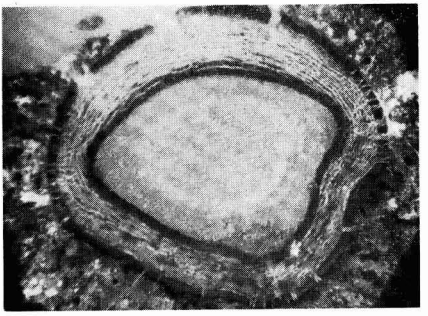

Fig. 1. Positive grid bar from battery after two years' open-circuit stand.

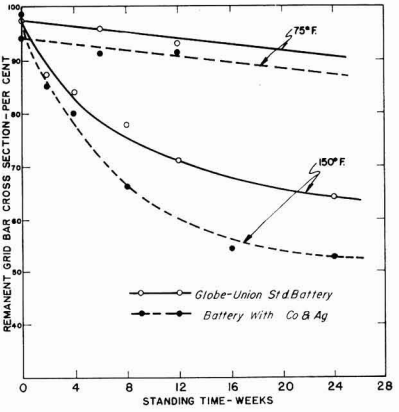

Fig. 2. Effect of open-circuit standing on positive grid corrosion.

Figure 2 shows data obtained on batteries standing at 75° and 150°F in the laboratory. The effect of Co and Ag additions are shown in the curves. At 150°F, which approximates under-the-hood temperatures, the addition of Co and Ag causes an approximate 50% increase in corrosion in 12 weeks.

Work on this project is continuing and it is hoped that a complete report will be ready for presentation at a future meeting of the Battery Division of the Society.

Diffusion of Oxygen in Zirconium and Its Relation to Oxidation and Corrosion

J. P. Pemsler (pp. 315-322, Vol. 105)

L. Young[65]: Dr. Pemsler makes use of the "Pilling-Bedworth number" (defined as the ratio of molar volumes of oxide and metal) to decide that the oxide on Zr is under compression. I would like to repeat the point which I made in a recent paper[66] that with flat surfaces there is no obvious reason why the oxide should be under compression if this number is greater than unity, and, furthermore, that despite the widespread impression to the contrary, Pilling and Bedworth made no such suggestion, at least not

[65] British Columbia Research Council, University of British Columbia, Vancouver 8, B. C., Canada.
[66] L. Young, *Acta Met.*, 5, 711 (1957).

in their original paper.[67] Their "hypothesis" was, in fact, the perfectly logical deduction that compressive stresses will be produced when the metal surface is convex and when oxygen—not metal—is mobile, so that fresh layers of oxide are produced in the space previously occupied by the metal from which they are formed. Obviously, other nonflat surfaces, or metal ion movement, require the application of other conditions to determine the general macroscopic stress, and rough surfaces and microscopic stresses are another case again.

[67] N. B. Pilling and R. E. Bedworth, *J. Inst. Met.*, 29, 529 (1923).

J. P. Pemsler: Recent papers by Young[66] and Vermilyea[68] have duly modified current thinking on what is commonly referred to as the Pilling-Bedworth volume-ratio concept. For cation diffusers, on samples with flat surfaces, the arguments against deciding *a priori* that the film is under compression are quite tenable. However, in cases where oxygen diffusion through the oxide controls the rate of oxidation, as is the case in the oxidation of Zr at low and intermediate temperatures, it is not clear whether the oxide should be under compression.

[68] D. A. Vermilyea, *Acta Met.*, 5, 492 (1957).

June 1959 Discussion Section

A Discussion Section, covering papers published in the July–December 1958 JOURNALS, is scheduled for publication in the June 1959 issue. Any discussion which did not reach the Editor in time for inclusion in the December 1958 Discussion Section will be included in the June 1959 issue.

Those who plan to contribute remarks for this Discussion Section should submit their comments or questions in triplicate to the Managing Editor of the JOURNAL, 1860 Broadway, New York 23, N. Y., *not later than March 2, 1959*. All discussion will be forwarded to the author, or authors, for reply before being printed in the JOURNAL.

Abstracts of "Recent News" Papers

Presented at Electronics Division Semiconductor Symposia

New York Meeting, April 28-30, 1958

Method of Growing Silicon Crystals without a Crucible

W. C. Dash, Research Laboratory, General Electric Co., Schenectady, N. Y.

In place of a crucible, a Si "pedestal" is used to support a melt heated directly by rf. The pedestal is a cylinder with a number of radial slots which prevent extensive heating. On top of it is placed a solid disk which is melted and held stably by electromagnetic levitation and surface tension. A seed is inserted into the melt and withdrawn as in the Czochralski method. Many crystals have been found to be free of dislocations as determined by etching and decoration, in support of earlier results on crucible grown specimens. Germanium crystals have also been grown by this method.

Nitrogen in Silicon

W. Kaiser and C. D. Thurmond, Bell Telephone Laboratories, Inc., Murray Hill, N. J.

Very little is known about the solubility of N in either solid or liquid Si. The phase Si_3N_4 which has two crystalline modifications is the only well-established Si-N compound. Liquid Si has been exposed to gaseous ambients containing varying concentrations of N_2 or NH_3. Under certain conditions Si_3N_4 needles may be grown on the surface and into the body of the melt. The solubility of nitrogen in molten Si is of the order of 10^{19} atoms/cm^3. During the crystallization of the liquid zone, precipitation of Si_3N_4 occurs in the last portion to freeze. The concentration of electrically active impurity states is less than 10^{12} atoms/cm^3.

Uniform Resistivity p-Type Silicon by Zone Leveling

E. D. Kolb and M. Tanenbaum, Bell Telephone Laboratories, Inc., Murray Hill, N. J.

Silicon single crystals 1 cm in diameter and 16 cm long have been grown with aluminum doping in an automatic floating zone apparatus. Crystals have been prepared with nominal p-type resistivity of 0.5 ohm-cm and resistivity variations of less than 5% along the crystal length. Variations of resistivity with rotation rate, growth rate, ambient gas flow rate, and other growth variables have been studied. Zone length variations in the automatic apparatus are reported.

Technique for Growing Crystals of Uniform Impurity Concentration

W. F. Leverton, Raytheon Manufacturing Co., Waltham, Mass.

A simple modification of the Czochralski or seed pulling method permits the growing of large single crystals containing a uniform concentration of doping element throughout their extent. The method, which has been thoroughly tested, is described with particular reference to the growing of Ge crystals. Results are presented. The use of this technique for growing Si crystals is discussed.

Small Scale Impurity Fluctuations in Silicon Crystals Grown from the Melt

R. L. Rouse, Associated Electrical Industries Ltd., Aldermaston, Berks., England

Impurity fluctuations in Si single crystals grown from the melt have been shown up by the technique of solid-state diffusion in compensated samples in which an impurity step was first incorporated by remelting and recrystallization. Fairly regular striations were found with a spacing of a few microns and corresponding to a change in relative impurity concentrations of order 1%.

Effects of Fast Neutron Irradiation on Electron Lifetime in p-Type Silicon

R. W. Beck, E. Paskell, and C. S. Peet, Battelle Memorial Institute, Columbus, Ohio

Studies of the change in minority carrier lifetime in p-type Si indicate that the change in reciprocal lifetime with fast neutron exposure is linear up to a dose of at least 10^{19} neutrons/cm^2. The rate of lifetime change was found to be about 3×10^{-6} reciprocal sec/neutron/cm^2 for p-type Si of resistivities from 15 to 50 ohm-cm. The radiation-induced recombination level appears to be near the middle of the forbidden band. Results of limited experiments with monoenergetic neutrons are reported also.

Hall Effect in p-type Germanium at High Electric Fields

J. Zucker and E. M. Conwell, Sylvania Electric Products Inc., Bayside, N. Y.

The Hall coefficient of a semiconductor depends not only on the number of free carriers but on the details of scattering processes and band structure. To obtain information concerning the latter in the "hot carrier" range, measurements of Hall coefficient were taken on p-type Ge as a function of electric field intensity up to 7000 v/cm at liquid nitrogen and room temperatures. Voltage was applied in pulses to avoid heating the sample. A null method was developed for measuring pulse heights. To minimize capacitive loading on the Hall probes, cathode followers and attenuators were used. Precautions were taken to minimize injection and prevent surface breakdown. For low magnetic fields the Hall constant of a high resistivity p-type sample was found to decrease 35% as the electric field increased from the Ohm's law region to 7000 v/cm. This does not imply an increase in carrier concentration since the sample was in the exhaustion region. An explanation of the decrease in terms of the band structure of p-type Ge* is presented.

* E. O. Kane, *J. Phys. Chem. Solids*, **1**, 82 (1956).

Methods of Measurement of Lifetime and Resistivity of Silicon without Contacts

I. R. Weingarten and M. Rothberg, Merck and Co., Inc., Rahway, N. J.

Resistivity and lifetime measurements of zone-refined Si crystals have been made without direct contacts by two methods.* One method employed inductive coupling for both resistivity and lifetime measurements but required calibration and had a minimum useful frequency of about 10 megacycles. Our measurements were made with a Twin-T bridge, however, instead of a Q meter as previously reported† and yielded more directly usable data. The other method employed capacitive coupling and yielded data that permitted direct calculation of resistivity based on either bridge or Q meter measurements. With capacitive coupling it was possible to use frequencies as low as 50 kilocycles, but best results were obtained in the vicinity of one megacycle. Lifetime was estimated by noting change of average resistivity under illumination with either type of coupling. This measurement required reference calibration. More precise lifetime measurement was made by

* W. Keller of Siemens, Pretzfield Lab., has developed similar methods which will be published shortly.

† H. K. Henisch and J. Zucker, *Rev. Sci. Instr.*, 27, 409 (1956).

photoconductive decay observed by use of capacitive coupling and a one-megacycle carrier.

Resistivity Homogeneity Evaluation of Germanium Single Crystals by Photovoltaic Scanning

J. Oroshnik and A. Many, Sylvania Electric Products Inc., Bayside, N. Y.

The photovoltaic effect due to inhomogeneities in the bulk of Ge single crystals is used to determine the resistivity uniformity of Ge wafers. A plot of photovoltage (microvolt range) vs. position for any one wafer gives a qualitative picture of the resistivity variation throughout it. One can then determine how to cut a wafer such that samples of maximum uniformity may be expected. In addition by using a sample of rectangular geometry, quantitative results can be obtained. This method is very sensitive and rapid, far more so than the usual resistivity scans. Resistivity variations of less than 0.1% in 10 ohm-cm Ge are easily detected. Results are presented. The photovoltaic method admits measurement of resistivity changes under conditions where ordinary probe methods are extremely difficult.

Experimental Studies of the Diffusion of Phosphorous into Silicon

J. E. McNamara and C. U. Darter, Motorola Semiconductor Division, Phoenix, Ariz.

A flowing gas method for diffusing phosphorous into Si is described. Using the pn junction-identification method to determine the diffusion gradients, the activation energy was found to be 79 ±3 kcal/mole. Surface concentrations tended to be lower than those reported by other investigators using another chemical form of phosphorous as the diffusant source. Possible explanations for this difference are discussed.

Use of a Radioactive Tracer in the Study of a Flowing Gas Method for Diffusing Antimony into Germanium

J. E. McNamara, D. H. Kouns, and C. U. Darter, Motorola Semiconductor Division, Phoenix, Ariz.

A radioactive tracer procedure is described for studying the diffusion of Sb into Ge from a flowing hydrogen ambient. Initial experimental results are presented.

A Double-Diffused, Silicon, High-Frequency Switching Transistor Produced by Oxide Masking Techniques

J. F. Aschner, W. F. J. Hare, J. J. Kleimack, and C. A. Bittman, Bell Telephone Laboratories, Inc., Murray Hill, N. J.

The relative merits of two double-diffused transistor structures are discussed, one of which employs a localized emitter. The merits of the localized emitter structure include greater ease of making a base contact, increased range of emitter surface concentrations, elimination of emitter etching, and better dimensional control. A process for producing the localized emitter structure is described employing the masking property of SiO_2 against the subsequent phosphorous diffusion. The dimensions of each emitter are closely controlled by etching away this oxide mask from only those regions not protected by a specially prepared photo resist coating. Transistors have been produced which switch 30 ma with a gain of 12, in times in which the sum of the turn "on," storage, and turn "off" time is less than 0.1 μsec. Small signal alphas of 0.97, and alpha cut-off frequencies in common base connection in excess of 300 mc have been achieved. Other typical parameters are collector to base breakdown voltage of 60 v, collector capacity 5$\mu\mu$f, and base resistance 200 ohms.

Surface Stabilization of Silicon by Thermally Grown Oxides

M. M. Atalla, Bell Telephone Laboratories, Inc., Murray Hill, N. J.

The properties of thermally oxidized Si surfaces on single conductivity crystals and on single and multiple junction devices have been studied. The following results are presented: (*a*) properties of the oxide; (*b*) density, distribution, and type of surface states obtained by the conventional a-c field-effect technique and by a new zero-frequency 4-point probe field-effect technique; (*c*) ambient effects and suppression of outer or slow states; (*d*) formation of "p-oxide" and "n-oxide" and dependence on process and impurity content of crystal; and (*e*) characteristics of thermally oxidized diodes and multiple junction devices.

Immersion Plating of Copper on Silicon

Pei Wang, Sylvania Electric Products Inc., Woburn, Mass.

Copper can be easily deposited from an aqueous solution on Si surfaces by an immersion plating technique. The deposit is very adherent and can be used for making low resistance contacts to Si. The mechanism of this reaction is believed to be a galvanic displacement.

Silicon Light Figures

P. Pennington and J. D. Turner, Hughes Aircraft Co., Los Angeles, Calif.

Light figures are the geometric patterns produced by the reflection of a light beam from a suitably etched single crystal surface. The figures produced by (111) oriented Si surfaces etched in NaOH and KOH solutions have been studied in detail. These figures varied from the familiar three-rayed star obtained with dilute etches, through triangular rings, to large circles obtained with concentrated solutions (60% or more). The figures vary regularly with time of etching, temperature of etch, and concentration and composition of the etch solution. Study of the optical system and of the etched surfaces has shown that the figures are produced from each pit by a simple reflection. The forms of the light figures then show how the bottoms of the etch pits deviate from planarity in a way varying regularly with etching conditions.

Ottawa Meeting, Sept. 29-Oct. 1, 1958

Preparation, Properties, and Stoichiometry of PbTe Single Crystals*

E. Miller, I. Cadoff, and K. Komarek, College of Engineering, New York University, New York, N. Y.

Single crystals of various compositions of PbTe were grown by the Bridgman technique using zone refined Pb and Te as starting materials. The lattice parameters were determined over the entire composition range of PbTe, and electronic properties were determined for crystals at and on either side of the stoichiometric point. Analysis of the data obtained gives evidence that the stoichiometric composition and congruent melting point of PbTe do not coincide.

* This research was supported by the U. S. Air Force under Contract No. AF33(616)-3883 monitored by the Aeronautical Research Lab., Wright Air Development Center.

The Etching of $Bi_2Te_xSe_{(3-x)}$

J.W. Faust, Research Labs., Westinghouse Electric Corp., Pittsburgh, Pa.

In studying the fundamental properties of these compounds, it is advantageous and often necessary to have a clean surface free of mechanical damage and to have a knowledge of the degree of perfection of the sample. Both of these can be accomplished by suitable etchants. Problems associated with surface preparation and with devising suitable etches are discussed. Etches for cleaning surfaces and for revealing macro and microstructure are given.

Effect of Certain Variables on the Photoconductivity of CdSe Polycrystalline Layers

G. S. Briggs, Radio Corp. of America, Lancaster, Pa.

In the preparation of polycrystalline layers of cadmium selenide, it was observed that the composition of the substrate, density of the preferred coating, nature of the atmosphere used during the sintering process, time and temperature of firing, and type of impurity present in the preparation have a profound effect on the photoconductivity of the resulting polycrystalline layer.

Cadmium-selenide layers prepared on substrates such as borosilicates, lime glass, and "Vycor" have lower resistivity and a poorer light-to-dark current ratio than comparable layers prepared on high-alumina substrates. The denser and/or thicker the coating (other things being equal) the higher the photo and dark currents. The degree of sintering and texture or homogeneity of the polycrystalline layer is markedly affected by the concentration of chloride and oxygen present during the firing process. In general, relatively high concentrations of oxygen and copper increase resistivity, while high levels of chloride and low levels of oxygen decrease resistivity.

Arsenic- and Carbon-Free Antimony for Intermetallic Compounds

R. R. Haberecht, A. Herczog (present address: Corning Glass Works,

Corning, N. Y.), and A. E. Middleton (present address: General Electric Co., Cleveland, Ohio), P. R. Mallory & Co., Indianapolis, Ind.

The paper describes methods of purification of Sb for the removal of metallic impurities, As, and C.

The As-Sb phase diagram indicates solid solubility of the two components for all compositions. The segregation coefficient for small quantities of As in Sb is expected close to unity. Therefore, zone refining has no appreciable effect of eliminating As from Sb. These unfavorable conditions of segregation can be modified, however, by addition of small amounts of Al to the As-containing Sb and by zone refining it thereafter. In this case, As shows a preferential segregation at the front end of the Al-containing part of the zone refined ingot while segregation of all other impurities is observed in the back. According to the amount of Al added and the number of refining passes, the segregation of both impurities can take place either at the front or at the back portion of the Sb ingot. An explanation is given for the mechanism of the observed segregation patterns and the possible application of this mechanism to other systems is discussed.

Another impurity contained in Sb in larger quantity is C. C appears to be present in Sb in the form of a volatile compound of low vapor pressure. C was removed from the Sb by vacuum double distillation of the metal.

Preparation and Properties of Some Ternary Semiconductor Materials*

D. R. Mason, L. Thomassen, D. F. O'Kane, and J. S. Cook, Dept. of Chemical and Metallurgical Engineering, University of Michigan, Ann Arbor, Mich.

A method for preparing intermetallic compounds from pure elements is described. Preliminary results indicate that not all the members of the homologous series $II^bIII^b_2VI^b_4$ (where II^b is Zn, Cd, or Hg, III^b is In or Tl, and VI^b is Se or Te) form single-phase compounds or have congruent melting points. Experimental evaluations of these materials are compared with results reported by Hahn, *et al.*** and Busch, *et al.*†

* Work supported in part by the National Science Foundation, and by Project MICHIGAN under a Signal Corps Contract.

** H. Hahn, G. Frank, W. Klinger, A. D. Storger, and G. Storger, *Z. anorg. u. allgem. Chem.*, 279, 241 (1955).

† G. Busch, E. Mooser, and W. B. Pearson, *Helv. Phys. Acta.*, 29, 192 (1956).

Precision Doping of Silicon Crystals

W. W. Greer, E. I. du Pont de Nemours & Co., Inc., Wilmington, Del.

The controlled doping of Si melts with master alloys to obtain Si crystals of reproducible resistivity levels is reported. The master alloys were produced by vacuum casting from doped Si melts into silica tubes. Results of master alloy uniformity checks, doping to various resistivity levels, heat treatment analyses, lifetime determinations, and dislocation density counts are among data included.

Dual Display System for Measuring Lifetime in Silicon Using Photoconductivity Decay

J. Mandelkorn, U. S. Army Signal Research and Development Lab., Fort Monmouth, N. J.

Although measurements of minority carrier lifetime in semiconductors may be made by one of several different means, the procedure used at present in the vast majority of laboratories is the photoconductivity decay method. A recent survey showed poor correlation between values of lifetime as measured at different laboratories, all of which used the photoconductivity decay method; the reasons for such poor correlations are significant.

Observations of instrumentation and techniques used at many laboratories to measure lifetime were made and an analysis of differences and possible sources of error which could lead to poor correlation between measurement was made. In addition, experiments were made with modifications of instrumentation to limit error in the measurement.

This paper encompasses practical observation and experience in lifetime measurement, including instrumentation and techniques, and discusses a dual display method which minimizes error in the measurement.

Plastic Deformation of Germanium by Alloying

W. J. Feuerstein, Motorola, Inc., Phoenix, Ariz.

It has been observed that after alloying single-crystal Ge with tin and thermally cycling the Ge in contact with the tin-doped alloy material, considerable plastic deformation of the Ge adjacent to the regrowth material occurs. Of several systems investigated, plastic deformation was observed only in the Ge samples in contact with a tin-doped regrowth material.

Precision Resistivity Measurements to Evaluate Silicon Single Crystals

S J. Silverman and C. L. Paulnack, Bell Telephone Laboratories, Inc., Allentown, Pa.

The development of a precision resistivity measurement technique has permitted an exact study of both the radial and the axial variations in Si single crystals as a function of growth parameters. Both n- and p-type specimens in the resistivity range from 30 to 0.05 ohm-cm have been investigated. The precision of a particular measurement at any one position on the specimen is sufficiently high to detect small fluctuations solely attributed to the impurity distribution within the material.

A more complete discussion is presented to enumerate the pertinent factors affecting these observations. This information is essential in optimizing those crystal growing conditions which influence resistivity homogeneity.

Electrical Properties of Dislocations in Silicon

R. A. Logan, D. A. Kleinman, and A. J. Peters, Bell Telephone Laboratories, Inc., Murray Hill, N. J.

N- and p-type floating zone Si have been plastically deformed with crystal orientation chosen so as to introduce parallel arrays of edge dislocations. Studies of the electrical properties of the dislocations, using Hall effect techniques, have been made over the temperature range 20°-300°K, with the current flow perpendicular to the direction of the dislocations. While the effects of the dislocations are small in p-type material, a new acceptor center and a markedly reduced carrier mobility have been observed in n-type Si. These effects are compared to similar measurements in Ge* and with the predictions of Read's theory.†

* R. A. Logan, G. L. Pearson, and D. A. Kleinman, *Bull. Am. Phys. Soc.*, 3, 261 (1958).

† W. T. Read, Jr., *Phil. Mag.*, 46, 111 (1955).

A Method of Pulling Single Crystal Strips from a Melt

G. K. Gaule, J. T. Breslin, and J. R. Pastore, U. S. Army Signal Research and Development Lab., Fort Monmouth, N. J.

A method of growing long, flat single crystals (strips) from a melt has been developed. The shape of the layer of the melt, closest to the growth interface, is controlled by the surface tension acting on the free surface of the liquid, and by electromotive forces acting on certain surface regions of the liquid. These forces are caused by an RF concentrator surrounding the growth interface. Experimental results are discussed.

A Turntable Method for Crystal Refining and Growth

G. K. Gaule, J. T. Breslin, and J. R. Pastore, U. S. Army Signal Research and Development Lab., Fort Monmouth, N. J.

Application of heat radiation followed by RF induction heating creates a molten pool on the surface disk (3 cm thick, 15 cm diameter). The disk, serving as a "crucible" for the molten material, rests on a slowly rotating "turntable." Since the pool is off center and remains stationary, an annular "track" of the material is melted and resolidified (and "zone refined"), while moving through the pool. Impurities accumulated in the pool can be "dumped" in a region off the "track." A single crystal is pulled from a new pool, constantly fed with refined material through the rotation.

Control of Solute Concentration in Crystals Grown from the Melt

J. R. Patel and J. Mullen, Raytheon Manufacturing Co., Waltham, Mass.

In the normal freezing process of crystal growth as exemplified by the Czochralski or Bridgman method, the concentration of a solute along the length of the crystal is determined invariantly by the effective distribution coefficient of the solute. By a suitable geometrical arrangement of containers it is shown that the solute concentration in the solid can be controlled regardless of the actual distribution coefficient. Analytical expressions have been derived for the solute concentration along the length of the crystal. The results predict the geometrical ar-

rangement necessary to provide the desired solute concentration in the solid.

Boron Diffusion in Silicon

B. T. Howard, Bell Telephone Laboratories, Inc., Murray Hill, N. J.

A process is described for producing diffused junctions in Si using B as the diffusant. The process consists of two parts, first, a thin layer of B is prediffused in the Si, and subsequently this prediffused layer is diffused into the Si to produce the junction required.

Results are presented to show that this process is capable of producing junctions with surface concentrations from 10^{18} cm^{-3} to 10^{20} cm^{-3} with a reproducibility of $\pm 5\%$. Junction depths may be obtained varying from less than 0.1 mil to about 1.0 mil with a reproducibility of $\pm 5\%$. The mechanism involved in the process is discussed, and measurements of the diffusion coefficient for B in Si are presented.

Diffusion of Antimony into Silicon through an Oxide Film

A. LaRocque, R. Yatsko, and A. Quade, U. S. Army Signal Research and Development Lab., Fort Monmouth, N. J.

When Sb is diffused into Si there is a problem of surface deterioration. Experimental evidence tends to indicate that this is due to minute areas of Si-Sb regrowth on the surface. It has been determined experimentally that the aforementioned surface impairment can be minimized by the process of pre-oxidizing the Si immediately prior to the antimony diffusion.

Experimental data have been obtained relating the diffusion conditions with the depth of junction formation. Techniques for determining this depth, as well as for the determination of oxide surface films, have been utilized. Electrical measurements, including reverse bias diode breakdown voltage, diode capacitance, and forward bias injection characteristics, have been obtained.

Etching of Silicon Carbide

J. W. Faust, Jr., Research Labs., Westinghouse Electric Corp., Pittsburgh, Pa.

Various methods of etching silicon carbide are mentioned. The use of molten salts as etchants is discussed in more detail. Dislocations revealed by these etchants are illustrated by photomicrographs.

Division News

Battery Division

The Battery Division luncheon and biennial election of officers was held in the Ballroom of the Chateau Laurier, Ottawa, on September 30, 1958. A feature of the luncheon was the presentation of the first Research Award of the Battery Division to Dr. John J. Lander of the Delco-Remy Division of General Motors. This award bestows on Dr. Lander a Life Membership in both the Society and the Battery Division.

The following Division officers were elected:

Chairman—J. C. White, Naval Research Lab., Washington, D. C.

Vice-Chairman—E. J. Ritchie, Eagle-Picher Co., Joplin, Mo.

Secretary-Treasurer—C. H. Clark, Signal Corps Engineering Labs. (Mail add: 34 Pleasant Place, Deal, N. J.)

Members-at-Large—Arthur Fleischer, McGraw-Edison Co.; and Wm. Herbert, Ray-O-Vac Co.

The Secretary-Treasurer reported that on September 21, 1958 the paid membership of the Division was 253, and that the cash balance after providing for outstanding bills was approximately $1576.00

E. J. Ritchie,
Past Secretary-Treasurer

Corrosion Division

A brief business meeting was held on October 1, 1958 at the Ottawa Meeting.

The Secretary's report described the Division's joint sponsorship of a symposium (with the Electrothermics and Metallurgy Division) at the Spring 1958 New York Meeting. The central topic was the stress corrosion cracking of stainless steel, on which six papers were given.

Officers for the 1958-1959 period were elected:

Chairman—M. A. Streicher, E. I. du Pont de Nemours & Co., Wilmington, Del.

Vice-Chairman—R. T. Foley, General Electric Co., Schenectady, N. Y.

Secretary-Treasurer—Milton Stern, Electro Metallurgical Co., Division of Union Carbide Corp., Niagara Falls, N. Y.

It is planned to devote a symposium at the Spring 1959 Philadelphia Meeting to unusual valence states associated with corrosion processes.

R. T. Foley,
Secretary-Treasurer

Theoretical Electrochemistry Division

The Nominating Committee of the Theoretical Division (E. B. Yeager, Chairman; W. J. Hamer, Paul Delahay) reports that the following have been nominated as candidates for officers of the Division:

Chairman—C. W. Tobias, University of California, Berkeley, Calif.

Vice-Chairman—Ralph Roberts, 3308 Camalier Dr., Washington 15, D. C.

Secretary-Treasurer—L. G. Longsworth, Rockefeller Institute for Medical Research, New York 21, N. Y.

Executive Committee (two to be elected)—Sigmund Schuldiner, 2101 "P" St., S. E., Washington 20, D. C.
Paul Rüetschi, Electric Storage Battery Co., Philadelphia 20, Pa.
A. J. deBethune, Boston College, Chestnut Hill 67, Mass.
Seymour Senderoff, National Carbon Research Labs., Cleveland 1, Ohio.

Each nominee has expressed his willingness to serve if elected.

The election will be held at the Society's Spring 1959 Meeting in Philadelphia.

E. B. Yeager, *Chairman*
Nominating Committee

Battery Division Extended Abstracts

Battery Division Extended Abstracts from the Ottawa Meeting, September 28-October 2, 1958, may be ordered from the Secretary-Treasurer, Chas. H. Clark, 34 Pleasant Place, Deal, N. J.

Their price is $2.00 per copy, postpaid, and payment must accompany all orders (by action of the Battery Division Executive Committee).

Theoretical Electrochemistry Spring 1959 Symposium

The Theoretical Electrochemistry Division announces that a symposium on "Electrode Processes" is to be held at the Spring 1959 Meeting of The Electrochemical Society to be held in Philadelphia, May 3-7. The symposium will include invited papers presented by distinguished foreign and U. S. scientists.

This symposium is being supported in part by the United States Air Force Air Research and Development Command through its Office of Scientific Research.

Section News

Mohawk-Hudson Section

The Section's first meeting of the 1958-1959 season was held on October 21, 1958. Speakers at this meeting were Dr. F. W. Clark, General Electric Co., who discussed recent advances in the field of insulation; and Dr. E. C. Pitzer, also of the General Electric Co., who gave a review of battery research and technology. Professor George Janz, of the Dept. of Chemistry, Rensselaer Polytechnic Institute, then gave a talk on homogeneous electrochemistry dealing chiefly with conductance transport and electrode phenomena in fused salts.

The meeting was attended by many students in the area who are being encouraged to join the national Society by being sponsored by members of the Local Section.

W. H. Smith,
Secretary-Treasurer

Personals

H. M. Scholberg has joined the research dept. at Monsanto Chemical Co. in St. Louis, Mo., as a group leader with the Inorganic Chemicals Division. Previously, he had served with the Minnesota Mining & Manufacturing Co., St. Paul.

F. J. Port, formerly manager of manufacturing and engineering, has been appointed general manager of the Automotive Division of the Electric Storage Battery Co., Philadelphia.

E. B. Saubestre has joined Enthone, Inc., New Haven, Conn., as assistant to the research director. He will assist Dr. W. R. Meyer, president and research director, in expanding Enthone's research and development program. He had been with Sylvania Electric Products Inc., Bayside, N. Y.

Worden Waring, formerly chemistry group leader in the Semiconductor Development Lab. of Raytheon Mfg. Co., Newton, Mass., has joined Fairchild Semiconductor Corp., Palo Alto, Calif., as head of the Chemistry Section.

News Items

Nominations for ECS Honorary Membership

Harold M. Scholberg, Chairman of the Honors and Awards Committee of The Electrochemical Society, would like to receive suggestions for candidates for two Honorary Memberships in the Society, to be awarded in May 1959.

Nominations should carry a resumé of the candidate's career and of his contributions to the Society and the Science.

Nominations should be submitted as soon as possible to H. M. Scholberg, Inorganic Division, Research Dept., Monsanto Chemical Co., Lindbergh & Olive St. Rd., St. Louis 24, Mo.

"Technology of Columbium (Niobium)" Now Available

The Electrochemical Society is pleased to announce the availability of the latest volume in the ECS Series, sponsored by the Society, and published by John Wiley & Sons, Inc.

"Technology of Columbium (Niobium)," published August 1958, is a compilation which includes most of the papers presented at the Symposium on Columbium (Niobium) of the Electrothermics and Metallurgy Division of The Electrochemical Society in Washington, D. C., May 15 and 16, 1958. It provides vital information on niobium, discussed by 25 authorities active in the field of high-temperature technology.

The 120-page book, listed at $7.00, is available to ECS members at the 33 1/3% member discount. To obtain the discount, orders must be sent to Society Headquarters, 1860 Broadway, New York 23, N. Y. The Society will forward orders to Wiley who will ship the volume with the invoice. Nonmembers, including subscribers, should send their orders directly to John Wiley & Sons, Inc., 440 Fourth Ave., New York 16, N. Y.

Electric Storage Battery Co. Scientific Research Center to Seek New Packaged Power Devices

A new research center that will probe a wide range of related scientific subjects—from packaged power sources of the future to artificial organs for medical use—was opened recently by the Electric Storage Battery Co., Philadelphia.

The 70-year-old pioneer of the battery industry moved its 41-man basic and applied research team, formerly at its Philadelphia plant, to a new and separate facility in Yardley, Pa., near Trenton, N. J.

Current projects include work on hermetically sealed storage battery cells, as well as studies of various primary energy cells, including chemical fuel cells.

The new center will also permit further extension of its research in such diverse areas as plastics; metallurgy, especially work in nonferrous metals; and special membranes for use in large-scale desalting of water.

The move initially more than doubles company research space to provide for current expansion and that already planned for the future, including a substantial increase in the scientific staff.

The corporate Research Center has individual divisions for fundamental scientific inquiry in electrochemistry, physical chemistry, organic chemistry, and solid-state physics. In a division of applied research, the knowledge unearthed by basic research is translated to a form suitable for use by separate development and engineering groups in the company.

The Electric Storage Battery Co.'s research department is headed by Captain Clifton G. Grimes, former deputy Chief of Naval Research, who reports directly to the company's president, Carl F. Norberg.

Research in Metal Sputtering Shows Printed Circuit Possibilities

Recent research in the field of cathode metal sputtering at Bell Telephone Labs. indicates that this century-old technique may be useful in producing precision printed circuits for modern communication equipment. It now appears that entire circuits, including resistors, capacitors, and leads, may be laid down by this technique, in which ionized gas molecules bombard a cathode, dislodging atoms of metal which then redeposit on nearby surfaces.

Harold Basseches of Bell Labs. has produced thin films of a number of electrically interesting high melting point metals. Tantalum and titanium, for example, melting at 3000° and 1670°C, respectively, can be laid down in films which show sufficient high resistivity to be useful as resistors in printed circuits. With proper masking of the substrate, lines and patterns of practically any desired shape and size can be formed, ranging in width

(Continued on page 258C)

A Few of the 800+ at the Ottawa Meeting

Row 1—W. C. Gardiner presenting Acheson Medal to W. J. Kroll; Dr. and Mrs. John Convey (General Chairman Ottawa Meeting and Chairman Ladies' Committee, respectively); J. C. White and J. J. Lander (first recipient of Research Award of the Battery Division of The Electrochemical Society). **Row 2**—Dr. and Mrs. J. W. Marden; Mr. and Mrs. G. W. Heise; W. Dingley, J. S. McCree (Ottawa Committee-Tours), G. Sirianni, I. I. Tingley, G. N. Banks, and H. C. Miller. **Row 3**—Julian Glasser and Dr. and Mrs. Morris Feinleib; Herbert Bandes and R. R. Heikes; J. H. Brennan, T. W. Clapper, and J. C. Schumacher. **Row 4**—R. A. Campbell (Ottawa Committee-Publicity), W. R. Inman (Ottawa Committee-Entertainment), and Mrs. Inman (member Ladies' Committee); Abner Brenner; W. W. Knipe, W. W. Palmquist, and C. S. Stokes. **Row 5**—John Convey; The Honorable Paul Comtois, Minister of Mines and Technical Surveys; Paul Tardif, Controller, representing Mayor George Nelms; an G. C. Monture, Vice-President, Stratmat Ltd.; Mr. and Mrs. C. A. Snavely; Dr. and Mrs. H. B. Linford, Dr. and Mrs. L. I. Gilbertson, and R. A. Schaefer.

Photographs by Newton

Row 1—Mrs. C. A. Hampel and Mr. and Mrs. T. H. G. Michael; Ella, Lottie, and Fred Fink; N. M. Winslow. **Row 2**—Dr. and Mrs. C. L. Faust; Mrs. H. A. Acheson, W. J. Kroll, and Mrs. W. C. Gardiner; Mr. and Mrs. R. K. Shannon. **Row 3**—Andrew Herczog and R. K. Willardson; M. P. Neipert and F. W. Koerker; William Blum and Dr. and Mrs. G. W. Vinal. **Row 4**—R. N. Hall and J. W. Faust, Jr.; Dr. and Mrs. R. R. Rogers (Ottawa Committee-Finance, and member Ladies' Committee, respectively), their son, and daughter; Dr. and Mrs. L. O. Case; J. V. Petrocelli, Morris Cohen (Ottawa Committee-Registration), D. L. Douglas, and Mrs. Cohen (member Ladies' Committee); J. J. Lander, C. K. Morehouse, and H. L. Hartzell; Mr. and Mrs. G. A. Ellinger.

News Items

(Continued from page 255C)

down to a few mils. These sputtered films generally are between a few hundred and a few thousand angstroms thick.

In addition to pure metals, alloys such as those of nickel-copper and nickel-chromium can be sputtered without difficulty, apparently retaining their approximate original composition.

R. W. Berry, also of Bell Labs., has produced "printed capacitors" by a combination of sputtering and chemical methods. A tantalum film of the proper shape and size is first sputtered onto the substrate and then anodically oxidized to form a tantalum oxide dielectric film. The counter electrode, a film of gold, can then be evaporated onto the dielectric to form the completed capacitor "sandwich."

Copper leads can be sputtered without difficulty to connect the various components. The technique is attractive since it eliminates the need of any organic adhesives.

RCA Awarded Air Force Contracts for High-Temperature Semiconductor Products

Two U. S. Air Force contracts totaling approximately $3,000,000 have been awarded to the Radio Corp. of America by the Air Material Command and Wright Air Development Center, for the development of high-temperature devices employing new semiconductor materials such as gallium arsenide and indium phosphide.

The contracts call for the development and production refinement of a computer diode, a power rectifier, a general-purpose transistor and a power transistor, to operate to temperatures of 400°C.

Pennsalt Completes Ammonium Perchlorate Plant for High-Energy Missile Fuels

A new plant for the production of ammonium perchlorate, a chemical used in high-energy solid state missile propellants, was put on stream recently by Pennsalt Chemicals Corp. at its Portland, Ore., works.

Ammonium perchlorate acts as the oxidizer when used in solid state rocket fuels, which have been employed in the second, third, and fourth stages in such operational rockets as the Army's Jupiter C used to put Explorer satellites into orbit, and the U. S. intercontinental missiles.

The new ammonium perchlorate plant is part of the company's current $55,000,000 expansion and improvement program. Pennsalt has also pioneered in the development of elemental fluorine and other high-energy chemicals used in both solid and liquid missile fuels.

American Institute of Physics Launches Two New Soviet Journals

The American Institute of Physics recently announced publication of *Soviet Physics—Crystallography* in cooperation with the American Crystallographic Association. It also announced publication of *Soviet Astronomy—AJ* in cooperation with the American Astronomical Society. The "AJ" in the title stands for *Astronomical Journal* as published by the Academy of Sciences of the USSR. The two bimonthly journals bring to six the translated Soviet journals published by the American Institute of Physics with the support of the National Science Foundation.

Notice to Members

By now you have received your official voting ballot from Society Headquarters. If you have not already done so, please return the ballot *by December 15* so that your vote can be included in the final election count.

Book Reviews

Insulation Engineering Fundamentals, by G. L. Moses. Published by Lake Publishing Corp., Lake Forest, Ill., 1958. 118 pages. Price: $2.75, paperbound edition; $6.00, clothbound reinforced library binding edition.

Electric Insulation has grown during the last 50 years from the academic interest of Debye into the sub-industry of today. There is still much academic interest in electric insulation, exemplified by the recently published books of Smyth, Whitehead, Frohlich, Bottcher, and von Hippel. From a professional engineering view, the older works of Peek and Miller serve as standard references.

For those people who find themselves gainfully employed in the field of electric insulation, either as suppliers or as fabricators, G. L. Moses has assembled a series of previously published essays under the title "Insulation Engineering Fundamentals." The articles proved quite popular when printed as a monthly feature of *Insulation* magazine. In the present form, they will undoubtedly serve, for the neophyte, as an introduction to the problems which confront the insulation specialist. Moses, with the collaboration of R. Lee and R. J. Hillen, has used photographs and drawings copiously. The book is written in simple, understandable terms and contains much of the jargon of the trade. This, of course, adds authenticity to much of what is based on the personal experience of the author.

T. D. Callinan

Surface Activity, Proceedings of the Second International Congress held in London, April 1957; in 4 volumes of approximately 1800 pages. Edited by J. H. Schulman. Published by Academic Press, Inc., New York City, and Butterworths Scientific Publications, London; 1958. Price of complete set, $50.00.

Vol. 1: Gas/Liquid and Liquid/Liquid Interface. Price, $15.00. Sections on Insoluble Films, Soluble Films, Foams, Evaporation Retardation, Monolayers Liquid/Liquid Interface, Solubilization and Micelles, Emulsions, General Phenomena.

Vol. 2: Solid/Gas Interface. Price, $12.60. Sections on Physical Adsorption, Chemisorption.

Vol. 3 (reviewed below): **Electrical Phenomena; Solid/Liquid Interface.** Price, $16.80; 621 pages.

Vol. 4: Solid/Liquid Interface (Washings, etc.); Cell/Water Interface (Biological). Price $12.60. Sections on Washing, Suspensions, and Agglomerations.

Vol. 3 of this four-volume report consists of both original contributions and reviews of fundamental work by prominent workers in the field of surface activity at solid/liquid interfaces. The papers are divided into two major categories: 1. Electrical Phenomena, and 2. Solid/Liquid Interfaces.

The first category (121 pages), Electrical Phenomena, consists of fifteen papers, all but two of which are primarily concerned with adsorption phenomena in the electrical double layer. The discussion at the end of this section is seven pages long and deals only with six of the papers.

The second category (about 500 pages), Solid/Liquid Interface, is subdivided into six subject headings: 1. Contact Angles, Spreading and Wetting (9 papers); 2. Flotation (17 papers); 3. Adhesion (6 papers); 4. Adsorption (9 papers); 5. Lubrication (5 papers); 6. Nucleation (5 papers).

The collection of papers given in this volume deals with a multitude of subjects and, therefore, a full review is impossible. The papers of especial interest to electrochemists begin with one by Ueda, Tsuji, and Watanabe on the so-called U-Effect, which is the a-c voltage generated on a solid/liquid interface which is mechanically forced to vibrate. This is followed by two papers on the electrical properties of dispersions. The majority of electrochemical papers, however, are concerned with the electrical double layer. These consist of a theoretical treatment of the double layer at non-iongenic interfaces by Benton and Elton; Tensammetry by Breyer; a thermodynamic evaluation of the Esin and Markov effect by Parsons; a study of the heat of specific adsorption of ions on a mecury surface by Anderson and Parsons; a report by Miller on the interaction of sodium salts of polyacids on mercury surfaces; a review by Frumkin on the adsorption of organic substances at the metal/solution interface and its influence on electrode processes; an electrokinetic study of ion adsorption on synthetic magnetite, by Anderson; a review by Hoare on inhibition of metallic corrosion by adsorbed organic molecules; a study of the relationship between wetting agents, hydrogen adsorption, and dissolution of iron, by Felloni and Bolognesi; a report by Watanabe, Tsuji, and Ueda on their work on double layer capacitance; Kamienski, on the role of water dipoles on the electrical potential; and a paper by Guastalla on Electro-adsorption.

A great many of the papers in the Solid/Liquid Interface section are of general interest to electrochemists and some deal specifically with electrocapillary phenomena. Some examples are: a paper by Cook and Wadsworth on hydrolytic and ion pair adsorption processes; electrokinetic properties of Scheelite, by O'Connor; a review of electrical phenomena in flotation, by Pomianowski; a paper by Derjaguin and coworkers on electrical phenomena accompanying the formation of new surfaces; and a review by Rehbinder and Lichtman of the effect of surface active media on strains and rupture in solids.

The papers in Vol. 3 present an important part of the current knowledge and theoretical interpretations in the areas covered and would be of interest primarily to research workers. One advantage of such a collection is the discussion section where various authorities in each field bring up to date their controversial interpretations of experiment and theory. The discussion sections of Vol. 3 vary considerably in this respect and it is unfortunate that, generally speaking, they are not as complete as could be hoped for. A minor weakness of the book is the lack of either an author or subject index.

S. Schuldiner

Zone Melting, by William G. Pfann. Published by John Wiley & Sons Inc., New York City, 1958. 236 pages; $7.50.

The first paper on zone melting was published in 1952. Now, six years later, the inventor of the method has written the first book on the subject. In the interval, the technique has been widely adopted for the manufacture of semiconductors and metals of extreme purity and for the production of materials containing controlled amounts of solutes. A comprehensive summary of the theory and practice has been badly needed. This book fills that need admirably.

The author begins with a general discussion of fractional crystallization and illustrates the application of the distribution coefficient. He then reviews the theory of zone refining, starting with concentration distributions resulting from a single pass of a zone, and proceeds to the determination of multipass distributions by calculation and by the use of analog computers. The next chapters, devoted to techniques and applications of zone refining and to continuous refining, will be especially valuable to those wishing to set up refining units.

The final chapters deal with more specialized topics such as zone leveling, growth of single crystals, means of altering the concentration at junctions, and zone melting under a temperature gradient. An appendix contains 20 graphs of computed zone refining curves showing solute concentration as a function of distance for various numbers of zone passes and for different values of distribution coefficient. These should prove extremely useful to designers of zone melting processes. The text is rendered more valuable by a comprehensive bibliography following each chapter.

It appears likely that the techniques of zone melting will in the future be applied to an ever-broadening spectrum of materials. This book should hasten the process.

M. Kolodney

Automatic Process Control, by D. P. Eckman. Published by John Wiley & Sons, Inc., New York City, 1958. 368 pages; $9.00.

The intended purpose of this book is to present the principles of automatic control to the undergraduate engineering student. The reader is assumed to have a knowledge of the fundamentals of calculus, differential equations, mechanics, thermodynamics, and fluid flow. The Laplace transform is not introduced until the

last chapter. The choice of topics is oriented toward the chemical or mechanical engineering student, and it would appear that the text was written for use in a survey type course on process controls for these people. A major portion of the text is devoted to a presentation of the principles of operation of various types of components and instruments found in process control systems. The treatment of closed-loop feedback theory is presented briefly in the last two chapters. It is regrettable that this material has not been presented earlier where it could serve as a focal point for the other developments. By the same token, if the Laplace transform were introduced earlier it could become a useful tool and point out vividly the concept of the transfer function and how the properties of individual components affect closed-loop system operation. The question of system stability, absolute and relative, is not discussed until the end of the book. In brief, the systems aspect of process control is not emphasized.

The treatment of the operation of various components is presented clearly and simplified to indicate the fundamental physcial principles involved. Most of the material is up to date and seems well chosen in terms of current practice. The text is well written, and there are problems at the end of each chapter with answers in the back of the book.

S. R. Parker

Constitution of Binary Alloys, by Max Hansen and Kurt Anderko. 2nd Ed., Metallurgy and Metallurgical Engineering Series. Published by McGraw-Hill Book Co., New York City, 1958. 1305 pages; $32.50.

This is an immensely valuable translation and revision of the well-known "Der Aufbau der Zweistofflegierungen" originally published in German by Max Hansen in 1936.

The original German edition became a metallurgists' "bible" and source book of phase diagrams. The present English edition represents an almost twofold expansion of the first in terms of systems covered and diagrams offered. Earlier constitution diagrams have been revised in the light of improved data and many new systems have been added. In particular, the multitude of binary systems that have been investigated as a result of developments in titanium metallurgy and in nuclear energy are thoroughly covered. Other welcome features include the pre-

sentation of data in terms of atomic per cent and the inclusion of lattice parameters of intermediate phases.

This book is a necessity in every metallurgical library. The U. S. Air Force is to be congratulated for its sponsorship of the formidable task of revision.

H. W. Salzberg

Radioisotopes, by Sidney Jefferson. Published by Philosophical Library, New York, 1958. 110 pages; $4.75.

This little book presents a brief survey of the industrial applications of radioisotopes. The examples chosen are British and cover such subjects as radioactive markers, leak detectors, thickness guages, etc. Only sufficient details are included to excite the interest of lay personnel. The book also includes a popular, nontechnical survey of radioactivity, atomic structure, atomic energy, detection of radiation, and health precautions. This book will provide insight into radioisotopes for the businessman and layman.

S. Edmonds

Dispersion of Materials, by Rolt Hammond. Printed in Northern Ireland by Universities Press, Belfast, for Philosophical Library, New York, 1958. x + 230 pages; $10.00

This book covers dispersion of materials by method (crushing, grinding, fluidization, flotation, liquid-dispersion techniques.) Major emphasis is on practical methods, including equipment, ranges of applicability, and types of materials used. Illustrative material is of good quality. The book is recommended to those who are concerned with industrial processes in these areas.

A section on "dispersion of gases and atmospheric pollution" constitutes a well-conceived summary of some air pollution topics but is somewhat forced within the over-all scope of the book. Although pollutants are frequently introduced to atmosphere by dispersion methods, their control at the source is frequently the reverse—a problem in collection. This distinction should be more clearly delineated.

Amos Turk

Announcements from Publishers

"Studies on Organic Fluorine Compounds," Vol. 3, J. E. Park, J. R. Lacher, and others, University of Colorado, for Office of Naval Research, Aug. 1945. Report PB 121702,* 296 pages; $5.50.

Report contains results of a study in thermochemistry designed to obtain information concerning heats of chemical reactions and, indirectly, to examine bond energies and the nature of their variation among compounds.

"A Hollow Cathode Discharge Tube for Isotopic Analysis: Progress Report," May 1958. AEC Report IDO-14432,* 15 pages; 50 cents.

"The Solubility of Zirconium Tetrafluoride in Nitric Acid from 0° to 80°C," April 1958. AEC Report IDO-14442,* 17 pages; 75 cents.

"High-Temperature Electrical Insulating Inorganic Coatings on Wire," C. G. Bergeron, A. L. Friedberg, P. F. Schwarzlose, R. J. Beals, and W. M. Faber, University of Illinois, for Wright Air Development Center, U. S. Air Force, March 1958. Report PB 131811,* 78 pages; $2.00.

"Thin Metal Films as Corrosion Indicators," R. B. Belser and F. E. Hankinson, Georgia Institute of Technology, for Wright Air Development Center, U. S. Air Force, May 1958. Report PB 131894,* 98 pages; $2.25.

"High-Temperature Insulation for Wire," J. D. Walton and J. N. Harris, Georgia Institute of Technology, for Wright Air Development Center, U. S. Air Force, March 1958. Report PB 131812,* 35 pages; $1.00.

"HRP Radiation Corrosion Studies: In-Pile Loop L-4-11," AEC Report ORNL-2152,* 1958. 48 pages; $1.50.

"Analyses of Experimental Power-Reactivity Feedback Transfer Functions for a Natural Circulation Boiling Water Reactor," AEC Report ANL-5850,* July 1958. 52 pages, $1.50.

*Order from Office of Technical Services, U. S. Dept. of Commerce, Washington 25, D. C.

Catalogs of Technical Reports

The Office of Technical Services, U. S. Dept. of Commerce, has published "Catalogs of Technical Reports" listing all research reports available from the OTS collection in the fields of powder metallurgy and semiconductors.

Many of the reports listed in the catalogs are the result of research conducted for the Army, Navy, Air Force, and other agencies of the U. S. Government. All reports listed are for sale to the public, some in printed form from OTS and others in microfilm or photocopy from the Library of Congress.

The CTR's may be ordered from OTS, U. S. Dept. of Commerce, Washington 25, at 10 cents each. They are: CTR-343, "Powder Metallurgy," 1929-1958; and CTR-340, "Semi-Conductors," 1933-1958.

U. S. Papers from Geneva Atom Conference Available from OTS

Technical papers presented by American nuclear scientists at the Second International United Nations Conference on Peaceful Uses of Atomic Energy held in Geneva, September 1-13, 1958, have been published by the U. S. Atomic Energy Commission and are for sale by the Office of Technical Services (OTS), U. S. Dept. of Commerce, Washington 25, D. C. A list of the U. S. technical papers is available from OTS; price, 25 cents.

The following papers are of especial interest to ECS members:

715—High temperature thermodynamic properties of reactor materials. R. J. Ackermann and R. J. Thorn.

914—Analysis for plutonium by controlled potential coulometry. F. A. Scott and R. M. Peekema.

917—Spectrographic determination of oxygen, nitrogen, and hydrogen in metals. V. A. Fassel and others.

923—Application of isotopes to boron hydride chemistry. W. S. Koski and J. E. Todd.

1833—Summary of analytical methods used in the chemical processing plants at Hanford. R. J. Brouns and R. A. Schneider.

2247—Recent advances in the basic chemistry of plutonium, americium, and curium. S. W. Rabideau and others.

517—Pyrometallurgical processing. P. Chiotti and A. F. Voigt.

520—Concentration and purification of uranium, plutonium, and neptunium by ion exchange in nuclearly safe equipment. F. W. Tober.

521—A rationale for the recovery of irradiated uranium and thorium by solvent extraction. T. H. Siddall, III.

523—Continuous processes for the direct reduction of uranium hexafluoride to uranium tetrafluoride of high purity and density. S. H. Smiley and D. C. Brater.

535—Recovery of uranium from highly irradiated reactor fuel by a

fused salt-fluoride volatility process. G. I. Cathers and others.

1434—Recent advances in the chemistry of liquid metal fuel reactors. R. H. Wiswall and others.

1780—Methods and equipment for low decontamination processing of metallic nuclear fuels. G. E. Brand and others.

784—A new fabrication technique for the production of stainless steel oxide dispersion fuel elements. S. Shapiro.

"Current Contents of Chemical Publications"

"Current Contents of Chemical Publications" is a new weekly designed to fill the chemical and allied industries' need for current research information. The inaugural issue is set for January 7, 1959. Research in pure and applied chemistry, physics, engineering, operations research, petroleum technology, etc., will be covered.

"Current Contents" consists of weekly pocket-size booklets containing photographic reproductions of advance or current tables of contents of more than 350 publications.

Three special features of the new service include coverage of chemical patents, translations of Russian and Japanese titles, and a magazine procurement service.

"Current Contents" is available on both a single subscription and a group basis. For a list of journals covered, specimen copies, and any additional information, write to Eugene Garfield Associates, 1523 Spring Garden St., Philadelphia 30, Pa.

Proceedings of Second International Conference on Peaceful Uses of Atomic Energy

The United Nations announces the publication in English of the complete "Proceedings of the Second International Conference on the Peaceful Uses of Atomic Energy," held in Geneva, September 1-13, 1958.

The complete English edition is expected to consist of 34 volumes of approximately 500 pages each, contents as follows: 1. Material relating to the objectives and operation of the Conference; 2. The record of all sessions; 3. The complete text of all papers submitted to the Conference (approximately 2200); 4. A detailed index volume (subject, numerical, and author).

The first volumes will be available in December 1958, and the last volumes are expected off the presses by July 1959.

The average price of the English edition of the Proceedings will approximate $15.00 per volume; price for the full set will approximate $510.00.

Orders can be placed at the United Nations and local bookstores.

Literature from Industry

Maccromates. A new group of compounds for producing chromate conversion coatings on zinc and cadmium plated work, on zinc diecastings, and on aluminum is fully described in Technical Data Sheet No. 76, a four-page usage and instruction sheet prepared by MacDermid Inc., Waterbury, Conn. Called Maccromates, the new line includes the following types of coatings: Single Dip Clear, Leach Type Clear, Iridescent Yellows and Bronzes, Olive Drab, Chemical Polishes for Zinc diecastings, Clear to Bronze on Aluminum. A wide variety of leaching compounds and dyes is also available.

Phosphotex. An iron-zinc phosphate process for rust-proofing steel, zinc base diecastings, zinc, and cadmium plate is fully described in Technical Data Sheet No. 27, available from MacDermid Inc., Waterbury, Conn. Called Phosphotex, the process promotes the adhesion and durability of paint finishes, provides a mechanical bond for paint, protection against rust around dents, nicks, and accidental scratches. MacDermid's Phosphotex treatment converts a steel surface into a nonmetallic phosphate coating of extremely fine grain size. Products processed in Phosphotex may be painted or finished with oil, wax, or other type finishes.

"Sylvania CR-405 Phosphor," a new technical bulletin, describes a blend of silver-activated zinc and zinc cadmium sulfides designed especially for use in aluminized television picture tubes. Copies of the bulletin may be obtained from Sylvania Electric Products Inc., Towanda, Pa.

"Synthetic Sapphire, An Infrared Optical Material." This 11-page booklet, written with the requirements of the infrared optical system designer in mind, is a resumé of single-crystal aluminum oxide growth, recent advanced shapes and sizes, and optical, thermal, and high-temperature physical properties of Linde synthetic sapphire. Available from: Crystal Products Dept., Linde Co., Div. of Union Carbide Corp., 30 E. 42 St., New York, N. Y.

Employment Situations

Please address replies to box shown, c/o The Electrochemical Society, Inc., 1860 Broadway, New York 23, N. Y.

Positions Wanted

Physical Chemist, Ph.D. 1958, desires research position in electrochemistry and/or solid state. Strong

Manuscripts and Abstracts for Spring 1959 Meeting

Papers are now being solicited for the Spring Meeting of the Society, to be held at the Sheraton Hotel in Philadelphia, Pa., May 3, 4, 5, 6, and 7, 1959. Technical sessions probably will be scheduled on Electric Insulation, Electronics (including Luminescence and Semiconductors), Electrothermics and Metallurgy (including a Projected Symposium on "Mechanical Properties of Intermetallic Compounds"), Industrial Electrolytics, and Theoretical Electrochemistry.

To be considered for this meeting, triplicate copies of abstracts *(not to exceed 75 words in length)* must be received at Society Headquarters, 1860 Broadway, New York 23, N. Y., *not later than January 2, 1959. Please indicate on abstract for which Division's symposium the paper is to be scheduled, and underline the name of the author who will present the paper.* Complete manuscripts should be sent in triplicate to the Managing Editor of the JOURNAL at the same address.

★ ★ ★

The Fall 1959 Meeting will be held in Columbus, Ohio, October 18, 19, 20, 21, and 22, 1959, at the Deshler-Hilton Hotel. Sessions will be announced in a later issue.

instrumentation background; research experience; publications; honor societies. Will consider position in New York City or Metropolitan New Jersey area only. *Reply to Box 365.*

Battery Chemist, 11 years' experience with manufacturers of automotive, stationary, and industrial lead-acid batteries. Thoroughly experienced in grid design and casting, oxide production, paste formulation, assembly, fast formation, and dry charging; development, quality control, and cost reduction. B.Sc. degree. Age 32. *Reply to Box 366.*

Positions Available

Electrochemist for Basic Studies in Corrosion, position open in small laboratory in Virginia. Opportunity for solid-state physics approach or conventional electrochemical approach to aqueous corrosion. Position is such that either a strong individualist or a team man could be happy. *Reply to Box A-277.*

Physical Chemist, Physicist, or Metallurgist. The British Columbia Research Council has a vacancy for a physical chemist, physicist, or metallurgist for research on anodic oxide films. Salary range to $7000 depending upon qualifications and experience. Applications with names of two referees should be sent to Dr. G. M. Shrum, Director, British Columbia Research Council, University of British Columbia, Vancouver 8, B. C., Canada.

Engineers (Aeronautical, Electrical, Electronic, Industrial, General, Mechanical, and Power Plant), **Electronic Scientists, Metallurgists, Physicists, Technologists**—Vacancies exist for professional personnel in the above positions. Starting salaries range from $4490 to $10,130 per annum. The Naval Air Material Center is currently engaged in an extensive program of aeronautical research, development, experimentation, and test operations for the advancement of Naval aviation. Experimental work is also being conducted in the guided missile field. Personnel are needed for work on projects involving modification, overhauling, and testing of aeronautical equipment, materials, accessories, power plants, launching and arresting devices, and for modification and structural testing of aircraft. Also, for work involving the basic design of catapults, launchers, arresting gear and their component parts; test and development work at shore stations and on board U. S. Navy ships; evaluation of new equipment and establishment of performance parameters, and applied research on the many problems relevant to this field.

Interested persons should file an Application for Federal Employment, Standard Form 57, with the Industrial Relations Dept., Naval Air Material Center, Naval Base, Philadelphia 12, Pa. Applications may be obtained from the above address or information as to where they are available may be obtained from any first or second class post office.

Advertiser's Index

The Electrochemical Society

Patron Members

Aluminum Company of Canada, Ltd., Montreal, Que., Canada
International Nickel Company, Inc., New York, N. Y.
Olin Mathieson Chemical Corporation, Niagara Falls, N. Y.
  Industrial Chemicals Division, Research and Development Department
Union Carbide Corporation
  Divisions:
    Electro Metallurgical Company, New York, N. Y.
    National Carbon Company, New York, N. Y.
Westinghouse Electric Corporation, Pittsburgh, Pa.

Sustaining Members

Air Reduction Company, Inc., New York, N. Y.
Ajax Electro Metallurgical Corporation, Philadelphia, Pa.
Allied Chemical & Dye Corporation
  General Chemical Division, Morristown, N. J.
  Solvay Process Division, Syracuse, N. Y. (3 memberships)
Alloy Steel Products Company, Inc., Linden, N. J.
Aluminum Company of America, New Kensington, Pa.
American Machine & Foundry Company, Raleigh, N. C.
American Metal Company, Ltd., New York, N. Y.
American Platinum Works, Newark, N. J. (2 memberships)
American Potash & Chemical Corporation, Los Angeles, Calif. (2 memberships)
American Zinc Company of Illinois, East St. Louis, Ill.
American Zinc, Lead & Smelting Company, St. Louis, Mo.
American Zinc Oxide Company, Columbus, Ohio
M. Ames Chemical Works, Inc., Glens Falls, N. Y.
Auto City Plating Company Foundation, Detroit, Mich.
Bart Manufacturing Company, Bellville, N. J.
Bell Telephone Laboratories, Inc., New York, N. Y. (2 memberships)
Bethlehem Steel Company, Bethlehem, Pa. (2 memberships)
Boeing Airplane Company, Seattle, Wash.
Burgess Battery Company, Freeport, Ill. (4 memberships)
C & D Batteries, Inc., Conshohocken, Pa.
Canadian Industries Ltd., Montreal, Que., Canada
Carborundum Company, Niagara Falls, N. Y.
Catalyst Research Corporation, Baltimore, Md.
Chrysler Corporation, Detroit, Mich.
Ciba Pharmaceutical Products, Inc., Summit, N. J.
Columbian Carbon Company, New York, N. Y.
Columbia-Southern Chemical Corporation, Pittsburgh, Pa.
Consolidated Mining & Smelting Company of Canada, Ltd., Trail, B. C., Canada (2 memberships)
Continental Can Company, Inc., Chicago, Ill.
Cooper Metallurgical Associates, Cleveland, Ohio
Corning Glass Works, Corning, N. Y.
Crane Company, Chicago, Ill.
Diamond Alkali Company, Painesville, Ohio (2 memberships)
Dow Chemical Company, Midland, Mich.
Wilbur B. Driver Company, Newark, N. J. (2 memberships)
E. I. du Pont de Nemours & Company, Inc., Wilmington, Del.
Eagle-Picher Company, Chemical Division, Joplin, Mo.
Eastman Kodak Company, Rochester, N. Y.
Electric Auto-Lite Company, Toledo, Ohio
Electric Storage Battery Company, Philadelphia, Pa.
The Eppley Laboratory, Inc., Newport, R. I. (2 memberships)
Federal Telecommunication Laboratories, Nutley, N. J.
Food Machinery & Chemical Corporation
  Becco Chemical Division, Buffalo, N. Y.
  Westvaco Chlor-Alkali Division, South Charleston, W. Va.
Ford Motor Company, Dearborn, Mich.
General Electric Company, Schenectady, N. Y.
  Chemistry & Chemical Engineering Component, General Engineering Laboratory
  Chemistry Research Department

Author Index (Vol. 105, 1958)

(D) Indicates Discussion
(E) Indicates Editorial

PAGES IN EACH ISSUE (Vol. 105, 1958)

Month	Technical	Nontechnical
January	1- 58	1C- 14C
February	59-108	15C- 30C
March	109-178	31C- 68C
April	179-238	69C- 88C
May	239-288	89C-102C
June	289-368	103C-114C
July	369-434	115C-140C
August	435-486	141C-180C
September	487-552	181C-202C
October	553-612	203C-222C
November	613-694	223C-244C
December	695-762	245C-264C

Subject Index (Vol. 105, 1958)

Following an item, (E) indicates an editorial, and (D) indicates discussion of material published in preceding volume of the JOURNAL

(Sustaining Members cont'd)

General Electric Company (cont'd)
Metallurgy & Ceramics Research Department
General Motors Corporation
Brown-Lipe-Chapin Division, Syracuse, N. Y. (2 memberships)
Guide Lamp Division, Anderson, Ind.
Research Laboratories Division, Detroit, Mich.
Gillette Safety Razor Company, Boston, Mass.
Gould-National Batteries, Inc., Depew, N. Y.
Grace Electronic Chemicals, Inc., Baltimore, Md.
Great Lakes Carbon Corporation, New York, N. Y.
Hanson-Van Winkle-Munning Company, Matawan, N. J. (3 memberships)
Harshaw Chemical Company, Cleveland, Ohio (2 memberships)
Hercules Powder Company, Wilmington, Del.
Hooker Electrochemical Company, Niagara Falls, N. Y. (3 memberships)
Houdaille-Hershey Corporation, Detroit, Mich.
Hughes Aircraft Company, Culver City, Calif.
International Business Machines Corporation, Poughkeepsie, N. Y.
International Minerals & Chemical Corporation, Chicago, Ill.
Jones & Laughlin Steel Corporation, Pittsburgh, Pa.
K. W. Battery Company, Skokie, Ill.
Kaiser Aluminum & Chemical Corporation
Chemical Research Department, Permanente, Calif.
Division of Metallurgical Research, Spokane, Wash.
Keokuk Electro-Metals Company, Keokuk, Iowa
Libbey-Owens-Ford Glass Company, Toledo, Ohio
P. R. Mallory & Company, Indianapolis, Ind.
McGean Chemical Company, Cleveland, Ohio
Merck & Company, Inc., Rahway, N. J.
Metal & Thermit Corporation, Detroit, Mich.
Minnesota Mining & Manufacturing Company, St. Paul, Minn.
Monsanto Chemical Company, St. Louis, Mo.
Motorola, Inc., Chicago, Ill.
National Cash Register Company, Dayton, Ohio
National Lead Company, New York, N. Y.
National Research Corporation, Cambridge, Mass.
Norton Company, Worcester, Mass.
Olin Mathieson Chemical Corporation, Niagara Falls, N. Y.
High Energy Fuels Organization (2 memberships)
Pennsalt Chemicals Corporation, Philadelphia, Pa.
Philips Laboratories, Inc., Irvington-on-Hudson, N. Y.
Pittsburgh Metallurgical Company, Inc., Niagara Falls, N. Y.
Poor & Company, Promat Division, Waukegan, Ill.
Potash Company of America, Carlsbad, N. Mex.
Radio Corporation of America, Harrison, N. J.
Ray-O-Vac Company, Madison, Wis.
Raytheon Manufacturing Company, Waltham, Mass.
Reynolds Metals Company, Richmond, Va. (2 memberships)
Schering Foundation, Inc., Bloomfield, N. J.
Shawinigan Chemicals Ltd., Montreal, Que., Canada
Speer Carbon Company
International Graphite & Electrode Division, St. Marys, Pa. (2 memberships)
Sprague Electric Company, North Adams, Mass.
Stackpole Carbon Company, St. Marys, Pa. (2 memberships)
Stauffer Chemical Company, Henderson, Nev., and New York, N. Y. (2 memberships)
Sumner Chemical Company, Division of Miles Laboratories, Inc., Elkhart, Ind.
Superior Tube Company, Norristown, Pa.
Sylvania Electric Products Inc., Bayside, N. Y. (2 memberships)
Sarkes Tarzian, Inc., Bloomington, Ind.
Tennessee Products & Chemical Corporation, Nashville, Tenn.
Texas Instruments, Inc., Dallas, Texas
Titanium Metals Corporation of America, Henderson, Nev.
Udylite Corporation, Detroit, Mich. (4 memberships)
Upjohn Company, Kalamazoo, Mich.
Victor Chemical Works, Chicago, Ill.
Wagner Brothers, Inc., Detroit, Mich.
Weirton Steel Company, Weirton, W. Va.
Western Electric Company, Inc., Chicago, Ill.
Wyandotte Chemicals Corporation, Wyandotte, Mich.
Yardney Electric Corporation, New York, N. Y.

How to make rust-and-scale removal an exact science: For more than 20 years, Enthone has studied metal finishing problems and developed specialized solutions. Among the rust and scale removal compounds perfected by Enthone research and proved in the field, are the Alka-Deox® series of alkaline materials which electrolytically or non-electrolytically remove rust and scale from steel, cast or malleable iron; Enthol® 42, a solvent acid cleaner for steel, zinc, aluminum and other metals; and Actane® 70, a replacement for hydrofluoric acid as a dispersing agent in acid pickles to remove colloidal and siliceous films from metals. Write us about your special oxide removal problems. Chances are we have the answer in stock. Enthone, Inc., 442 Elm Street, New Haven 11, Connecticut.

ENTHONE

ENTHONE, INC. IS A SUBSIDIARY OF AMERICAN SMELTING AND REFINING COMPANY